Late Palaeozoic and Mesozoic evolution of the Amu Darya Basin (Turkmenistan, Uzbekistan)

MARIE-FRANÇOISE BRUNET[1*], ANDREY V. ERSHOV[2], MAXIM V. KOROTAEV[2], VLADISLAV N. MELIKHOV[3], ERIC BARRIER[1], DMITRIY O. MORDVINTSEV[1,4] & IRINA P. SIDOROVA[4]

[1] *Sorbonne Universités, UPMC Univ. Paris 06, CNRS, Institut des Sciences de la Terre de Paris (iSTeP), 4 place Jussieu 75005 Paris, France*
[2] *Geological Faculty, Moscow State University, Vorobievy Gory, 119899 Moscow, Russia*
[3] *A.P. Karpinsky Russian Geological Research Institute (VSEGEI), Sredny prospect 74, 199106 Saint Petersburg, Russia*
[4] *Institute of Geology and Geophysics of the Academy of Sciences of Republic of Uzbekistan, Olimlar 49, 100041, Tashkent, Uzbekistan*

*Corresponding author (e-mail: marie-francoise.brunet@upmc.fr)

Accepted May 15, 2017, *In:* BRUNET, M.-F., MCCANN, T. & SOBEL, E. R. (eds) *Geological Evolution of Central Asian Basins and the Western Tien Shan Range*. Geological Society, London, Special Publications, **427**.

Abbreviated title: **Evolution of the Amu Darya Basin**

Abstract

The Amu Darya Basin (ADB) has been studied primarily for its important hydrocarbon reserves but less for its geodynamic evolution. The ADB is located on the southeast portion of the Turan Platform, between the sutures of the Turkestan and Palaeo-Tethys oceans, which closed during the Late Palaeozoic and Early Mesozoic, respectively. Blocks and island arcs accreted to Eurasia during the Palaeozoic form a poorly defined, heterogeneous basement underlying the ADB. They played an important role in shaping its composite structure into variously oriented sub-basins and highs. In this paper, depth-structure and isopach maps, and regional cross-sections are analyzed to unravel the location and origin of the main structural elements and to characterize the subsidence evolution of the ADB. The main tectonic events leading to the formation and evolution of the ADB took place: (1) in the Late Palaeozoic-Early Triassic (back-arc, rollback, extension/strike slip); (2) from Middle-Triassic to the Triassic-Jurassic boundary (Eo-Cimmerian collision of Gondwana-derived continental blocks with Eurasia); (3) during the Early to Middle-Jurassic (post collision extensional event). The last part of this evolution reflects shortening and flexure due to Cenozoic collisions to the south. Palaeotectonic maps are used to relate these events to the geodynamics of the Tethyan domain.

The Amu Darya Basin (ADB) is a large structural depression in western Central Asia, east of the Caspian Sea, where about 15 km of sediments have been deposited since the Palaeozoic. The ADB has been studied particularily for its petroleum resources, the province being mainly gas prone (Clarke 1988, 1994; Ulmishek 2004). The area of the ADB is larger than 417 000 km^2 (Klett *et al.* 2012), lying mainly in Turkmenistan but also in Uzbekistan along its NE margin and in Afghanistan and Iran along its southern segments. The present NW-SE to WNW-ESE elongated shape (Fig. 1) is delineated by surrounding topographic highs or ranges uplifted during several orogenies since the Late Palaeozoic. The ADB is located on the so-called Turan Platform (e.g. Clarke 1988; Thomas *et al.* 1999a; Natal'in & Şengör 2005), composed of a series of blocks/terranes accreted during the Late

Palaeozoic Variscan orogeny, when the Turkestan Ocean closed, forming the Turkestan suture (Fig. 1). The Turan Platform (or Turan Plate) was then part of the southern active margin of Eurasia until the closure of the Palaeo-Tethys to the south. This collision formed the Palaeo-Tethys suture (Fig. 1) in the Mesozoic by accretion to Eurasia of the Cimmerian terranes, which were detached from Gondwana in the Permian. The uplift of the Southwestern Gissar Range, a consequence of northward indentation of the Pamir during the Alpine Himalayan orogeny, partly separated the ADB from the neighbouring Afghan-Tajik Basin. Although these two basins constituted one single basin from the early Mesozoic until Miocene time (Ulmishek 2004), our study is focused on the ADB.

A substantial published literature, mainly in the Russian language, has developed since the middle of the last century on the structure, lithostratigraphy, palaeogeography, deep geophysics and hydrocarbon resources of the ADB; much less work has been done on its geodynamics. Therefore, the reference list of this paper is far from complete, as hundreds of papers, books or reports exist on the ADB. However, we refer to several important papers where details can be found related to the available data and discussions, helping to understand the ADB evolution, and providing internet links to access several of the papers. Most of the work was published from the 1960s to the 1980s, corresponding to time when the bulk of the data was acquired (wells and geophysics) and interpreted (e.g. Vol'vovskiy *et al.* 1966; Beliayevsky *et al.* 1968; Ryaboy 1968; Yegorkin & Matushkin 1970; Babadzhanov *et al.* 1986); some data were reprocessed in the 1990s (e.g. Pavlenkova 1996; Sheikh-Zade 1996). They are either part of books on the geology or geophysics of the former Soviet Union (e.g. Antropov 1957; Bakirov *et al.*, 1979; Maksimov 1987, 1992; VNIGNI & Beicip Franlab 1992) or more focused on the ADB (e.g. Amurskii 1966; Babayev 1976). More recent studies on the geology of the Turkmenistan part often reinterpret the same data or make syntheses about the entire ADB, either in Russian or English (e.g. Clarke 1988, 1994; Melikhov 2000, 2013, 2017; Ulmishek 2004). More recent data on the central part of the ADB in Turkmenistan are not readily accessible to the international community. Nevertheless, a large suite of recent papers issued from the CNPCI's (China National Petroleum Corporation International) Amu Darya Natural Gas Project (e.g. Zheng *et al.* 2011, 2013, 2014; Xu *et al.* 2012, Liu *et al.* 2013; Lu *et al.* 2013; Nie *et al.* 2013a, b, 2015, 2016; Ba *et al.* 2015) presents some new data and interpretations on the deep northern margin of the ADB in Turkmenistan, an area named the right bank of the Amu Darya River. In the Uzbekistan portion of the northern margin of the ADB, an abundant literature, mainly in Russian, has existed from the 1960s with publications in journals, books, internal reports of the Uzbekistan organizations IGIRNIGM and Uzbekgeofizika, as well as theses (e.g. Gavrilcheva & Pashaev 1993; Besnozov & Mitta 1995; Abdullaev & Mirkamalov, 1998, 2001; Fortunatova 2000, 2007; Babadzhanov & Abdullaev 2009; Radjabov 2009; Abdullaev *et al.*, 2010; Babadzhanov 2012; Troitskiy 2012; Evseeva 2015a,b).

Only a few publications about the southeastern margin of the ADB in Afghanistan are available; these contain the main tectonic, lithostratigraphic and hydrocarbon geology informations on its evolution (Kingston 1990; Kingston & Clarke 1995; Brookfield & Hashmat 2001; Klett *et al.* 2006; Abdullah & Chmyriov 2008; Montenat 2009; Wang *et al.* 2014a). Similarly, a few publications are available that focus on the southern and southwestern margins near Iran (e.g. the Dauletabad-Donmez area, Clarke & Kleschev 1992) and their link with the Kopet-Dagh (Robert *et al.* 2014).

Detailed studies of the northern and northeastern margins of the Amu Darya and Afghan-Tajik basins can be found within this volume (Brunet *et al.* (eds) 2017). McCann (2016 a, b) presents sedimentological and stratigraphic studies of the Jurassic of the Central Kyzylkum and the Cretaceous of the South Kyzylkum and Nuratau region bordering the northern ADB (Fig. 1). Mordvintsev *et al.* (2017) present cross-sections and describe the evolution of the Bukhara and Chardzhou steps, to the east of the northern margin of the ADB. Fürsich *et al.* (2015) detail the Jurassic clastic series in Southwestern Gissar (northeastern margin of the ADB and northwest of the Afghan-Tajik Basin). Siehl (2015) provides a review of the Variscan basement of the Turan Plate and the links with the Afghan orogenic segment to the south.

The ADB appears at first glance to be a jigsaw puzzle of many sub-basins and highs with various orientations. The aim of this paper is not to make a detailed review of the geology of the ADB with

its more than 15 km of sediments, but rather to provide a better understanding, at the basin scale, of the main structuring events leading to the formation and evolution of the ADB as it is known today. For this purpose, we use maps, cross-sections and subsidence analysis to focus on the evolution of the ADB during the Late Palaeozoic to Mesozoic with a special emphasis on the Jurassic. We refer the reader to some publications where the litho-stratigraphy and general geology or geophysics of the ADB are described in detail, limiting our discussion to the most controversial points about the ages and tectonics that directly influence the precision of the tectonic chronology.

The Late Palaeozoic is the earliest and main episode recognized in the formation of the ADB (e.g. Clarke 1988; Thomas *et al.* 1999a; Ulmishek 2004; Natal'in & Şengör 2005), with several kilometres of volcanoclastic sediments deposited; however, it is also the least well known, as the exact geometry, thickness and age of the sub-basins established on a mosaic of lithospheric blocks is not well constrained. The inherited Palaeozoic structures play an important role in the tectonic complexity of the ADB. Indeed, the ADB is subdivided into highs and troughs with structural features of various orientations, formed or reactivated by repeated collisional and extensional events. The Early-Middle Jurassic event is the main one discussed in this paper because it dominated the formation of the present shape of the basin and its hydrocarbon system. We go on to relate the tectonic events and their timing to the key features of the geodynamic evolution of this part of the Tethyan domain.

The work reported in this paper took place in the framework of the Darius International Programme of research on Middle East and western Central Asia. As some of the series of the deep ADB crop out in the Southwestern Gissar (Fig. 1), this study benefitted from close interactions with companion research performed in Uzbekistan in the frame of a Group of Research-Industry cooperation "GRI Total UPMC Northern Tethys", a thesis on the Bukhara-Khiva region (composed mainly of the Chardzhou and Bukhara steps) and on the Southwestern Gissar, using seismic data and subsidence analysis (Mordvintsev 2015; Mordvintsev *et al.* 2017), and field studies in the Southwestern Gissar on the palaeogeography and stratigraphy of the Lower and Middle Jurassic siliciclastics (Fürsich *et al.* 2015), and of the Upper Jurassic carbonates (Carmeille *et al.* 2014, 2016).

Geological setting

The Amu Darya Basin (ADB), also named the Karakum Basin (e.g. Seregin *et al.*, 1979; Melikhov 2000, 2017), is bounded to the north, south and west by ranges and basement highs. To the south, these are the Kopet-Dagh in Iran, Bande Turkestan and Paropamisus in Afghanistan, to the north, in Uzbekistan, the Sultanuizdag Mountains, the Kyzylkum High or Kuldzhuktau and Zirabulak Mountains, the western part of the South Tien Shan and to the west, in Turkmenistan, the Tuarkyr and the Great Balkhan (Fig. 1). The ADB extends towards the east-southeast into the Afghan-Tajik Basin, surrounded as well by mountain ranges to the north (Gissar in the South Tien Shan) and east (Hindu Kush, Pamir), and by basement highs to the south in northern Afghanistan. These two neighbouring basins have been closely linked since the end of the Palaeozoic and through the Mesozoic until the uplift of the Southwestern Gissar Range during the Miocene (Ulmishek 2004). The NE-SW-oriented Southwestern Gissar Range includes outcrops of the sediments that are elsewhere buried on the northeastern margin of the ADB.

Because of their petroleum interest, the definition of these two basins is often considered in terms of petroleum provinces, thus grouping several small peripheral areas. Accordingly, different authors depict different contours for the two petroleum provinces or modern basins and the peripheral structures they choose to include. Wynn *et al.* (2016) present different versions of basins boundaries, defined by AAPG, Tellus and USGS. Figure 1 displays a different outline of the ADB and Afghan-Tajik Basin or petroleum provinces, modified from Melikhov (2000).

Main structural subdivisions of the Amu Darya Basin

The surface topography of the ADB is rather flat, mostly covered by the Karakum Desert. However, at depth, the ADB has a complicated structure (Fig. 1) with varying orientations often inherited from

the Palaeozoic assemblage of underlying crustal blocks. The ADB is subdivided into several sub-basins, separated by high areas and often by faults; its margins are termed steps.
A series of NW-SE-oriented faults shapes the northeast margin. Several northern faults lie between the Zirabulak Mountains and the Mubarek High, and continue towards the west as the Central Ust Yurt Fault (e.g. Ulmishek 2004; Natal'in & Şengör 2005), which joins the Manghyshlak region; these mark the northern edge of the Bukhara Step and also the northern boundary of the ADB. An important zone of faults and flexures with a range of names, including Bukhara-Gissar, Aral-Gissar, Gissar-Manghyshlak, Bukhara (e.g. Blackbourn 2008; Babadzhanov & Abdullaev 2009) or Uchbash-Karshi Flexure Fault Zone (UKFFZ) (Abidov & Babadzhanov 1999) separates the Bukhara from the Chardzhou steps. Towards the south, the Amu Darya Fault separates the Chardzhou Step from the Bagadzha Step and the Karabekaul Trough. To the east, the NE-SW-oriented Beshkent Depression borders the similarily oriented Southwestern Gissar Mountain; these are the most apparent features linked to the NE-SW-oriented faults structuring the Bukhara and Chardzhou steps (e.g. Mordvintsev & Mordvintsev 2011; Babadzhanov *et al.* 2012; Lu *et al.* 2013).
The WNW-ESE-oriented Repetek-Kelif zone of uplifts is a major feature in the eastern part of the ADB. It is the only area of the ADB where movements of the Upper Jurassic salt occur; the intensity of diapirism decreases from east to west with the thickness of salt (e.g. Clarke 1988). Salt domes, reaching an amplitude of 1-2 km, sometimes pierce the entire Cretaceous and Paleogene sequence, creating a narrow elongated zone of uplifts about 450 km long. From the centre of the ADB towards the east, this zone of uplifts separates the northeastern margin of the ADB, the Zaunguz Depression, the Bagadzha Step and the Karabekaul Trough (or North Amu Darya Depression for Bakirov 1979) in the north from the Murgab Depression in the south (e.g. Clarke 1988; VNIGNI & Beicip Franlab 1992; Ulmishek 2004). The Repetek-Kelif zone is bordered on the north by the Repetek or Repetek-Yerbent deep fault zone. In the western part of the ADB, where the Jurassic salt decreases in thickness and pinches out, the E-W Repetek Fault is not associated with domes and runs south of the Ilim Trough and the Beurdeshik Step, until south of the Central Karakum Arch in the west.
The Murgab Depression, which is the main part of the ADB, is itself divided into several sub-basins and highs: the main depressions are the Obruchev, North Mary, North Badkhyz, North Karabil and Dauletabad troughs. The southern margin of the ADB with the Badkhyz-Karabil and Maimana steps is shaped by WNW-ESE to E-W-oriented structures such as the Alburz Mormul, Andarab, Bande Turkestan faults (e.g. Brookfield & Hashmat 2001; Siehl 2015) as well as several NE-SW-oriented faults.
The medial part of the ADB is marked by N-S to NNW-SSE-oriented lineament and faults (the main ones being the Khiva Murgab Lineament and the Murgab Fault) along which exist relative highs in the sedimentary succession; to the west, the Khiva Murgab Trough encompasses the Balkui, Illim and Kalandar troughs. The NW-SE-oriented Pre-Kopet-Dagh Foredeep with the Ashgabat and Kaahka depressions, bordered to the north by the Bakhardok Slope and to the southwest by the Ashgabat Fault, constitute the southwestern sub-basin and margin of the ADB.

Stratigraphic framework

Here we give a general overview of the sediment fill of the ADB, summarized by a simplified synthetic sedimentary column (Fig. 2); the reader is referred to more detailed stratigraphic descriptions elsewhere (e.g. VNIGNI & Beicip Franlab 1992; Clarke, 1988; Melikhov 2000; Ulmishek 2004; Klett *et al.* 2006).
The Intermediate Complex (e.g. Maksimov 1992; Thomas *et al.* 1999a) comprises the oldest sediments filling the troughs underlying the ADB; the depositional onset is poorly dated as the basement is never reached by boreholes in the sedimentary depocentres. The Intermediate Complex begins at least in the Early Carboniferous, recognized in some boreholes in the Daryalyk-Daudan Trough, or even possibly in the Devonian (e.g. Melikhov 2000), and ends in the Permian-Triassic (e.g. Babadzhanov *et al.* 1986; Clarke 1988, 1994; Shayakubov & Dalimov 1998). It contains marine Early Carboniferous coarse clastics, and carbonates, and then volcanics. These are overlain by coarse-grained continental red beds (shale, sands and conglomerates) and volcanics, deposited after

retreat of the sea concommittent with the Late Carboniferous collision. The complex has a maximum thickness of 4 to 8 km, thinning to 1-2 km on the edges. The margins were often eroded during the Late Triassic Eo-Cimmerian orogeny; consequently, basement or partially eroded and deformed Intermediate Complex are overlain with an angular unconformity by Lower to Middle Jurassic siliciclastic strata. The presence of this unconformity in the central part of the ADB is not clear because of the great depths and the absence of accessible deep seismic profiles.

The earliest Jurassic deposits are continental clastics, comprising organic rich lacustrine sediments and thin coal beds at least near the margins (e.g. Egamberdiev & Ishniyazov 1990; Ulmishek 2004; Fürsich *et al.* 2015). The age of the beginning of the unit is not precisely known, especially in the centre of the ADB and the southeastern part of the Pre-Kopet-Dagh Foredeep where the unit is not penetrated by wells; it has been extensively explored by wells only in shallow sub-basins and on the margins, and by outcrops in the Southwestern Gissar (Fig. 3b). The siliciclastic sequence may begin in the latest Triassic, in the Hettangian or a bit later. On the Uzbekistan margin, in the Yangikazgan area, the Sandzhar Formation (name of the basal Jurassic in this area) is dated by a spore-pollen assemblage as Pliensbachian or even possibly Late Sinemurian (Aliyev *et al.* 1983) but the lower part may be missing on the margin and present at the bottom of the ADB. Indeed, the Lower to Middle Jurassic siliciclastic unit remains unexplored in the Murgab Depression and the Pre-Kopet-Dagh Foredeep. The unit is up to more than 2000 m in thickness in the NE of the ADB. Continental clastics of the Lower Jurassic and lower Middle Jurassic pass to marine clastics with a Late Bajocian transgression (e.g. Krymholts *et al.* 1988; Fürsich *et al.* 2015). The Lower-Middle Jurassic siliciclastic unit is the main source rock of the ADB, it contains mainly humic organic matter concentrated in shale and siltstone (e.g. VNIGNI & Beicip Franlab 1992).

The Lower Callovian sequence, the upper part of the siliciclastic unit, is progressively enriched in carbonates (see also the description in the Southwestern Gissar by Fürsich *et al.* 2015); it is thus difficult to precisely define whether the age of the contact upper boundary with the overlying Middle to Upper Jurassic marine carbonate unit takes place inside the Lower Callovian sequence (e.g. Evseeva 2015b end of the Baysun Formation in Uzbekistan) or at its roof (e.g. Aliyev *et al.* 1983; Krymholts *et al.* 1988).

The carbonate unit (also named the Kugitang sequence, c. 800 m maximum thickness) consists mainly of carbonates (Fig. 3c-d), which range from carbonate build-ups along part of the margins and high areas, constituting the main reservoir rocks of the ADB, to more basinal carbonates and carbonaceous shales in central parts of the ADB. The age at the top of the carbonate unit is controversial, ranging between the latest Oxfordian and the end of Kimmeridgian and will be discussed below. The carbonate unit is overlain by an evaporitic unit (Fig. 3e), the Gaurdak Formation, up to 1000-1500 m in thickness, composed principally of alternating levels of anhydrite and salt. In the south and northwest of the ADB, the Upper Jurassic sequence terminates with carbonates. In the centre of the ADB, the Gaurdak Formation is often overlain by red clastic beds of the Karabil Formation (latest Jurassic to Early Cretaceous age), which were deposited in a lagoonal to alluvial environment (Ulmishek 2004).

The Lower Cretaceous clastics and carbonates were deposited in continental, lacustrine and shallow water conditions; the environment was predominantly marine during Aptian-Albian times. The Upper Cretaceous strata, in general marine, consist of sandy shales with subordinate development of sandstones and carbonates unconformably overlying the Lower Cretaceous deposits with some erosion on the basin margins. The maximum thickness of the mainly clastic Cretaceous deposits is c. 2300 m.

Paleogene deposits consist of limestone, dolomite, gypsum and sandstone. The Neogene clastic deposits are marine in the west and continental in the east; they overlie older sediments above an erosion surface.

More details on the ages, lithologies, facies and stratigraphic allocations of the Jurassic formations, as well as erosion periods and their location through the whole evolution, will be discussed below. These details directly impact calculation of the subsidence evolution of the ADB, which is one of the main aims of this study.

Methods and data

In order to characterize the evolution of the Amu Darya Basin (ADB) during the Late Palaeozoic and the Mesozoic at the basin scale, various kinds of data have been analysed. The first step is to provide an overview of the Palaeozoic basement structure on which the subsequent tectonic events will play, in order to try to distinguish the role of inherited structures and how they were reactivated. The bulk of the following data consists of depth-structure maps to different levels, isopach maps and cross-sections through the basin, supplemented by general geophysical and borehole data.

Methods

To know the respective position of structures and compare them at different times, all of the maps are georeferenced in the Arcgis ESRI system using a conformal projection (Projection World Mercator), which preserves angles but not distances. The maps and cross-sections are simplified and redrawn to highlight the Mesozoic subsidence evolution of the ADB. They are modified from Melikhov (2000, 2008, 2017), where more detailed maps and cross-sections are available.
The original maps and cross-sections were constructed by Melikhov (2000) on the basis of a large set of data. A compilation was made of existing maps at different scales. The compilation was controlled and enriched by well data (about 1200 wells mostly in Turkmenistan, reaching variable depths but few in the oldest units), seismic data (reflection CDP, Common Depth Point, and refraction) mainly from the 1980s and more recent deep seismic lines, as well as gravimetric models and other geophysical models for the deepest levels. Unfortunately, in Turkmenistan many boreholes did not recover samples; the stratigraphy has sometimes been determined by correlation of geophysical well logs. Another constraint for the construction of maps and cross-sections, at the basin scale at which they are drawn, is that the stratigraphic subdivisions chosen must be available for the entire area of the ADB. Thus, ages that are only well defined on the margins and not in the central part were not used.

Subsidence analysis with 2D backstripping of simplified cross-sections and drawing of 1D tectonic subsidence curves in the deepest parts of the ADB allow visualizing the evolution of the ADB through time and dating tectonic episodes. Backstripping removes the effect of sedimentary loading by progressively subtracting the isostatic and compaction effects of sedimentary layers from the top downwards (Steckler & Watts 1978). The remaining sediments are sequentially decompacted and depths are isostatically restored. The 2D flexural backstripping of the cross-sections is computed using Moscow University software, taking into account compaction of sediments, regional flexural isostasy and a palaeobathymetric model. For the 1D subsidence analysis, we use the software SUBSID (Brunet 1981) and associated lithology-based decompaction laws. Subsidence curves (total and tectonic subsidence for an air-filled basin) and the rates of tectonic subsidence are then drawn. The tectonic subsidence is obtained after subtracting the load-induced component (sediments and water) from the total basement subsidence (with sediments). It should reflect solely the tectonic or driving mechanisms of the subsidence of a basin. The characterization of periods of acceleration of the tectonic subsidence in the history of a basin allows elucidation of the timing of tectonic events. The resulting tectonic calendar is subsequently interpreted in context of the geodynamics of the area to identify the tectonic causes of these events.

Basement of the Amu Darya Basin

The basement of the ADB is mainly known from geophysical data: magnetic and gravimetric anomalies (Fig. 4), and deep seismic profiles, supplemented by some drilling on the margins of the ADB. The basement underlying the ADB is heterogenous. It consists of a mosaic of crustal blocks and slivers, of pieces of volcanic arcs accreted in the Carboniferous (e.g. Thomas *et al.* 1999a; Natal'in & Şengör 2005; described by Siehl 2015), locally of pre-Palaeozoic sediments intruded by granites or granodiorites as in the Central Karakum Arch (e.g. Seregin *et al.*, 1979; VNIGNI &

Beicip Franlab 1992) and of Palaeozoic sediments strongly tectonized and metamorphosed during the Variscan orogeny.
Crustal scale structural columns in several areas of the ADB and surroundings are presented by Natal'in & Sengör (2005). These authors identify Palaeozoic arc and forearc subunits from the characteristics of the crust derived from various geophysical data as well as boreholes reaching the basement in the areas with thinnest sedimentary cover. A compilation of geochronological ages (see map fig. 20 in Zanchetta *et al.* 2013) and characteristics of the basement intrusive and volcanic rocks reached by boreholes in the Turan Platform and northern Iran area completes Natal'in & Sengör's scheme (2005).

Geophysical anomalies. Magnetic and gravimetric anomalies have a dominantly NW-SE strike (e.g. Pavlenkova 1996; Natal'in & Şengör 2005), reflecting the main orientation of the structures of the Turan Platform, located between the two large bounding sutures zones: the Turkestan or South Tien Shan suture to the north and the Palaeo-Tethys suture zone to the south. Figure 4 displays magnetic (Emag2) and gravimetric (GRACE) anomalies in the ADB and Afghan-Tajik Basin. The Turkestan suture is WNW-ESE-oriented prior to joining the north-south-oriented Urals in the west (Fig. 1), although the two orthogonal collisional systems – the South Tien Shan and the Urals – are independent and of different ages (e.g. Alexeiev *et al.* 2009; Dolgopolova *et al.* 2016).
The NW-SE-oriented Palaeo-Tethys suture zone is more linear than the Turkestan suture. Between the two main sutures, the magnetic anomalies of the ADB (Fig. 4a) reveal a division of the basin into two areas with different characteristics. In the west (Central Karakum Arch area) the anomalies are not regularly organized while in the east, they have a clear NW-SE direction pinching out in the north. These latter linear anomalies are interpreted from boreholes to be caused by basic volcanic remnants of Carboniferous volcanic arcs (Ulmishek 2004; Natal'in & Sengör, 2005).
The western and eastern parts of the ADB are delimited by a medial area where Palaeozoic sub-basins exist but are not well known. In the northern part of the ADB, troughs are located along the N-S-trending Khiva-Murgab Lineament (KML Figs. 1, 4), often drawn displaced by the WNW-ESE-trending Central Ust Yurt and Repetek left lateral strike-slip faults (Khain *et al.* 1991; Clarke 1994; Ulmishek 2004). A shift in the anomalies appears in the Repetek area (Fig. 4a). In the southern part of the ADB, the Palaeozoic troughs and some anomalies are NW-SE inclined; troughs are fragmented as for example by the NNW-SSE Murgab Fault.
The strong negative gravity values in the basins (Fig. 4b) reflects the position of the sedimentary depocentres: the deepest ones are NW-SE-oriented for the Pre-Kopet-Dagh Foredeep and more E-W-oriented for the Obruchev and Afghan Tajik basins. Some smaller basins are also visible on the gravimetric map: the Assakeaudan, Daryalyk-Daudan, Karabekaul, North Mary, Rometan troughs for example and the Zaunguz, Kaahka and Beshkent depressions. Steps and highs appear with weak negative anomalies and belts with high positive anomalies.

Deep seismic data. Deep seismic profiles obtained using Deep Seismic Sounding technique (DSS) or continuous seismic profiles complete the basement database (Beliayevski *et al.* 1968). Prodehl & Mooney (2012) reviewed the history of deep seismic investigations in the USSR which used chemical explosions or peaceful nuclear explosions from the end of the 1960s through the 1980s. The ADB has been explored by a network of profiles; unfortunately, some remain to be published, such as the BAZALT profile (e.g. Morozov *et al.* 2006), which crosses the ADB from Kara Bogaz in the west to the centre of the basin in the area of Yelan and then runs NE-SW towards the NE Uzbekistan margin. The BAZALT profile has the potential to bring interesting new data on the crust underlying the ADB. Some other profiles were published with various kinds of reprocessing and interpretations, the crystalline basement being generally located deeper when reprocessing allowed identification of Palaeozoic sediments. Deep profiles provide data on the thicknesses and velocities of the crustal and sedimentary layers. They are not replicated here but their interpretation can be seen in the cited papers. Such profiles were usually linked with magnetic and gravimetric recordings; gravity models of thickness and densities are then often associated with the interpretation of the profiles. They allow

inferring regional faults, large intrusions and basement depth, which are necessary for locating the Palaeozoic rifts and drawing a depth-to-basement map.
The north-south Aral Kopet-Dagh profile goes through the Pre Kopet-Dagh Foredeep in the south, where 10 to 20 km of sediments are inferred, the Central Karakum Arch with less than 3 km, and to the north of the Karakum Arch, the Daryalyk-Daudan basin with nearly 10 km of sediments, of which more than 5 km comprises Palaeozoic to Triassic sediments (e.g. Slikin 1966; Ryaboy 1967; Yegorkin & Matushkin 1970; Babadzhanov & Zunnonov, 1998; Zakirov 2011; Sidorova & Golovko 2015). A crustal scale section, the Tien Shan geotraverse, running from the Black Sea to the Tien Shan (Beliayevsky *et al.* 1968; Kosminskaya *et al.* 1969) was constructed from DSS profiles. It displays thick sediments in the central part of the ADB and a Moho uplift, indicating a rift below the Bukhara Khiva zone, north of the Amu Darya Fault.
A series of profiles exists on the better studied northeastern margin of the ADB, such as the NE-SW Farab-Tamdybulak (Yegorkin & Matushkin 1970) and Karabekaul-Koytash (e.g. Abetov 1992) profiles. These profiles demonstrate the importance of the long NW-SE-oriented regional fault zones separating the steps: a northern fault (sometimes named the North Gissar Fault) between the Zirabulak Mountains and the Mubarek High, marking the north side of the Bukhara Step and also the northern boundary of the ADB, the Bukhara-Gissar or Uchbash-Karshi Flexure Fault Zone (UKFFZ) between the Bukhara and Chardzhou steps, and the Amu Darya Fault between the Chardzhou Step and the Karabekaul Trough. The Farab-Tamdybulak profile as well as more detailed studies and gravimetric models of the Bukhara Khiva area (e.g. Mordvintsev 2004) reveal the presence of the Kimerek or Karakul rift on the Chardzhou Step, limited to the north by the UKFFZ and to the south by the Alat Fault. The Karabekaul-Koytash profile is in fact the northern part of a profile running from Tedjen/Dushak in the south of the ADB near the Kopet-Dagh, to Karabekaul (Yegorkin & Matushkin 1970). The Dushak-Karabekaul profile (Yegorkin & Matushkin 1970), crossing the entire ADB, reveals the presence of several kilometres of pre-Mesozoic sediments in the centre of the basin, possibly of Permo-Triassic age or older, sometimes down to c. 15 km depth.
Another interesting profile is the WNW-ESE-oriented Farab-Babatag profile, running through the Chardzhou Step, the Beshkent Depression, the Southwestern Gissar to the Surkhandarya Depression (= deepest part of the Afghan-Tajik Basin) in the east (e.g. Pavlenkova 1996; Makarov *et al.* 2005). Under the Southwestern Gissar, the crust has been affected by Cenozoic compression, creating more complex structures. There, the average velocity is lower and the crust is thicker, reflected by a Moho depth greater than 50 km, compared to the central part of the Turan Platform in the west, where the Moho is a bit more than 40 km deep and the crustal thickness is 35-40 km (e.g. Pavlenkova 1996). A significant thickness of sediments is imaged below the Beshkent and Surkhandarya Depressions.

Uncertainties regarding age and depositional environment of the upper Middle-Upper Jurassic formations

Comparing the Jurassic series in the deepest, Turkmenistan portion of the ADB and on the northeast Uzbekistan margin where they are better known because they are shallower or even crop out in the Southwestern Gissar (Fig. 3; see also Mordvintsev *et al.* 2017 for more details) highlights disagreement in the literature about the ages of the end of carbonate deposition and of the beginning of the overlying Gaurdak Formation. This comparison also investigates the possible synchronous deposition of some formations as well as the environment and hence palaeobathymetry at the top of the series. As the subsidence calculations use these data, which have a direct impact on the tectonic subsidence evolution, they need to be further discussed.

Carbonate unit. The carbonate unit (or Kugitang sequence) is subdivided into two parts. The lower part extends from Middle Callovian to Early or Middle Oxfordian (Kandym and Mubarek Formations in Uzbekistan). The age of the end of the upper part is controversial, taking place sometime between the end of Oxfordian and the end of Kimmeridgian time. The limestones of the lower part of the carbonate unit are generally dense, fine-grained and bedded, often dark grey with beds of organo-clastic and algal limestones and bioherm build-ups in the upper member of the Mubarek Formation

(e.g. Abdullaev 1997, 2004; Evseeva 2015b). Their thickness is rather homogeneous and increases towards the centre of the basin with an increase in the depositional water-depth towards the top of the sequence (e.g. Evseeva 2015b). In the literature, the age of the boundary between lower and upper carbonates is often taken as the passage from Middle to Late Oxfordian. Nevertheless, Nugmanov (2010) uses the change of climate conditions between the Early and Middle Oxfordian to refine the age of the boundary between the Lower and Upper Kugitang carbonates, proposing an older age between the Early and Middle Oxfordian, based on ammonite affinity and the model of Cecca *et al.* (2005) in the Tethyan and Peri-Tethyan domains. On the basis of geochemical data and biogeographical distribution (mostly coral reefs) over a wide area, Cecca *et al.* (2005) propose a Late Callovian-Early Oxfordian cooling followed by a Middle Oxfordian warming, leading to greenhouse type conditions and accompanied by the change from cold to warm water (e.g. Martin-Garin *et al.* 2012). Nugmanov (2010) links the reversal of ammonite fauna in the Kugitang Mountain (in Southwestern Gissar, Fig. 1; Mesezhnikov 1988; Abdullaev 2004; Kim *et al.* 2007; Mitta & Besnosov 2007) to this climate change. Extensively-developed cold affinity boreal ammonites in the Lower Kugitang carbonates are replaced by fauna of warmer water affinity appearing in the carbonates of the Upper Kugitang sequence (thermophilic ammonites, colonial corals and rudists).

In comparison to the lower part of the carbonate unit, the upper part of the unit is much more variable in thickness and in facies, with carbonate build-ups in localized high positions and on the edges of the platform margin. On the Uzbekistan margin, three types of environments have been proposed according to lithological variations of this upper part (e.g. Abdullaev 2004; see Evseeva 2015b for an overview): (1) for the margins of the basin, limestones alternating with anhydrite and gypsum, deposited in a lagoonal environment (e.g. Abdullaev 2004) or open platform (Nugmanov 2010) in a back-reef position (Ulmishek 2004); (2) carbonate build-ups (Fig. 3d) at the rim of the shelf, where most of the hydrocarbon reservoirs are located, with important variations in thickness, and (3) a deeper basinal facies with thin dark shales or shaly limestones. The synchroneity of these environments is debated and linked to the problem of correlating horizons in the upper part of the carbonate unit in the northeastern margin of the ADB and also between this NE margin and the Murgab Basin. Indeed, several different correlations exist with variations in the name of the formations and in the nomenclature of the horizons identified with roman numbers (e.g. Abdullaev 2004; Melikhov 2000; Nugmanov 2010). The age assigned to the end of the carbonates is also highly variable: in Turkmenistan it is often placed near the end of the Oxfordian (e.g. Aliyev *et al.* 1983; VNIGNI & Beicip Franlab 1992; Melikhov 2000); or later, at the end of the Early Kimmeridgian in the ADB (e.g. Ulmishek 2004) or on the Uzbekistan margin (e.g. Khusanov 1984; Besnosov and Mitta 1995; Kim *et al.* 2007; Nugmanov 2010). In a set of Uzbekistan papers from IGIRNIGM (Khusanov 1995; Abdullaev & Mirkamalov 2001, 2006; Abdullaev 2004; Abdullaev *et al.* 2010; Evseeva 2015b, 2016), the end of the Kimmeridgian is even proposed for the end of the carbonates, on the basis of assemblages of ammonites, Scleractinia and foraminifers, but with no species that are restricted only to the Late Kimmeridgian.

Recent studies of the borehole Samantepe 53-1, in the Samantepe gas field (central southern part of the Chardzhou Step in Turkmenistan, to the east of Chardzhou city), provide more information on the Upper Jurassic carbonates in a reefal area. A detailed litho-stratigraphic column with well logging and interpretations is given for this interval; the carbonate unit in this borehole is c. 380 m thick (Zhang *et al.* 2010; Zheng *et al.* 2011, 2013; Wen *et al.* 2012; Wang *et al.* 2014b). Comprehensive sedimentary microfacies to facies interpretations are given as well as reservoir properties with environmental and diagenetic interpretations, based on thin sections, fluid inclusion analysis, carbon and oxygen isotopic data (isotope $\delta^{13}C$ and $\delta^{18}O$; Zheng *et al.* 2013), combined with petrological and other geochemical information. The authors make also hypotheses on the role of climate and sea-level changes (Zheng *et al.* 2013) and propose a sequence stratigraphy evolution (Xu *et al.* 2012; Wang *et al.* 2014b).

The carbon isotopic study in the Callovian-Oxfordian portion of the Samantepe 53-1 borehole reveals an Oxfordian $\delta^{13}C$ curve for the ADB, consistent with the global sea-level curve and comparable to relevant areas in Europe and China (Louis-Schmid *et al.* 2007; Zheng *et al.* 2013). Two positive carbon-isotope excursions are identified; the main one identified in open platform carbonates above

reefal carbonates is correlated to the end of the *plicatilis* Ammonite zone and the transition to the *transversarium* zone. The basal age of the *Gregoryceras* zone (last zone of the Middle Oxfordian) is 160.09 Ma (Gradstein *et al.* 2012; Ogg *et al.* 2012; Cohen *et al.* 2013, International chronostratigraphic chart updated in 2016) with a duration of 0.65 My (duration of ammonite zone estimated by study of astronomically forced sequences, Boulila *et al.* 2010). This dating seems to confirm the interpretation of Nugmanov (2010) of a Middle rather than Late Oxfordian age for the beginning of the upper carbonates. Above this approximately dated upper Middle Oxfordian horizon in the Samantepe 53-1 borehole lies c. 15 m of open platform limestones without reef facies. Then come c. 60 m of alternating carbonate and anhydrite beds, constituting a transition in a restricted platform area, below a layer marked as "lower anhydrite" (Wang *et al.* 2014b) of the Gaurdak Formation. As the carbonate strata may be condensed and the bathymetry may have increased, the duration of their deposition is unknown.

This transitional sequence is similar to the Gardarya Formation identified in the shallow platform area, behind the reefs, with thickness ranging from 60 to 200 m (Abdullaev *et al.* 2010). The Gardarya Formation corresponds to the lagoonal facies in the barrier reef model (e.g. Fortunatova 2007; Abdullaev *et al.* 2010; Evseeva 2015b) in which it is synchronous with reef building.

The sediments forming the top of the carbonate unit in the basinal area of the ADB are poorly known and studied, except in the deep northeast margin of the ADB in Uzbekistan. There, the basinal deposits terminate with the "black shales" of the Khodjaipak Formation (Akramkhodjaev *et al.* 1982), penetrated by a number of wells between isolated bioherms and near the reefs contouring the basin, and cropping out in the Tubegatan area of Southwestern Gissar (e.g. Besnosov and Mitta 1995; Abdullaev *et al.* 2010). Another outcrop exists to the southwest of Tubegatan, in the Gaurdak area in Turkmenistan (Dolitskaya *et al.* 1984; Besnozov and Mitta 1995) (see location of Tubegatan and Gaurdak in Fig. 1). The basinal facies is the third element of the barrier reef model (e.g. Fortunatova 2007; Abdullaev *et al.* 2010; Evseeva 2015b); this is synchronous with the barrier reef facies (Urtabulak Formation), as grading is observed between the carbonate build-ups and the basin shales, and is also synchronous with the lagoonal facies. Besnosov & Mitta (1995) and Mitta & Besnosov (2007) studied the thin layer (c. 10-17 m) of the Khodjaipak Formation, especially in outcrops. This formation is characterized by dark colours and a high radioactivity and is often known as the "Gamma active pack"; this high activity is due to the high content of shale and tar (e.g. Abdullaev and Mirkamalov 2001). Before the deposition of gypsum or anhydrite in the overlying evaporites, the Khodjaipak Formation ends with a thin layer of c. 1-2 m of detrital and algal limestone with oncoliths (e.g. Besnosov & Mitta 1995; Nugmanov 2010; Evseeva 2015b). This level is similar to the Kushab Formation ending the carbonate unit above or near the reefal carbonates (e.g. Abdullaev *et al.* 2010; Evseeva 2015b).

From the northeast margin of the ADB, Besnosov & Mitta (1995) extend the location of the black shales southwards in the eastern part of the ADB in eastern Turkmenistan. A c. 100 m thick layer of marine shales with an organic matter content of 0.3-0.7% is discussed by VNIGNI & Beicip Franlab (1992) and Ulmishek (2004) describes Oxfordian marine black shales and marls, known also as the "radioactive bed", but the location is not specified in these two publications. Belenitskaya (1999, 2000) shows a cross-section of the ADB through the Bagadzha Step to Sandykachi area (North Karabil Trough) where a thin layer of carbonaceous shales is drawn between the reefal build-ups and probably hypothesized in the central part of ADB. The basinal facies occurs at great depths in the sedimentary column, in areas away from the reefs; as potential reservoir structures are absent, there are few or no boreholes. Therefore, references in the literature are scarce for the Turkmenistan part of the ADB and the distribution of the black shales is not well defined, either over a large area in the deep basin, or in a more restricted area near the reefs and passing to dark clayey limestones in the basin. Nevertheless, this basinal facies is important for its source rock properties (e.g. Klett *et al.* 2006, 2012), and in our study to characterize the depositional environment in the basin.

Upper Jurassic. The carbonate unit is covered by the sealing evaporites of the Gaurdak Formation. Many papers deal with the evaporite unit (e.g. Khudaykuleyev, 1986; Gavrilcheva & Pashaev 1993; Pashayev *et al.* 1993; Belenitskaya 1999, 2013; Abdullaev & Mirkamalov 2006; Darman 2010;

Wynn *et al.* 2016), which is often divided into five layers: lower anhydrite, lower salt, middle anhydrite, upper salt, upper anhydrite, but some levels may not exist in specific parts of the ADB (e.g. Khudaykuleyev, 1986; Gavrilcheva & Pashaev 1993). The estimates for the age of the base of the evaporites ranges from the Latest Oxfordian-Early Kimmeridgian to the Early Tithonian. The lowest layer (lower anhydrite) correlates in the central part of the basin with a transitional level between the carbonate and the evaporite units. This c. 80-100 m thick transitional level is composed of carbonate layers (dolomites) mixed with anhydrite and is named the carbonate-evaporite or sulfate-carbonate level, often considered to be latest Oxfordian-Early Kimmeridgian in age (e.g. Khudaykuleyev, 1986; VNIGNI & Beicip Franlab 1992; Melikhov 2000). The boundary between the carbonate and evaporite units is still more difficult to fix; as most wells were not cored, well-logs are almost the only data source. Even when cores exist, fossils are almost absent; when present, they are often from species that cover a wide age range.

The salt is present only in the central part of the basin and thins towards high areas and the ADB margins. There, the Gaurdak Formation is composed of anhydrite or gypsum or even replaced by dolomites or limestones (southern Pre-Kopet-Dagh Foredeep) (e.g. Melikhov 2000).

The boundary between the Jurassic and the Cretaceous is not easily recognized because there are few fossils, the formations often being continental or deposited in shallow water with some intercalations of gypsum or anhydrite. Different opinions exist on the age of the Karabil Formation, which conformably overlies the evaporitic succession of the Gaurdak Formation (Ulmishek 2004) in the centre of the ADB. According to different authors, the Jurassic-Cretaceous boundary is placed either at the base, middle or top of the Karabil Formation. For example, the variegated red clastic Karabil series (up to 340 m) are of Tithonian-Valanginian age (VNIGNI & Beicip Franlab 1992) or Late Tithonian to Early Berriasian (Ulmishek 2004). Alternatively, a poorly constrained Berriasian age is proposed, based on a few ostracods and crustaceans in terrestrial and lagoonal deposits of the Gissar (Kim *et al.* 2007).

Maps and cross-sections

Depth-structure maps

The depth-to-basement structure map presented in Figure 5 displays the basement map of Melikhov (2000) for western Uzbekistan and all the areas situated to the south of the Turkmenistan-Uzbekistan border. For most of the Bukhara-Khiva area, it shows a simplified basement map constructed from Uzbek data (O. Mordvintsev, in Babadzhanov 2008), indicating several Palaeozoic depocentres which were not present on the original map (Melikhov, 2000). Some of these correspond to relative topographic highs in the present sedimentary successions, either with less subsidence during the later evolution or inverted before the Mesozoic.

The depth-to-basement map integrates tectonically-driven subsidence, driven by both extensional and compressional events which occurred since the Late Palaeozoic until the Present. It corresponds to the total thickness of sediments deposited since about the Carboniferous, reduced by some periods of erosion, mainly on the basin margins. The largest depths, reaching more than 15 km, are observed in several troughs: in two NW-SE-oriented areas of the Pre-Kopet-Dagh Foredeep, in the NS Kalandar and the NW-SE-oriented Mary troughs in the very central part of the Amu Darya Basin (ADB). Other large thicknesses are present in the north within the NS-oriented Ilim Trough and towards the south and east, in the North Badkhyz, North Karabil and Obruchev troughs, all more or less NW-SE-oriented. These troughs together comprise a single larger depocentre, approximately WNW-ESE. Some faults control either the formation or the subsequent, possibly strike-slip, evolution of troughs as they bound large differences in depth to basement. This is the case, for example, of the Khiva Murgab Lineament, which forms an abrupt eastern boundary of the Ilim and Kalandar troughs.

In addition to the depth-to-basement map, four other depth-structure maps are shown (modified after Melikhov 2000, 2017): the base of the Jurassic (Fig. 6a), the top of the upper Middle-Upper Jurassic carbonates (Fig. 6b), the base of the Cretaceous (Fig. 6c) and the top of the Paleocene (Fig. 6d).

These isodepth maps provide an overview of the shape of the basin and give an idea of the progressive influence of the tectonic events that are superimposed to shape the ADB. Accordingly, we look first to the more recent depth-structure map to distinguish the influence of the recent compressional deformation in order to better recognize the older events, the recent subsidence being added to the depths of the surfaces of the older levels.

The map of depth to the top of the Paleocene (Fig. 6d) indicates the influence of Cenozoic compression. We observe two depocentres with more subsidence: a NW-SE orientated basin near the Kopet-Dagh and an ENE-WSW-oriented sub-basin in the southeast of the ADB. The Cenozoic subsidence of the Pre-Kopet-Dagh Foredeep occurs in a foreland flexural basin driven by compression of Arabia against the Iranian blocks and the uplift of the Kopet-Dagh with thrusting towards the ADB (e.g. Lybérys & Manby 1999; Thomas *et al.* 1999b; Smit *et al.* 2013; Robert *et al.* 2014). The southeast basin starts from the North-Badkhyz Trough, goes through the North-Karabil Trough and east of the Obruchev Trough to join the Afghan-Tajik Basin, where probably much more than 10 km of subsidence has occurred since the Neogene (Nikolaev 2002). This subsidence also developed in a flexural basin context due to regional compression and hence thrusting and topographic growth; however, on the eastern side of the ADB, it is the India-Pamir collision that induced NW compression. The WNW-ESE-oriented faults (Alburz-Mormul, Andarab) of the southeastern margin are clearly visible in the topography and are active in this interval.

The border and change of orientation between the two main Cenozoic sub-basins occur in the middle of the ADB, south of the roughly NS-oriented boundary between the two halves of the ADB (i.e. the Khiva-Murgab Lineament and the series of NS then NW-SE Palaeozoic sub-basins). This medial area is also marked by a slightly larger amount of subsidence in comparison to lower subsidence in the east (Bagadzha Step, Uchadzhi Arch) and in the west (Central Karakum Arch). Some subsidence also occurred to the north (Daryalyk-Daudan Trough) and west of the Central Karakum Arch (Upper Uzboy and Uchtagan troughs).

An important feature of the depth to the top of the Paleocene map is the WNW-ESE-oriented trace of the Palaeo-Amu Darya River, which incised down to Cretaceous strata. It partly follows the track of the Repetek Fault and, in the east, of the Repetek-Kelif zone of uplifts (see location on Fig. 1). The Palaeo-Amu Darya River drained westwards during the Pliocene towards the South Caspian Sea where a delta developed until probably the Pleistocene, when a very recent regional uplift diverted the Amu Darya River towards the Aral Sea to the north (e.g. Thomas *et al.* 1999b, Torres 2007).

The depth-structure map to the base of the Cretaceous (Fig. 6c) more precisely represents a Berriasian surface, as it corresponds to the top of possibly Berriasian aged Karabil Formation, although it is grouped with the Upper Jurassic in this paper and in much of the literature. The map displays a smoothed shape of the ADB, quite similar to the top of the Paleocene, suggesting that no important tectonic event occurred during the Cretaceous. The Upper Jurassic is absent from the Central Karakum Arch and western areas and also from the southern margin. The Badkhyz-Karabil and Mainana steps as well as the North Afghan High were positive structural elements during the Late Jurassic (Klett *et al.* 2006), with no deposition of the Jurassic carbonate series (Klett *et al.* 2006, Wang *et al.* 2014a) or the evaporite series. However, a pre-Valanginian erosional event also occurs on the Afghan margin (Klett *et al.* 2006).

The depth-structure map of the top of the upper Middle-Upper Jurassic carbonates (Fig. 6b) and equivalents (or the base of the evaporitic Gaurdak Formation) indicates a change in the shape of the ADB and the orientation of the depocentres in the east. The ADB is more uniformly a WNW-ESE-oriented basin, as usually known. The deepest parts are the Pre-Kopet-Dagh Foredeep, as discussed above, and the Obruchev Trough, which is much wider and extends westwards in comparison to the younger structure maps. This overall WNW-ESE-oriented shape of the ADB is complicated by an indentation towards the north, in the middle of the ADB, corresponding to the Ilim Trough and the Zaunguz Depression. This depocentre lies between two shallower areas: the Central Karakum Arch and western areas of the ADB in the west, and most of the Bukhara and Chardzhou steps in the east. Other areas which have greater depths in comparison to the previous maps include the Beshkent Depression, the western part of the Obruchev and Karabekaul troughs and the North Mary Trough.

The general WNW-ESE orientation of the ADB is even better defined in the depth-structure map to the base of the Jurassic (Fig. 6a). This map includes the cumulative Mesozoic (since the end of the Triassic) and Cenozoic subsidence following the Eo-Cimmerian unconformity. Two regions with large subsidence due to Cenozoic compression are still visible: the Kopet-Dagh Foredeep and the eastern prolongation of the ADB (east of the Obruchev Trough) into the Afghan Tajik Basin. Nevertheless, the ENE-WSW-oriented Cenozoic depocentre is no longer identifiable on the southeastern margin, as it is counterbalanced by the absence of Upper Jurassic sediments on this margin, which is in a high structural position. The western part of the Obruchev Trough, the North Mary Trough, as well as a NE-SW area joining the Kaahka Depression to the Khiva Murgab line are more noticeable.
On the two maps of depths to Jurassic surfaces, the Repetek-Kelif zone of uplifts is visible as it is bounded to the north by the Repetek Fault, which is probably of Jurassic age or older (e.g. Ulmishek 2004), later reactivated as a strike-slip fault (e.g. Otto 1997, Ulmishek 2004) along which the strata are uplifted. The sub-salt Jurassic sediments form a narrow arch with an amplitude of 250 to 300 m and dip angles of 6 to 7° (Clarke 1988).

Isopach maps

Isopach maps identify sub-basins with the greatest thicknesses. They do not necessarily indicate all the areas which had significant subsidence during the time interval mapped because areas with increasing palaeobathymetric depth and thin sediments will not be seen. Conversely, an initially deep basin can be filled by sediments without having a large tectonic subsidence during the time represented by the map. Accordingly, to illuminate the tectonic subsidence evolution, it is necessary to consider the entire set of isopach maps (Fig. 7) showing the evolution of the position and orientation of the depocentres, as well as a combination of thicknesses with corrections for palaeobathymetry through tectonic subsidence analysis.
The isopach map of the Lower-Middle Jurassic siliciclastics (Fig. 7a) includes the sediments between the Triassic-base of Jurassic regional unconformity and the end of the Bathonian. The depocentres occur in two NW-SE elongated areas. The main one runs from the Ilim Trough to the Karabekaul Trough with two maxima reaching more than 2000 m in the east, corresponding to the area around the Repetek-Kelif zone of uplifts and to a NE-SW-oriented depocentre in the Beshkent Depression. Another depocentre begins towards the Afghan Tajik Basin in the extreme east of the map area. The second main depocentre of the ADB is situated in the western part of the Pre-Kopet-Dagh Foredeep, joining an important area of subsidence towards the west near the South Caspian Basin. Although the depocentre is not drawn over the present Kopet-Dagh Range due to a lack of data, this was a time of important subsidence in the Kopet-Dagh Basin. During this period, the Kopet-Dagh Basin was the southeastern continuation of the South Caspian Basin (Brunet *et al.* 2007, 2010; Taheri *et al.* 2009). The deposits are thin on the Central Karakum Arch as well as on the E-W elongated southern margin of the ADB.
The isopach map of the upper Middle-Upper Jurassic carbonates (Fig. 7b) reveals a broader area of depocentres but retains the same NW-SE orientation. The Lower Callovian deposits, which complete the siliciclastic unit with a progressive enrichment in carbonates, are grouped in this map with the carbonate unit. The age of the upper boundary of the unit is controversial, as discussed above, ranging between the end of the Oxfordian and the end of the Kimmeridgian. The maximum thickness is located to the east of the Obruchev Trough, to the south of the depocentre of the previous map, but the central depocentre, between the Ilim Trough and the Zaunguz Depression, has the same location as during the Early-Middle Jurassic. The Pre-Kopet-Dagh depocentre borders the thick Kopet-Dagh Basin; active subsidence there continuing during the Callovian and partly during the Oxfordian in the west (Shahidi 2008; Brunet *et al.* 2010). The hydrocarbon reservoirs hosted by this carbonate series (reefal build-ups and bioherms) occur mainly in the area covered by the sealing salt (a dashed line indicates the boundary of salt in the overlying Upper Jurassic Gaurdak Formation). The two largest southern fields are Yashlar and Iolotan-Osman. The South Iolotan (Yoloten), Osman, and Minara gas fields comprise a cluster renamed as the Galkynysh gas field, which it is the second largest in the

world. The reservoirs of Upper Jurassic carbonates are found at depth ranging from 3.9 to 5.1 kilometres.
The depositional area of the Upper Jurassic Gaurdak Formation to the Karabil Formation and its equivalents during the Berriasian displays a simple pattern (Fig. 7c). A single WNW-ESE-oriented depocentre runs from the middle of the ADB, where it is located on the northern part of the North Mary Trough, towards the east, between the Karabekaul and Obruchev troughs, roughly along the Repetek-Kelif zone, quite near the depocentre of the Lower-Middle Jurassic siliciclastic series (Fig. 7a). The bulk of the deposition shown on this map is comprised of up to c. 1500 m of evaporites of the Upper Jurassic Gaurdak Formation and lateral equivalents; the overlying upper Tithonian carbonates are thin and the Karabil Berriasian series have a maximum thickness of c. 300 m. The salt disappears in the west, where it is replaced by anhydrites or gypsum, as well as on the southern margin. The simple geometry of the isopachs suggests the Late Jurassic filling of a depression created in earlier Jurassic times.
The isopach maps for the beginning of the Lower Cretaceous (Berriasian or Valanginian to Lower Barremian) and of the Upper Barremian-Aptian (Fig. 7d-e) only reveal an important depocentre in the area of the Kopet-Dagh Basin and Pre-Kopet-Dagh Foredeep. The rest of the ADB presents only a thin layer progressively thickening towards the southwest; no active event can be discerned at this time. The NW-SE-oriented contour of Hauterivian salt accumulation (Fig. 7d), laterally equivalent to the clastic productive Shatlyk Formation (Pashayev *et al.* 1993), shows an area which was probably the deepest in the ADB, open towards the eastern Afghan-Tajik Basin; this salt layer is interpreted as resulting from the reprecipitation of salt coming from the salt-bearing Gaurdak Formation on the northeastern margin (Pashayev *et al.* 1993). A Barremian extensional event that is observed in northern Iran (in Alborz and Kopet-Dagh, Shahidi 2008; Brunet *et al.* 2010) is not identifiable in the central part of the ADB from the isopachs maps. The Albian-Cenomanian map (Fig. 7f) displays a depocentre in the north central part of the ADB, mainly around the Zaunguz Depression, widening in a NW-SE direction from the Beurdeshik Step to the Karabekaul Trough and towards the east. It corresponds to a reactivation of subsidence and probably to a new extensional event. During the Turonian-Maastrichtian (Fig. 7g), thicknesses are greater in the eastern half of the ADB with an E-W orientation, and in two small NE-SW depocentres in the area of the Kaahka Depression and to the southeast of it, crossing the Iranian border.
To complete the stratigraphic succession, the basin geometries depicted on three maps of the Cenozoic (Paleocene, Eocene-Oligocene and Neogene, Fig. 7g-i) mainly reflect the influence of Cenozoic compression; flexural sub-basins are NW-SE-oriented near the Kopet-Dagh Range and ENE-WSW-oriented in the southeast, near the Afghanistan border. A shallow depocentre developed in the medial area of the ADB (Khiva-Murgab Trough), localized to the north (Balkui Trough and north of the Zaungunz Depression) during the Neogene (Fig. 7i).

Cross-sections of the ADB

Some attempts at palaeo-reconstruction along cross-sections appear in publications (e.g. Babayev 1976; Nie *et al.* 2013b); however, these publications neglect or only partially account for compaction, regional flexure and palaeobathymetry. In this study, a set of three general cross-sections from the literature are 2D backstripped, helping to visualize the general evolution of the ADB through time (Fig. 8).
The first NE-SW cross-section is the one most frequently displayed in publications (e.g. Dikenshteyn *et al.* 1977; Bakirov 1979; Maksimov 1987; VNIGNI & Beicip Franlab 1992; Thomas *et al.* 1999a; Isaksen & Khalylov 2007; Xu 2009; Knepel 2010), about which different hypotheses exist on the age of the lowest and thickest level: most of the authors suggest various Palaeozoic to Triassic ages, or even Late Triassic to Early Jurassic for Brookfield & Hashmat (2001, after Knyazev & Mavyyev 1974). As Carboniferous strata were drilled in the Daryalyk-Daudan Trough, our preferred interpretation is a Carboniferous to Triassic age, but the proportion of Carboniferous-Lower Permian compared to Upper Permian-Triassic is impossible to know. The data of cross-sections 2 and 3 are modified from VNIGNI & Beicip Franlab (1992). Some Palaeozoic strata are missing in the oldest

publications and do not account for the recent Uzbek data on the Palaeozoic, for example, below the Chardzhou Step in cross-sections 1 and 3.

2D backstripping is applied to these cross-sections assuming a maximum palaeobathymetry of 200 m at the end of the deposition of the Jurassic carbonates. The ADB is taken to be filled and in a continental environment after the deposition of the evaporites. A water depth of c. 150 m is restored at the end of the Early Cretaceous. Layers are smoothed for the backstripping computations in the vicinity of the Repetek-Kelif zone of uplifts. On the three cross-sections, the importance of the oldest Palaeozoic-Triassic level is evident; it corresponds to the initial event of the ADB evolution. Considering the size and the often asymmetrical geometry of the thick sub-basins such as the Khiva-Murgab Trough on cross-section 3 (Fig. 8d), we relate this event to extension associated in the subsidence models to thinning of crust and lithospheric mantle. The Lower-Middle Jurassic succession also appears, to a lesser extent, to have a variable thickness, implying that another tectonic event shaped the ADB. During the end of the Middle to Late Jurassic, the paleobathymetry of the ADB increases in its middle part and is shallow towards its margins, including towards the Kopet-Dagh (south of cross-section 1, Fig. 8b), where Jurassic deposits are nevertheless thick, due to the Middle Jurassic extensional event (Brunet *et al.* 2010). The area of Late Jurassic relatively deep paleobathymetry is then filled by the Gaurdak evaporites during the post-rift thermal subsidence of the basin. In the southern part of cross-section 2 (Fig. 8c), the Badkhyz-Karabil and Mainana steps are in a high position during the Late Jurassic with neither carbonates nor evaporites deposited. In the north of the same cross-section 2, the Uchadzhi Arch became a high only from the Early Cretaceous onwards. During Middle-Late Jurassic, it was part of the basin as demonstrated by boreholes which recover deep water carbonates rather than shallow water reefal carbonates as expected in this hydrocarbon potential structure, now in a high position (Melikhov 2000).

On all the cross-sections, the Cretaceous layers have a smooth geometry indicating an absence of any important local tectonic events and a small magnitude, long wave-length subsidence (thermal post-rift possibly supplemented by a mantle influence or far-field deformation). Even the areas previously in high positions are covered by thick Cretaceous series, such as at the Karakum Arch (west of cross-section 3) and the northeastern margin of the ADB (north of cross-sections 1 and 2), deposited when the Cretaceous sea reached the north of the ADB in the Kyzylkum area in the Aptian (e.g. Thomas *et al.* 1999a; McCann 2016b). Finally, the Cenozoic succession displays long wavelength thickening in the east, near the Gissar (eastern part of cross-section 3) and particularly in the south, near the Kopet-Dagh (southern part of cross-section 1 shows the thickening trend although the section stops before the thickest area) and Afghanistan (south of cross-section 2 in the Kalaymor Trough), suggesting subsidence due to compression.

Six more detailed cross-sections (Fig. 9) depict the variations in thicknesses of the main sub-basins of the ADB and its margins. They have not been backstripped as we could only recently access these cross-sections, after the end of our DARIUS project. The stratigraphic levels, with indications of the location of boreholes that helped in their construction, are grouped in colours to cover the same time span as the isopach maps presented in Figure 7. On the edges of cross-sections which extend into Iran or Afghanistan, some parts of the Jurassic or Cretaceous are unconstrained, as this data is sparser than elsewhere. A full version of these 6 cross-sections, with more stratigraphic levels, as well as some other cross-sections, can be found in Melikhov's work (2000).

The important variations in thickness of the Carboniferous-Triassic level emphasize the major tectonic events that influenced the formation of the ADB. The Lower-Middle Jurassic siliciclastic layer also shows variations in thickness, but the base of the Jurassic drawn on the sections is often uncertain as it is hypothesized from very few available seismic data, and it may be deeper in some areas. In general, the Cretaceous has few rapid thickness variations even on the Central Karakum Arch. The location and orientation of Cenozoic depocentres is linked to the areas influenced by the collision affecting the Kopet-Dagh and the Pamir.

Cross-section 4 (Fig. 9) is oriented N-S through the three main features of the western half of the ADB: the Daryalyk-Daudan Trough to the north, the Central Karakum Arch and the Pre-Kopet-Dagh Foredeep in the south. The depth of the basement and the base of the Jurassic are derived from geophysical data acquired along the Aral-Kopet-Dagh deep seismic profile, located near cross-

section 4. The Daryalyk-Daudan Trough is a thick Palaeozoic sub-basin penetrated by some wells where Middle Carboniferous strata as well as Lower Permian salt were recognized (Melikhov 2000). It is the only Palaeozic sub-basin of the ADB where a boundary between the Upper-Permian-Triassic and the Carboniferous-Lower Permian layers can be drawn. The Intermediate Complex is not divided in the other sections of the study. The area of the Central Karakum Arch had little subsidence during the Jurassic, but was no longer identified as a high during the Cretaceous when the ADB as a whole was subsiding. The Pre-Kopet-Dagh Foredeep shows the superimposition, on an older trough, of the Cenozoic foredeep of the Kopet-Dagh Range which gives its name to the sub-basin. The foredeep sub-basin, formed due to compression-driven subsidence and filled with coarse clastic sediments (e.g. Thomas *et al.* 1999b), is underlain by an important Palaeozoic rift. The subsidence was also active during the Middle Jurassic and Early Cretaceous towards the Kopet-Dagh Basin, which developed to the south and west in continuity with the South Caspian Basin (Brunet *et al.* 2007, 2010; Taheri *et al.* 2009). The main sedimentation in the foredeep occurs in the Upper Eocene (as seen from the original cross-section by Melikhov 2000) and Pliocene-Quaternary strata, during the periods of main shortening and Kopet-Dagh uplift (e.g. Lybérys & Manby 1999; Thomas *et al.* 1999b). The Pliocene incision of the Palaeo-Amu Darya River occurred on the southern slope of the Karakum Arch (Bakhardok Slope) after the westwards retreat of the sea from the western part of the ADB. Erosion incised to the top of the Cretaceous and the valley was subsequently filled by Quaternary sediments.

Cross-section 5 (Fig. 9) follows, in places, close to the backstripped cross-section 1 (Fig. 8b). It is the classical representative section of the ADB, perpendicular to the main NW-SE-oriented northeastern margin. It illustrates, as does cross-section 6, the Repetek-Kelif zone of layers uplifted along a deep fault, as well as the Palaeo-Amu Darya River incision. A main difference compared to similar profiles in the literature is the presence here of small Palaeozoic-Triassic sub-basins below the Chardzhou Step and a broader and thicker sub-basin below the Bagadzha Step.

Cross-section 6 (Fig. 9) cuts the ADB diagonally from the northwest in the central Balkui Trough to the deep central part of the Murgab Depression. The southern part of the section crosses, almost perpendicularly, the NE-SW-oriented Neogene-Quaternary depocentre (cf. Fig. 6d and 7i), showing the influence of the Pamir collision. The northwestern part of the section shows subsidence in the Balkui Trough (Fig. 7i) during the same time interval.

Cross-section 7 (Fig. 9) runs along the northeastern margin of the ADB from the Sultan Sandzhar Arch, in the northwest, where it is underlain by an inverted thick Palaeozoic basin, to the south of the Southwestern Gissar, where it crosses the deep, but presently narrow, link between the ADB and Afghan Tajik Basin and its important Neogene depocentre.

Cross-sections 8 and 9 (Fig. 9) are E-W-oriented and cut the ADB in its full, largest extent. These follow the system of Palaeozoic grabens situated either in the eastern half of the ADB or in the south, the northern part of the Pre-Kopet-Dagh Foredeep, then the North Badkhyz and North Karabil troughs. Upper Jurassic salt clearly pinches out westwards on the slopes of the Central Karakum Arch. Cross-section 9 depicts the Lower Cretaceous thickening towards the west, near the South Caspian Basin and the Kopet-Dagh Basin; these basins have a large amount of subsidence at this time. The Neogene-Quaternary is thick across this entire cross-section, which lies within the southern part of the ADB that was affected by Cenozoic compression and flexural basins formation. The wide Neogene-Quaternary depocentre in the middle of cross-section 8 corresponds mainly to the filling of the Palaeo-Amu Darya River incision. This portion of the cross-section runs parallel to and near the Repetek-Kelif zone. The eastern end of this cross-section reaches the western part of the huge Neogene depocentre of the Afghan-Tajik Basin.

Except for cross-section 7 in the easternmost portion of the ADB, no N-S-oriented cross-section traversing the deepest central part of the Obruchev Trough is depicted in the literature. This is probably because few or no deep wells exist in this area due to both the great sedimentary thicknesses and because it was deposited in a deep basin environment during the Jurassic, with less reefs and potential hydrocarbon reservoirs to explore. However, it is one of the most interesting part of the ADB for the subsidence evolution. Although the deep central Kalandar Trough is another important area for unravelling the ADB evolution and for understanding the influence of the medial roughly north-south sub-basins, few data are available.

Discussion

Palaeozoic-Triassic troughs

The greatest depths to basement (Fig. 5) are more than 15 km in the Amu Darya Basin (ADB) and often correspond to the presence of underlying Palaeozoic-Triassic troughs; in some places, the total subsidence is also large to the south of the ADB due to Cenozoic collisional processes. Other Palaeozoic-Triassic troughs exist in shallower areas that have not been subjected to strong Mesozoic reactivation or Cenozoic flexure. All these troughs are generally interpreted as rifts (e.g. Thomas *et al.* 1999a; Clarke 1988; Melikhov 2000; Ulmishek 2004). Their base (the basement) is not reached by boreholes except on the Uzbekistan northeast margin (Babadzhanov & Abdullaev 2009) and even the upper part of their infill, the Intermediate Complex, is not drilled in the central deep part of the ADB. Thus, they are not all well identified in terms of their ages, exact locations and orientations. This is why it is difficult to draw a reliable thickness map of their infill over the entire ADB, especially in the deepest, central part. Nevertheless, some maps based on geophysical data were published, for example by Babayev (1976), with depocentres slightly exceeding 5 km of Upper Palaeozoic-Triassic sediments or by Thomas *et al.* (1999a), with thicknesses of over 10 km of Upper Permian-Triassic strata. The great difference in the thicknesses is probably related to how different authors have interpreted Carboniferous sediments at the base of the troughs, recognized by boreholes in the Daryalyk-Daudan Trough, north of the Karakum High. Some authors consider the entire infill to be of Permian-Triassic age. The c. 3-8 km thick Intermediate Complex comprises four layers of slightly metamorphosed rocks (Melikhov 2000): the Lower-Middle Carboniferous (clastics, carbonates, volcanics), Upper Carboniferous-Lower Permian (tuffaceous clastics and effusive rocks), Upper Permian-Lower Triassic (continental clastics and effusive rocks), and Middle-Upper Triassic (tuffaceous clastics, predominantly marine) strata with pre-Upper Permian and pre-Jurassic erosional levels. The lowest Carboniferous units are mainly known from the Daryalyk-Daudan Trough but this differentiation is not possible in the central part of the ADB where the Upper Permian-Lower Triassic (c. 1.5-2 km) is reputed to be thicker than the Carboniferous deposits (Melikhov 2000). The Middle-Upper Triassic terrigenous-tuffogenic complex (c. 1-2 km) is the most widespread in the south of the ADB (Badkhyz-Karabil region and northern Afghanistan); it was uplifted synchronously with the inversion of the Bande Turkestan rift during the Eo-Cimmerian collision.

The N-S to NNW-SSE central rift, including the Khiva Murgab Trough, is part of the longer c. 1000 km Aral-Murgab rift system (Khain *et al.* 1991; Clarke 1994; Ulmishek 2004), with a width of 40-70 km in the north to 100-120 km in the south (Melikhov 2000). It has an asymmetrical profile (see schematic section in Clarke 1994) as seen from the basement depth map (Fig. 5) and looks more like a half graben, bounded on its abrupt eastern side by a substantially vertical fault (Khiva-Murgab Lineament) and by a more gentle slope towards the western Beurdeshik Step.

The Priamudarya system (paleorift system of Abidov *et al.* 1996) lies on the northeastern margin of the ADB. It consists of the Beshkent Depression, Kyzylkum Trough or Karakul rift, south of the Bukhara-Gissar or Uchbash-Karshi Flexure Fault Zone and other smaller troughs; the Karabekaul Trough is sometimes considered as belonging to this system. A section of the Karakul rift is named the Kimerek graben or rift, well expressed as a half graben by the thicknesses of Jurassic sediments (see Mordvintsev *et al.* 2017 and references therein). It was already active with a much larger extent during the Palaeozoic. It likely continues southeastward to the Beshkent Depression, and possibly corresponds to a continuation of the South Gissar rift recognized in the Gissar (e.g. Brookfied 2000; Konopelko *et al.* 2016). The existence of a rift below the Chardzhou Step was discussed in several papers (e.g. Abidov *et al.* 1996; Mordvintsev 2004; Babadzhanov 2005; Babadzhanov & Abdullaev 2009; Radjabov 2009; Troitskiy 2012; Abetov *et al.* 2015). The area of the rift is characterized by an extended, thinned crust having different characteristics from the surrounding crust (seismologically more transparent, fewer intrusions, and overlain by less metamorphosed sediments) (Abetov *et al.* 2015). Near the southern edge of the Farab-Tamdybulak DSS profile (Yegorkin & Matushkin 1970),

the Alat Fault marks the southern border of the Moho uplift corresponding to the Karakul rift, which was more active in the Jurassic.
A Palaeozoic rift underlies the Pre Kopet-Dagh basin, which was initially known only as a foredeep of the Cenozoic Kopet-Dagh Mountains. Using a model combining gravity, topography, heat flow and geoid data, Motavalli Anbaran *et al.* (2011) show a Moho uplifted to 38 km, indicating more crustal thinning than in previous interpretations of the Aral-Kopet-Dagh DSS profile (e.g. Yegorkin & Matushkin 1970), where it was about 45 km deep.
The remaining major Palaeozoic-Triassic troughs lie in the central-southern part of the ADB and are not well defined. To the south, the NW-SE-oriented North Badkhyz, North Karabil, and Dauletabad troughs comprise the E-W-trending Sandykachi system. In the centre of the ADB, between the Repetek Kelif zone and the Yashlar to Andkhoy zones of uplifts, the North Mary Trough and the Obruchev Trough open towards the Afghan-Tajik Basin in the east; the Obruchev Trough lies slightly to the south of the Jurassic depocentres (Fig. 7a-c).

Northeastern part of the Amu Darya Basin

The central part of the ADB is poorly known but its northeastern part (Uzbekistan margin and right bank of the Amu Darya River in Turkmenistan) has been better studied because of its hydrocarbon reserves and potential. As this area is located near the main Jurassic depocentres of the ADB, examining this region may help understand the evolution of the basin during this period. A compilation of the main structures of this northeastern part of the ADB, summarized by a cross-section and some recent seismic lines (Figs 10-11), relates the formation of the Early-Middle Jurassic depocentre to the location and directions of the main inherited or newly formed structural features. This analysis also helps to explain the subsequent Late Jurassic palaeogeographic evolution.
A composite map (Fig. 10a) displays the main faults compiled from several studies of different parts of the margin (Blackbourn 2008; Melikhov 2008, 2017; Lu *et al.* 2013; Mordvintsev 2015; Mordvintsev *et al.* 2017; Nie *et al.* 2016) and the distribution of the depositional environments of Late Jurassic carbonates (e.g. Fortunatova 2007; Babadzhanov 2012; Evseeva 2015b; Wang *et al.* 2014b). The composite Amu Darya Fault separates the Charzhou Step and the Beshkent Depression in the north from the Bagadzha Step and Karabekaul Trough in the south. It has a broken track, with NW-SE-oriented segments relayed by WNW-ESE segments. Other faults appearing on the seismic lines (Fig. 10c) are numbered to help orient the reader on the map (Fig. 10a). Faults names as well as the location and, to some degree, the fault orientations vary on the published maps. The location of Jurassic carbonates is taken from the barrier reef model (Fortunatova 2007; Abdullaev *et al.* 2010; Evseeva 2015b). Even if carbonates do not form a continuous barrier (e.g. Nugmanov 2010), this model indicates an envelope for the location of the main build-ups at the edges of the margin during the end of carbonate deposition, when the central deeper basin was well compartmentalized. Isolated reef build-ups are only shown in the Uzbekistan part and the right bank of the Amu Darya in Turkmenistan, as we do not have information for the southernmost areas. The Chinese studies (e.g. Xu *et al.* 2012; Wang *et al.* 2014b; Zheng *et al.* 2014) present the formation of carbonate build-ups as patch reefs on a carbonate ramp during the Callovian, changing to a ramp-rimmed platform in the Oxfordian. A similar model of patch reefs forming on a carbonate ramp has been proposed for the Callovian carbonates of the Southwestern Gissar (Carmeille *et al.* 2014, 2016).
Some recent seismic lines from the northern margin of the ADB illustrate the presence of faults and their possible play in the deeper part of the sedimentary pile (Fig. 10c modified after Lu *et al.* 2013; courtesy of Dr. Shi Kuo Lu). These seismic lines are part of the intensive study performed by CNPC on this deep part of the Chardzhou Step, the “right bank of the Amu Darya River”. They display an organization of the margin with two main orientations: towards the SW with the succession of steps towards the ADB and towards the SE Beshkent Depression (Fig. 10c). Four main fault orientations exist: NW-SE, NE-SW, ENE-WSW, and nearly E-W with various mechanisms, normal then reverse, thrust or strike-slip (Lu *et al.* 2013). These seismic lines show only the lowest part of the sedimentary pile, without the Cenozoic. They are calibrated by two wells situated on the upper part of the

Chardzhou Step: Samantepe 24, reaching the basement on the A-A' profile located in the northwest of the area, and Metedzhan 2, penetrating the Oxfordian layer on the line D-D'.
The two lines perpendicular to the margin, A-A' to the northwest and B-B' to the southeast, display the well known steps towards the SW deeper part of the Chardzhou margin and the centre of the ADB. Towards their southwestern ends, they cross the important NW-SE trend of the Amu Darya Fault. The southern part of the B-B' line reaches the edge of the Chardzhou Step and the threshold of the Karabekaul Trough.
The two NW-SE-oriented sections (C-C', D-D'), longitudinal to the Chardzhou Step, display normal faults with small steps deepening towards the southeast in the Beshkent Depression. These faults often affect the basement, are markedly active during the Early and Middle Jurassic and most of the time are sealed by the Late Jurassic. The northwesternmost NE-SW-oriented fault (noted F5 in Fig. 10a), seems to be present up to the Upper Cretaceous on line C-C' but, if it is indeed the same fault, it affects only the Jurassic until the top of the carbonate succession on line D-D' where it bounds the Metedzhan structure. The F3 series of faults comprises an important structural feature marking a step towards the Beshkent Depression; it was a normal fault during the Early-Middle Jurassic and was reactivated as a thrust during the Cenozoic. Faults in the upper part of the sections are often located in places where deep faults are present below, corresponding to reactivations during the Cenozoic compressions. These faults are sometimes visible just above the J_3 evaporites layer and delineate NE-SW-oriented folds.
A segment of cross-section 7 (seen in Fig. 9 and enlarged in Fig 10b) follows the same trend and is quite near the seismic lines D-D' and C-C' (Fig. 10c). It shows a larger thickness of the Jurassic siliciclastic layer corresponding to the NE-SW-oriented Early-Middle Jurassic depocentre (Fig. 11a). The location of the eastern part of the line H-H' of Mordvintsev *et al.* (2017) is indicated for comparison, this line being situated to the north, closer to the basin margin.
An ENE-WSW structural trend underlines the northwestern, deepest part of the depth to base of Jurassic map. A shift in magnetic anomaly pattern marks the northwestern part of the Karabekaul Trough across the Amu Darya Fault (Fig. 11b). In between, a prominent topographic boundary seems to exist near the location of the F3 fault on line C-C' (Fig. 10c). This structural orientation is long-lived and inherited from the Late Palaeozoic strike-slip structures. The layout of bioherms, aligned along ENE-WSW, NE-SW structures (for example Beshkent, Kamashi build-ups; G. Evseeva in Babadzhanov 2012), south of the Karshi Fault, indicates that these structural trends formed highs during the deposition of the carbonates (see also Mordvintsev *et al.* 2017). The thickest part of the Lower-Middle Jurassic siliciclastics of the Beshkent Depression is situated more to the southeast, with a more inclined NE-SW orientation (Figs. 10b, 11a and complete isopach map Fig. 7a).
The existence of a basinal area in the Beshkent Depression during the Middle-Late Jurassic is highlighted by the palaeogeographic reconstructions. On the basis of facies studies in the available boreholes and seismic lines from the right bank of the Amu Darya area, Chinese studies (Xu *et al.* 2012; Wang *et al.* 2014b; Zheng *et al.* 2014) have constructed palaeogeographic maps and a NW-SW sequence stratigraphic correlation profile for the Callovian-Oxfordian interval. They characterize a Middle-Upper Jurassic basin area in the Beshkent Depression at the same location as the Lower-Middle Jurassic siliciclastics depocentre, to the southeast of the margin where patch reefs formed on the slope during the earliest steps of the carbonates formation. Reefal bodies (considered as the barrier in the "barrier reef model") became wider on the top edge of the slope during the later stage of carbonate deposition and the deepening of the basin.
The presence of Jurassic normal faults (NE-SW, ENE-WSW) on the slope of the Beshkent Depression as well as a NE-SW-trending depocentre of Lower-Middle Jurassic siliciclastics overlain by upper Middle-Upper Jurassic deeper basinal facies in the same location provides evidence for the formation of this part of the ADB by a crustal extensional event during at least the Early-Middle Jurassic and a subsequent basin deepening by post-rift thermal subsidence. Some of the faults were reworked as thrusts during the Neogene uplift of the Southwestern Gissar and the flexural subsidence in the Beshkent Depression (see cross-section 7 in Fig. 9 and cross-sections A-A', G-G', H-H' in figures 8 and 12 of Mordvinstev *et al.* 2017). The NE-SW orientation, different from the main NW-

SE trend of normal faults active at the same time in the northeast of the ADB might be explained by the role of inherited structures in proximity to the western part of the Tien Shan.

Late-Palaeozoic-Mesozoic subsidence evolution of the Amu Darya Basin

The tectonic subsidence evolution of the ADB, with 1D backstripping and subsidence curves, is depicted at four points (Fig. 12): two in the central part of the ADB in the North Mary and Obruchev troughs, one in the Kimerek rift of the northeastern margin, and one in the Pre-Kopet-Dagh Foredeep in the south. Subsidence curves have been plotted for other wells on the Bukhara-Khiva northeastern margin (Mordvintsev 2015).
After an initial rapid subsidence phase, the subsidence curves display a general pattern of exponential decay corresponding to thermal subsidence following the periods of extension and thinning. However, it is more interesting to consider the tectonic subsidence rates (Fig. 12c), as the peaks directly show the periods of active tectonic events (e.g. Steckler & Watts 1978).

Central part and northeastern margin of the ADB. We first examine three representative localities for the evolution of the central part and northeastern margin of the ADB. The first is the Bayramali pseudo-well, which corresponds to one of the thickest areas of the ADB, situated in the North Mary Trough. The data used are a c. 15 km synthetic thickness column starting in the Late Palaeozoic, derived from cross-section 5 (Fig. 9; Melikhov 2000, 2017) and the lithologies from a set of boreholes in the Bayramali field area (VNIGNI & Beicip Franlab 1992). Unfortunately, it is located in a zone of Neogene uplift and erosion and a part of the Paleogene sediments is eroded, but it represents the deep Late Palaeozic-Triassic North Mary Trough.
The East Kulach pseudo-well represents the northwestern part of the Obruchev Trough. It is located to the northwest of the Palaeozoic trough and west of the Jurassic depocentres. It is the closest point to the Early-Middle Jurassic siliciclastics and Gaurdak Formation depocentres (Fig. 7a and 7c), where some data are available from boreholes (wells Kulach and East Kulach reaching the Callovian-Oxfordian) and the cross-section 8 (Fig. 9). No data are available further east at depth. This location records the extensional event during the Early-Middle Jurassic.
The Kimerek locality uses the data from the Kimerek 4 borehole, which reaches the base of the Jurassic on the Chardzhou step of the northeastern margin (Mordvintsev 2015). The Palaeozoic sediments are not considered here as the well is situated quite near the Uchbash-Karshi Flexure Fault Zone and penetrates diorites below the Jurassic; the Palaeozoic sediments of the rift are located somewhat to the south-southeast. The reconstruction thus begins to record extension in the Lower Jurassic.
The Bayramali and to a lesser extent the East Kulach tectonic subsidence rates (Fig. 12c) indicate the oldest important event that created the rifts underlying the ADB, with a maximum of c. 8 km of Late Palaeozoic to Triassic sediments. The age of the oldest strata cannot be precisely determined. Our curves average the entire Late Permian-Triassic period, thus over a total duration of c. 60 My. In fact, as Carboniferous strata are identified in some boreholes north of the Karakum Arch, they are probably present at the base of the troughs but their thickness is not known. Therefore, the duration of the infill is likely much longer. The main event is probably restricted to a shorter period of time: during the Late Permian to Early or Middle? Triassic, as in northern Iran (Brunet *et al.* 2010), perhaps with a duration of c. 15-30 My which would imply a much higher tectonic subsidence rate (about double) and possibly a Late Triassic reactivation of extension. The proportion of Middle-Late Triassic sediments cannot be deciphered from the total thickness of the Intermediate Complex. The age of the sediments above the main unconformity are not known in the deepest part of the ADB. We choose here to begin in the Hettangian in the central part of the ADB, thus the rate is very low for the Early Jurassic. If the oldest sediments are Sinemurian or Toarcian in age, the rate would be slightly higher. The latter is observed at the Kimerek well; there, a Toarcian age is taken because the Jurassic sediments appear to be a bit younger on the northeast margin.
The tectonic subsidence rate clearly increases during the Aalenian-Bajocian and attains the highest values during the Bathonian. The rate decreases after the Bathonian, during deposition of the

carbonate unit. We must note that in the data from the central part of the ADB, the end of the siliciclastic unit deposited during part of the Early Callovian is grouped with the carbonate unit; consequently, the age of the end of the tectonic subsidence peak is not accurate. In the Kimerek well plot (Fig. 12), where the data are more precise and the end of the siliciclastic unit is accurately placed in the late Early Callovian, the peak of tectonic subsidence occurs during the Toarcian to Early Callovian, with the highest values during the Aalenian-Bajocian.
The Early Cretaceous data from the central part of the ADB are not accurate enough to distinguish the age of the episode of diffuse extensional reactivation. The subsidence rate calculated for the Kimerek well is even lower. In the central part of the ADB, some subsidence persists until perhaps the Turonian, but the magnitude depends on the assumed bathymetries, for which we have no constraints. The Late Cretaceous subsidence is generally uniform, with a long wavelength evolution of the depocentre thicknesses corresponding to thermal cooling after the Jurassic extensional event and to possible additional causes such as far-field deformation or mantle cooling.
Considering the uncertainties on the depositional ages during the Middle-Late Jurassic, several tests have been performed by changing the age of the boundary between the carbonate and evaporite units, and thus the duration of the periods important for the tectonic subsidence rate; we also tested various water depths. The curve presented for the Bayramali area (Fig. 12c) presents a low tectonic subsidence rate of 7 m/My, corresponding to the longest possible duration of c. 14 Ma (Callovian to end of Kimmeridgian; e.g. Abdullaev *et al.* 2010) for the carbonate deposits and a shallow water depth of 180 m. Reducing the duration to a minimum of c. 9 My (Callovian-Oxfordian), the tectonic subsidence rate increases accordingly to 14 m/My with a different sea-level correction at the end of Oxfordian. Even in the case of a short duration, the tectonic subsidence rate decreases sharply at the end of the Lower-Middle Jurassic siliciclastic unit. The duration of deposition of the evaporite formation varies accordingly. A bathymetry of c. 200 m is sufficient to explain the deposits of the overlying Gaurdak Formation filling the Jurassic basin. A greater water depth would slightly increase the tectonic subsidence rates during the extensional event. The basin bathymetry during the deposition of the evaporitic Gaurdak Formation is a matter of debate, being either very shallow (dessication) or deep (salt deposited at the bottom of a brine basin with poor bottom water circulation). The almost complete isolation of the ADB may anyway reconcile the hypotheses as local dessication may have occurred during a local sea-level drop. This does not affect the calculated values of tectonic subsidence, as the bottom of the basin defined using the backstripping method is always located with respect to a zero present level, so a deep bathymetry or a shallow bathymetry with a local sea-level drop are equivalent.

Pre-Kopet-Dagh southwestern margin. The Izgant pseudo-well is representative of the Pre-Kopet-Dagh Foredeep and of the trough situated underneath, along the Kopet-Dagh; it is more precisely located in the Ashgabat Trough to the south of the Central Karakum Arch. It is part of the ADB petroleum province but its evolution appears closely related to the southern Kopet-Dagh. The synthetic column thickness is based on the cross-section 4 (Fig. 9) detailed in Melikhov (2000) for the Cretaceous and Cenozoic and the well Izgant 2, which reaches the Turonian-Cenomanian. From the Lower Cretaceous layers downwards, the thicknesses and their exact ages are sometimes not well constrained, based on some seismic lines calibrated by correlation with the Bakhardok southern slope of the Central Karakum Arch. The first important event, as in the central part of the ADB, appears with a high peak of tectonic subsidence rate during the Late Palaeozoic-Triassic extensional event. One part of the Late Palaeozoic succession, which cannot be determined, was actually deposited earlier than drawn in the curves, during the Carboniferous. The second high peak displays the Early-Middle Jurassic extension, which is also well expressed in this southern trough. It displays the birth of the Kopet-Dagh Basin as a continuation of the South Caspian Basin after the Eo-Cimmerian collision (see below). We consider that Jurassic deposition began in the Aalenian, as no deposits older than the Kashafrud Formation (beginning in the Late Bajocian) exist in the Kopet Dagh and Aalenian strata have been drilled to the north in the Bakhardok Slope. The peak of tectonic subsidence occurs from the Aalenian to the Middle Callovian, determined here by correlation with the Bakhardok Slope. The subsequent evolution during the Cretaceous and the Cenozoic is much

more variable than in the main part of the ADB as it is largely influenced by the development of the Kopet-Dagh Basin followed by the Arabian collision and uplift of the Kopet-Dagh Range. An extensional reactivation occurred during the Barremian-Aptian, with the highest peak during the Aptian. The same extensional event is recorded in the Kopet-Dagh with an increase from east to west (Shahidi 2008; Brunet *et al.* 2010). A large part of the preceeding Hauterivian event may be more closely related to compression-driven subsidence rather than to the subsequent extension as it occurs just after the Late Cimmerian collision when the erosion of topographic highs provided clastics sediments. The Hauterivian thickness is possibly also slightly overestimated, due to the poor age constraints.
The Cenozoic evolution is marked by the influence of the collision of the Arabian plate with the Central Iranian blocks and subsequent shortening. The initial collision of the Arabian Plate is recorded by a large flexure of the foredeep basin during the Late Eocene. The second large flexural event takes place during the Pliocene-Quaternary, after formation of the pronounced angular unconformity between the Miocene and Pliocene due to regional uplift (negative peak in subsidence rate but of uncertain duration and thus magnitude) and strong erosion (see cross-section 4 Fig. 9 and the Amu Darya River incision after the uplift). This deformation and erosion reflects the uplift of the Kopet-Dagh Range and north-vergent thrusting onto the Pre-Kopet-Dagh Foredeep.

Main results. In our tectonic subsidence reconstruction, after the Late Palaeozoic-Triassic extensional event creating the rifts, the eastern NW-SE-oriented ADB was progressively formed during the Jurassic. High Jurassic tectonic subsidence rates are a result of the Early Jurassic to Early Callovian phase of extension; lower rates occurred during the following period, until the Oxfordian or Kimmeridgian. The depth of the resulting basin and ongoing thermal subsidence are sufficient to explain the thickness of the evaporites filling the basin without requiring an additional Late Jurassic extensional event. Another extensional event is recorded during the Early Cretaceous. Although this is diffuse in the central part of the ADB, it is mainly expressed in the south in relation to the Kopet-Dagh Basin evolution. The Cenozoic evolution of this Pre-Kopet-Dagh Foredeep provides a good record of the collisional events which are not preserved in the subsidence record of the Kopet-Dagh Basin itself, because it was later inverted into the Kopet-Dagh Range (Shahidi 2008; Brunet *et al.* 2010).

Existing subsidence models of the Mesozoic Amu Darya Basin evolution

Except for general remarks on the subsidence of the ADB in the published literature, only a few papers have dealt with the subsidence evolution of the ADB and its tectonic driving mechanism prior to the Cenozoic inversion (VNIGNI & Beicip Franlab 1992; Thomas *et al.* 1999a; Holt *et al.* 2015; Abbasov 2015).
Geohistory curves and thermal maturation simulations for the hydrocarbon potential exist for some ADB boreholes (VNIGNI & Beicip Franlab (1992). Indeed, hydrocarbon generation from the rich organic matter of the Khodjaipak Upper Jurassic black shales and Lower-Middle Jurassic siliciclastic source rocks constrains the tectonic evolution of the Beshkent Depression proposed by Abbasov (2015); this analysis used a 1D thermal model that assumed a Late Triassic-Early Jurassic rifting event associated with high heat flow. Using isopach maps, cross-sections and tectonic analysis, Thomas *et al.* (1999a) examined the entire evolution of the ADB, partly following the same analysis of the data as in the present paper. Here we have taken into account more detailed recent data, combined with tectonic subsidence reconstructions from backstripping.
Following the study by Natal'in & Şengör (2005), Holt *et al.* (2015) based a model of ADB subsidence on a Palaeozoic initiation event: the amalgamation of arc and forearc terranes floored by oceanic crust. They explain the general exponential decay of the subsidence rate of the ADB since the Permian by a model of a unique thermal evolution of this accretionary orogeny, without requiring later orogenic extension. They assume that the onset of accretion occurred with a normal crust and a thin mantle lithosphere; subsequent cooling and thickening of the mantle caused isostatic subsidence. The data used for four backtripped subsidence curves and forward modelling come from an E-W

cross-section of the ADB published by Thomas *et al.* (1999a), similar to our cross-section 3 (Fig. 8d). The best fits are obtained for a final crustal thickness of 28 km beneath the Khiva central Palaeozoic depression, north of the Ilim Trough and 31 km beneath the Chardzhou Step, as well as a final lithosphere thickness of 155 km. They point out the poor definition of the starting points of their curves, due to uncertainty on the Permian onset and the Triassic termination of the event. Although they recognize that accretion and rifting lasting until the Middle Triassic could affect the interpreted initial conditions for basin evolution, they propose that no crustal extension occurred and that such rifting was only local, rather than underlying the entire ADB.
In fact, considering the location of the points studied, the data used by Holt *et al.* (2015) deal with only a small part of the ADB (N-S central rift and Chardzhou Step); they do not consider the eastern central part of the ADB, where the Jurassic basin is the thickest and best expressed. Their model is nevertheless interesting and shows a slight crustal thinning to 28-31 km; as seen from the DSS studies, the Moho below the Turan Platform is now rather homogeneously more than 40 km deep and the unthinned crust is more than 35 km thick. Their concluding model of long-lived thermal subsidence associated with lithospheric cooling after accretion could provide a background mechanism for tectonic subsidence of the ADB. However, we claim that crustal extension-driven thinning is superimposed upon this lithospheric cooling. Extension may have begun during the Late Palaeozoic-Triassic, as depth-to-basement maps (Fig. 5) and cross-sections (Figs 8-9) show that many Palaeozoic-Triassic troughs exist below the ADB, besides the north-south and Chardzhou margin troughs. On the other hand, Jurassic crustal extension-driven thinning is decisive in localizing and shaping the eastern part of the ADB and its neighbour, the Afghan-Tajik Basin. Our study also shows that the Jurassic depocentres are located slightly to the north of the Upper Palaeozoic-Triassic ones in the eastern ADB. The tectonic subsidence (Fig. 12) and normal faulting (see also Mordvintsev *et al.* 2017 on the northeastern margin) were active during the Early-Middle Jurassic, implying a new extensional event occurred at this time.

The Amu Darya Basin in the context of the regional geodynamical evolution

Palaeotectonic maps from the Late Permian onwards (modified from Barrier and Vrielynck 2017) allow us to relate the different stages of the evolution of the Amu Darya Basin (ADB) to the general geodynamics of this part of western Central Asia (Figs 2, 14). We place special emphasis on the Jurassic history.

Establishment of the Turan Platform at the end of the Palaeozoic

The Turkestan Ocean closed during the Palaeozoic by subduction towards the north below the Kazakh-Kyrgyz continent (e.g. Filippova *et al.* 2001; Burtman 2006; Alexeiev *et al.* 2009; Biske & Seltmann 2010; Seltmann *et al.* 2011; Biske *et al.* 2013; McCann *et al.* 2013; Nurtaev *et al.* 2013; Dolgopolova *et al.* 2016; Konopelko *et al.* 2016). This is a part of the vast Variscan orogeny that lead to the construction of the Pangea supercontinent. To the south of the Turkestan Ocean lay the Gissar basin, another much smaller basin underlain by oceanic crust. The existence of the Gissar Basin is interpreted based upon the remnants of sutures observed in the Gissar area, although whether the location of its western extension lies to the north of or below the ADB northeastern margin is controversial (e.g. Brookfield 2000; Troitskyi 2012; Nurtaev 2015; Dolgopolova *et al.* 2016; Konopelko *et al.* 2016). The Turkestan Ocean and Gissar oceanic basin closed in the latest Carboniferous (e.g. Dolgopolova *et al.* 2016; Konopelko *et al.* 2016), allowing the accretion, to the south of the Turkestan suture, of a stack of blocks/terranes/microcontinents; together, these comprise the Turan Platform. These blocks include the Alay block, hosting the Turkestan accretionary complex and the Kyzylkum area, the Karakum block or microcontinent that underlies the entire ADB, and the Tajik block in the east. Considering the varied orientations of major structures, the Karakum block is itself probably constituted of several blocks, as the Central Karakum block, corresponding to the western half of the ADB, is joined to a set of NW-oriented blocks constituting the eastern part of the ADB (e.g. Filippova *et al.* 2001; Heubeck 2001). This model is derived from the orientations and nature of the magnetic anomalies (Fig. 4a) and from the various compositions of drilled basement

with remnants of volcanic arcs, as discussed above (e.g. Natal'in & Şengör 2005; Zanchetta *et al.* 2013). Strike-slip faults are superimposed upon the late collisional system. Late-collisional left-lateral strike-slip faults occurred along the southern border of the Kazakhstan continent during the Early Permian, coincident with the age of the main phase of granitoid magmatism in the Uzbek western Tien Shan (e.g. Dolgopolova *et al.* 2016). Offset caused by this left-lateral strike-slip regime may explain the gap in the Aral-Murgab N-S-trending rift system along the WNW-ESE-trending Central Ust Yurt and Repetek faults in the medial area of the ADB (see above and Fig. 1) and the left-lateral shift of the magnetic anomalies (Figs 4a, 11b). The episode of pre-Late Permian regional erosion observed in the ADB (e.g. Melikhov 2000) corresponds to a geodynamic change at the end of the Variscan collision. The movement changed from left-lateral to a broader right-lateral system in the Late Permian (e.g. Natal'in & Şengör 2005; Dolgopolova *et al.* 2016 and Muttoni *et al.* 2009; Berra & Angiolini 2014 for the large Pangea dextral rearrangement during the entire Permian).

Palaeo-Tethys subduction and Eo-Cimmerian collision

At the end of the Palaeozoic (Permian map, Fig. 14), the Palaeo-Tethys was subducting towards the north below the Turan Platform, which had already been accreted to Eurasia after the closure of the Turkestan Ocean to the north (e.g. Thomas *et al.* 1999a, Garzanti & Gaetani 2002, Barrier & Vrielynck 2017), and Cimmerian blocks detached from Gondwana since the Early Permian.

South of the ADB, a system of arc and back-arc basins developed during the subduction of the Palaeo-Tethys; this is preserved in the Aghdarband area to the east of Kopet-Dagh (e.g. Zanchetta *et al.* 2013), and in the north of Afghanistan (Montenat, 2009; Siehl 2015). During the Late Permian-Early Triassic, rifts basins also existed to the north of the ADB, as for example in the Ustyurt Plateau (e.g. Krylov & Grizik 2015), far from the subduction zone. Subduction rollback may have resulted in a N to NE-directed extension of the overriding plate, in an area broader than the northern margin of the Palaeo-Tethys where back-arc extension was taking place. This extension was an important element in the subsidence evolution of the ADB, as it created the thick Permo-Triassic Troughs of the ADB, and the steps along its margins, mainly along the accreted blocks underlying the Turan Platform.

Throughout the Permian, the Turan Platform was located within a long Intra-Pangean dextral shear zone (e.g. Muttoni *et al.* 2009; Berra & Angiolini 2014). According to Natal'in & Sengör (2005), the Permian-Triassic evolution of the Turan Platform was unlikely to be related solely to extension but rather to extension linked to transtension and/or pull-apart basins along right lateral strike-slip faults. They propose a model of general dextral strike-slip, associated with the closing of the Palaeo-Tethys, until the Triassic for the Turan Platform and the Middle Jurassic for the Scythian Platform in the west, allowing for displacement along the Eurasian margin and stacking of slivers of arcs and blocks separated by steep faults. Unfortunately, subsurface data are too scarce to test this model and its implied large displacements; alternatively, the blocks could have been stacked with much less lateral displacement. In any case, a series of long NW-SE faults do mark the northern boundary of the ADB as well as the division of its northeastern part into several steps and troughs (Fig. 1).

The NW-SE-oriented Bukhara-Gissar Fault or Uschbash Karshi Flexure Fault zone played a major role in the tectonics of the northeast margin of the ADB, bounding the Late Palaeozoic Karakul rift, which was reworked into an important, more localized, Early Jurassic rift in the Kimerek area. A part of the Late Palaeozoic-Triassic extension in the ADB probably results from transtension accommodated by strike-slip reactivation of the faults bounding the blocks (e.g. Thomas *et al.* 1999a for the NS to 160°N trending basins; Natal'in & Sengör 2005: transtension being the main mechanism for all the troughs).

New radiometric ages from post-collisional granitoids suggest that the Palaeo-Tethys closed before Middle-Norian times in northern Iran (Zanchetta *et al.* 2013). The accretion of Iranian blocks to Eurasia represents the first event of the so-called Eo-Cimmerian collision (Norian map, Fig. 14). Due to the oblique convergence, Triassic-age left lateral movements occurred in the Aghdarband area, parallel to the collisional belt (Zanchi *et al.* 2016). All of the Cimmerian blocks did not arrive at exactly the same time along the Palaeo-Tethys margin; the precise chronology is still a matter of

debate and study. The composite Band-e Bayan-Helmand block (e.g. Siehl 2015) had not yet accreted to Eurasia in the Norian and the Qiantang block to the east accreted later, around the end of the Triassic or very beginning of the Jurassic, which generated deformation far from the collision zone (Jolivet 2015). Accretion of these eastern blocks, the second part of the Eo-Cimmerian collision, resulted in the major angular unconformity observed in the ADB between the Jurassic and the Upper Palaeozoic-Triassic folded sediments eroded on the margins.

Jurassic extension

At the beginning of the Jurassic, a widespread, roughly N- to NE-oriented post-orogenic extensional setting occupied the areas affected by the Eo-Cimmerian orogeny (Toarcian map, Fig. 14). At the same time, erosion of the previously uplifted areas sourced the siliciclastic series that filled the newly created basins in the south and central part of the ADB (Lower-Middle Jurassic siliciclastic unit in the ADB, e.g. Ulmishek 2004, similar to the Late Triassic-Early Jurassic Shemshak Group in northern Iran, Fürsich *et al.* 2009a). On the northern margin of the ADB, clastics deposits were sourced from remnants of Palaeozoic highs to the north (e.g. Natal'in & Şengör 2005; Brookfield 2000; McCann 2016a). At the beginning of the Middle Jurassic, focused extension lead to the development of a series of basins: the South Caspian and Kopet-Dagh basins, the ADB, the Afghan-Tajik and Pamir basins to the east, and the Farah Basin-Waras-Panjaw ocean in Afghanistan as well as the Central Iranian basins to the south (e.g. Brunet *et al.* 2003, 2010; Taheri *et al.* 2009; Wilmsen *et al.* 2009; Siehl 2015; Barrier & Vrielynck 2017).

The Early-Middle Jurassic extension reactivated mainly NW-SE-, and NE-SW-oriented Late Palaeozoic structures as normal faults; some new faults were also created (e.g. Mordvintsev *et al.* 2017). The Central Karakum Arch is a block which experienced less extension and subsidence during the Jurassic; it forms the western boundary of the Jurassic ADB, which acquired it's present form at this time. Indeed, strong extension almost ceased at the end of the Middle Jurassic, as shown by the sharp decrease of the tectonic subsidence rate (Fig. 12c) and the termination of normal faulting (Brookfield & Hashmat 2001). Only a few normal faults are observed to have been active later in lower Upper Jurassic carbonates, for example in places where a sharp change of topography occurred over a short distance between the northeast margin and the basin area during the Late Jurassic (e.g. Nugmanov 2010; Mordvinstev *et al.* 2017).

The Jurassic depocentres created in the northeast of the ADB were first filled with continental clastics of the thick Lower-Middle Jurassic siliciclastic unit; deposition in this area as well as the Kopet-Dagh and Alborz Mountains becomes marine during the Late Bajocian transgression (e.g. Fürsich *et al.* 2009b, 2015). The marine transgression was facilitated by increasing subsidence of the ADB. Carbonate production increased progressively during the Early Callovian; the amount of clastics decreased concurrent with a possible climatic change from humid to semi-arid conditions (e.g. Fürsich *et al.* 2015). Deposition of the carbonate unit commenced during the Middle Callovian as carbonate ramps with patch reefs; at the same time, the extension rate decreased drastically.

A minor unconformity formed either during or at the base of the Early Callovian; the timing is uncertain because the accuracy of the data varies spatially. This is described at the base of the Middle-Late Jurassic carbonate unit in the northeast of the ADB and in the well Samantepe 53-1 (e.g. Zheng *et al.* 2013; Wang 2014). It is described as a slight angular unconformity in the late Early Callovian in the Southwestern Gissar (Fürsich *et al.* (2015). On the southern margin of the ADB, in the Kopet-Dagh, Robert *et al.* (2014) describe erosion and an angular unconformity in the west of Kopet-Dagh, between the Kashafrud Formation (Bajocian-Bathonian) and the Chaman Bid Formation (beginning in Callovian). An erosional gap is observed at the top of the Kashafrud on seismic lines in the east of the Kopet-Dagh (Robert *et al.* 2014). An erosion surface exists between the Bathonian and Callovian to the north of the Kaahka Depression (east of the Pre-Kopet-Dagh Foredeep), as well as on the southern margin of the ADB in the Kopet-Dagh foothills and the Badkhyz-Karabil Step (Melikhov 2000). Where the Lower-Middle Jurassic succession is absent, the Callovian directly overlies the Upper Triassic (see southern part of the cross-sections 5, 6 Fig. 9). However, in the basinal parts of the ADB, there is no erosion and the transition to the Callovian is

gradual (Melikhov 2000). The age of the unconformity corresponds to the end of the period of important extension and could mark a post-rift unconformity. However, the unconformity could also be linked to an as yet undefined tectonic event. Such an unconformity, at either the base or within the Callovian and limited to the margin, is also locally known in the northern Caucasus margin, where Bathonian sediments are gently folded (e.g. Saintot *et al.* 2006). It could also correspond to the last western phase of sliver stacking in the Caucasus in the frame of the large dextral shear zone model of Natal'in & Şengör (2005).

The bathymetry of the central part of the basin continued to increase during the rest of the Callovian and the Early Oxfordian, resulting from thermal subsidence following extension and from a decreasing influx of clastic sediments due to drier climatic conditions and decreasing relief of the source areas. At this same time, sedimentation changed from siliciclastics to carbonates, leading to a well differentiated basin with relatively deep shaly carbonates in the centre, reef build-ups on its margins, and surrounded by shallow platforms during the Middle Oxfordian and possibly also the Kimmeridgian (cf. Callovian-Oxfordian map, Fig. 14). At approximately 20 m from the top of the carbonate unit, carbonates were sometimes deposited in very shallow platforms or lagoons, as dinosaur traces are sometimes observed in Gissar (Mirkamalov *et al.*, 2005) and in the Kugitang Mountain in Turkmenistan (Fanti *et al.* 2013). In other places, carbonates without reefs overlie the reef build-ups. The termination of reef deposition may result from increasing water depths and also from increasing water salinity as the basin became progressively restricted.

The development of the reefal carbonates on the edges of the platforms was favoured by an Oxfordian climate warming, shown by faunal changes (e.g. Cecca *et al.* 2005; Nugmanov 2010). The basinal part, where black shales or dark shaly carbonates were deposited, was possibly stratified with poor bottom circulation and undisturbed anaerobic bottom water. A similar interpetation has been proposed for other source rocks, such as the Devonian Domanik facies on the Russian Platform or Palaeozoic high gamma ray black shales in North America (e.g. House *et al.* 2000; Sarg 2001; Moore & Wade 2013).

At the end of the Jurassic (Tithonian map, Fig. 14), a large basin was established that included the ADB and continuing to the east as the Afghan-Tajik and Pamir basins. It was partly bounded by exposed areas that were being uplifted in the south and east by deformation related to the onset of closure of southern basins such as the Waras-Panjaw ocean in Central Afghanistan (e.g. Siehl 2015; Barrier & Vrielynck 2017). The combination of a strongly restricted environment and drastic aridification allowed the deposition of thick evaporites. The basin was probably only open in the west (e.g. Barrier & Vrielynck 2017) to periodically receive regular marine input necessary for the deposition of the thick evaporitic sequence comprising the Gaurdak Formation. The subsidence evolution shows that there was not an additional extensional tectonic event at this time (Fig. 12). Therefore, the evaporite unit appears to represent the filling of a depression formed earlier, during the Early-Middle Jurassic extensional event. The lower anhydrite and lower salt layers filled the inherited Jurassic topographic irregularities; they are thin or absent on top of the reefs and on the back-reef shelf. The lower salt layer thickens abruptly over areas of deep-water deposits of the carbonate unit. The thickness of the upper salt layer is less variable, being several hundred meters thick in the central basin area and thinning gradually towards the basin margins (Khudaykuleyev, 1986).

At the end of the Jurassic, due to the same climatic conditions and restricted environments, thick evaporites comprising the Hith Formation (Fig. 15) were deposited on the southern margin of the Neo-Tethys in intra-platformal basins of Arabia, isolated in hypersaline conditions behind reefs or shoal rims (e.g. Hughes & Naji 2008). Similarly to the Gaurdak Formation, the Hith Formation seals carbonates with hydrocarbon potential (Arab Formation), beginning with a transitional facies with interbedded carbonates and anhydrites related to sea-level fluctuations and terminating with a carbonate layer marking the overlying transgression. In the absence of chronostratigraphic markers, the age of the Hith Formation is as difficult to constrain as is the age of the Gaurdak Formation. A Tithonian age is proposed by Hughes & Naji (2008), based on the stratigraphic position of the Hith Formation between the top of the Arab Formation, dated Late Kimmeridgian, and the Sulaiy Formation of Late Tithonian to Berriasian age.

Late Cimmerian collision and Cretaceous evolution

Between the end of the Jurassic and the beginning of the Early Cretaceous, the southern basins of Central Iran and Central Afghanistan closed, and collisions occurred during the Early Cretaceous in the east; these are often grouped as the Late Cimmerian orogeny. This event is recorded by poorly identified unconformities of various Early Cretaceous ages, and by clastic deposits, at least partly continental, such as the Shurijeh Formation (Hauterivian) in the eastern Kopet-Dagh (northern Iran) (e.g. Mortavazi *et al.* 2014). Northern Afghanistan was uplifted due to the closure of the Waras-Panjaw oceanic basin (Montenat, 2009; Siehl 2015); an erosional event is recorded on the southern Afghan margin of the ADB (Melikhov 2000; Ulmishek 2004; pre-Valanginian age for Klett *et al.* 2006). Even further north in the ADB, the Uchadzhi area, which was in a basinal environment in the lower Late Jurassic, was uplifted between the very end of Jurassic and the Early Cretaceous to become an arch (e.g. Klett *et al.* 2006 and reference therein; backstripped cross-section 2 Fig. 8c). Uplift was probably caused by transpressional strike-slip reactivation of the Repetek Fault which bounds the Uchadzhi Arch, resulting from shortening in the southeast.

A regional post-Barremian unconformity affected the Turan domain and its surroundings; deformation was especially intense in the eastern part in Afghanistan (Thomas *et al.* 1999a and references therein). The Lhasa terrane accreted in the east, at the end of the Early Cretaceous (e.g. Jolivet 2015).

The sedimentary environment at the beginning of the Cretaceous alternated between continental and marine; later it became solely marine. Until Late Aptian time, the northern boundary of the marine area was located along the southern slope of the Central Kyzylkum system of uplifts (Middle Aptian map, Fig. 14), then a regional transgression took place, covering a significant part of the territory of Central Asia to the north (e.g. Nugmanov 2010; McCann 2016b). Tectonic subsidence was reactivated in an extensional setting between the Barremian and the Albian or Albian-Cenomanian (Fig. 12), synchronous with extension in the Kopet-Dagh Basin (e.g. Brunet *et al.* 2010; Barrier & Vrielynck 2017). Thermal subsidence of the entire ADB followed during most of the Late Cretaceous with deposition of a rather homogeneous thickness of marine clastic or carbonate strata.

Cenozoic collision

The Cenozoic tectonic evolution of the Turan Platform was influenced by the collision of two indenters with southern Eurasia. The Arabian Plate collided with the Iranian blocks in the west and the Indian Plate collided with Tibet and the Pamir in the east. These collisions, which have differing timing, vectors and velocities, drove far-field deformation in Central Asia. These collisions resulted in roughly synchronous uplift (c.a. 5 Ma) of belts such as the Alborz, Kopet-Dagh, Pamir and in flexure of adjacent basins. Farther north from the collision areas, there was a broad zone of intraplate deformation characterized by fault reactivations (reverse thrusting and strike-slip accommodation), as well as uplift and subsidence (e.g. Nikishin *et al.* 1997; Otto 1997; Lybérys & Manby 1999; Thomas *et al.* 1999a, b; Brunet *et al.* 2003; Jaboyedoff *et al.* 2005; Smit *et al.* 2013). Utilizing a model of lithospheric folding based on the observed alternation between areas of uplift with areas of subsidence in Central Asia, several studies note the importance of a NE-SW boundary, the so-called Kugitang-Tunka line (Fig. 14, map). This boundary separates two areas with different crustal and upper mantle structures behaviours (e.g. Nikishin *et al.* 1993, 1997; Smit *et al.* 2013; Robert *et al.* 2015) and a change of orientation of the structures on opposite sides of this line. Variations in the thermo-mechanical structure of the lithosphere and of the orientation and convergence velocities of the Iranian and Pamir indenters may explain the interference of lithospheric folding patterns in Central Asia (e.g. Smit *et al.* 2013) and the differences in observed topography and gravimetry. The Kugitang Mountains, south of the Kugitang-Tunka line, are part of the Southwestern Gissar, marking the boundary between the ADB and the Afghan Tajik Basin. Southwestern Gissar was uplifted and thrust towards the northwest onto the Beshkent Depression during the Late Cenozoic (Tevelev & Georgievskii 2012). The southernmost part of this uplifted zone is visible on cross-section 7 (Fig. 9),

near the border between Turkmenistan and Afghanistan. During this episode of tectonic shortening, several likely inherited Palaeozoic structures were reactivated as strike-slip faults. An example is the dextral Ashgabat Fault, reactivation of which resulted in Late Pliocene parallel, northeast-southwest trending folds (e.g. Lybérys & Manby 1999; Torres 2007). Other examples of apparently reactivated structures are located near the northern boundary of the ADB (e.g. Thomas *et al.* 1999a), and within the ADB, such as the Repetek Fault (e.g. Otto 1997, Ulmishek 2004), allowing the localization of the Palaeo-Amu Darya River and possibly the Bukhara-Gissar or Uchbash-Karshi Flexure Fault Zone (e.g. Thomas *et al.* 1999b). North-south-oriented structures of the central Khiva-Murgab Trough were also probably reactivated, as the Khiva Murgab Lineament is in continuity with the roughly NS-oriented faults and the similarly oriented East Iran Ranges, all lying between the Lut block in Iran and various tectonic blocks in Afghanistan. The Iranian structures were active during the Cenozoic Arabian collision, coeval with the N to NNE movement of the Lut and Iranian blocks. The strike-slip reactivations of inherited structures contribute to the tectonic complexity of the ADB.

Conclusions

A study of depth-structure maps, isopach maps and cross-sections drawn at the scale of the entire Amu Darya Basin (ADB), as well as subsidence analysis of several key localities, illuminates the basin evolution, allowing it to be related to the geodynamic events in western central Asia. The Late Palaeozoic-Mesozoic subsidence evolution of the ADB may be explained by two important extensional events that occurred during Late Palaeozoic-Triassic and Early-Middle Jurassic times, after the closure of the Turkestan and Palaeo-Tethys oceans respectively and the subsequent collisions. The complex structure of the ADB, displayed by the wide range of orientations of structural highs and sub-basins, results mainly from the reactivation of inherited structures of the underlying inhomogeneous Turan Plate, which consists of several blocks. These reactivations occurred during both extensional periods and collisions. Contractile deformation induced thrusts and flexural subsidence near the collisional belts as well as far-field deformation driven by lithospheric folding and strike-slip faulting resulting from the obliquity of collisions. The Early-Middle Jurassic extension was principally localized in the eastern half of the ADB between its northern NW-SE-oriented and southern more E-W-oriented margins, which were built by the Late Palaeozoic-Early Mesozoic closure of oceans and collisions of terranes. This extension is responsible for the formation of an elongated deep basin and may explain the entire Jurassic sedimentary infill of the ADB. At the same time, there were several Jurassic climatic changes from humid to semi-arid, then arid, and changes of temperatures from cool to warm (e.g. Cecca *et al.* 2005; Nugmanov 2010; Fürsich *et al.* 2015; Jolivet 2015). The combination of extension-driven subsidence and this climatic history created the important Jurassic hydrocarbon system of the Amu Darya Basin. The upper Middle-Upper Jurassic carbonate build-ups on the edges and high points of the ADB constitute high quality reservoirs, supplied by the locally organic-rich source rocks of the Lower-Middle Jurassic siliciclastics, and the marine carbonaceous shales of the Middle Upper Jurassic that were subsequently sealed by the Upper Jurassic evaporites.

This work was funded by the International Darius Programme and benefited from tight interactions with the interdisciplinary program “Groupe de Recherche-Industrie UPMC-TOTAL Northern Tethys” on the geological evolution of western Central Asia. We thank the Institute of Geology and Geophysics of Tashkent for allowing field works, IGIRNIGM and Uzbekgeofizika for providing subsurface data and reports and allowing publication. Dr. Shi Kuo Lu is acknowledged for allowing the use of seismic lines from the right bank of the Amu Darya River area. Jean-François Brouillet, Frédéric Kaveh and particularly Anne-Claire Laurent Morillon (CNRS-UPMC) are thanked for their active participation in the georeferencing of documents, drawing of maps, and cross-sections. We also acknowledge the reviewers Randell Stephenson and Gabor Tari, and the editor Edward Sobel for their scientific advice and patient assistance in improving the English.

References

ABBASOV, S. 2015. Background and basis of prediction of Jurassic petroleum deposits in the Central part of Beshkent trough with the software PETROMOD 1D. *Eurasian Union of Geoscientists*, **7** (16), 131-135 [in Russian].

ABDULLAH, S. & CHMYRIOV, V. M. (eds) 2008. *Geology and Mineral Resources of Afghanistan. 2 Volumes*. British Geological Survey, Occasional Publications, **15**. Accessed on March 8, 2017, at http://www.bgs.ac.uk/data/publications/pubs.cfc?method=listResults&pageSize=100&pubName=Afghanistan&author=&simpleSearch=Go

ABDULLAEV, G. S. 1997. Detailing of stratigraphy of Upper Jurassic Carbonate Complex of Western Uzbekistan - Basis for Increasing Effectiveness of Oil-Gas exploration. *Uzbekskiy Geologicheskiy Zhurnal*, **4**, 69–79 [in Russian]. English Abstract in *Petroleum geology*, **33** (1999), 297-304.

ABDULLAEV G. S., 2004. Biostratigraphy, lithofacies and oil and gas perspectives of the Amu-Darya northern margin Jurassic carbonates. Abstract of the thesis, Geology and Geophysics Institute, archives, Tashkent, 40 p. [in Russian]. Accessed on March 8, 2017, at http://dlib.rsl.ru/loader/view/01000179240?get=pdf.

ABDULLAEV, G. S. & MIRKAMALOV, H. H. 1998. Unification of stratigraphic nomenclature of commercial horizons of Jurassic carbonate formations of the southern and southwestern Uzbekistan. *Uzbek Oil and Gas Journal,* **4**, 13–16 [in Russian].

ABDULLAEV, G. S. & MIRKAMALOV, H. H. 2001. Stratigraphy of the Jurassic high-gamma activity rocks of the Bukhara-Khiva region and its importance for the modelisation of the carbonate formation. *Geology and oil and gas perspectives of Uzbekistan*, Tashkent, 13–24 [in Russian].

ABDULLAEV, G. S. & MIRKAMALOV, H. H. 2006. Volume and age of the Jurassic Gaurdak formation of the Southwestern Gissar and the Bukhara-Khiva region. *Uzbekistan oil and gas journal*, 2, 17–21 [in Russian].

ABDULLAEV, G. S., MIRKAMALOV, H. H. & EVSEEVA, G. B. 2010. Oil and gas bearing reefal facies of the Jurassic carbonate unit of the Amu-Darya basin (Southern and Southwestern Uzbekistan) and their relationship with reef formation within the paleobasins of the Tethys. In proceedings of the conference 12 Octobre 2009 *"Theoretical and practical aspects of the oil and gas geology of Central Asia and the solutions for the modern problem of the domain", NGGI,* Tashkent, 39–49 [in Russian].

ABETOV, A. E., AHMETOV, E. M., ZHYLKYBAEVA, G. A. & ABETOVA, S. A. 2015. Geological structure and geodynamics of consolidated crust of the junction zone between the Southern Tien Shan and the Turan Plate. *Vestnik KazNTU*, **2**, 3-13 [in Russian with English abstract]. Accessed on March 8, 2017, at vestnik.kazntu.kz/files/newspapers/99/3209/3209.pdf

ABETOV, A. V., ATABAYEV, KH. A., BABADZHANOV, T. L., DOLGOPOLOV, F. G., ZUYEV, YU. N., MATASOVA, L. M., PAK, V. A., RZAYEVA, V. A., KHAMRABAYEV, K. KH., KHASANOV, P. KH., CHIRIKIN, V. V., SHARIPOV, R. A., SHATOKHIN, A. I., SHEYKH-ZADE, E. R., ERGESHEV, T. E., YUSUPKHODZHAYEV, KH. I. & YACHMENNIKOV, YU. M. 1992. Deep structure of Central Asia. *In*: V. V. BELOUSOV, N. I. PAVLENKOVA & G. N. KVYATKOVSKAYA (eds) Structure of the crust and upper mantle of the former USSR. *International Geology Review*, **34**, 279-297.

ABIDOV, A.A & BABADZHANOV, T.L. 1999. Map of the tectonic regionalization of the oil and gas provinces of Uzbekistan, 1:1 000 000. Uzbekgeofizika, Tashkent.

ABIDOV, A. A., ATABEKOV, I. U., DOLGOPOLOV, F. G. & KHODZHIMETOV, A. I. 1996. Late Paleozoic Rift System of Bukhara-Khiva Region as a New Regional Structure for Oil-Gas Exploration in Uzbekistan. *Uzbekskiy Geologicheskiy Zhurnal*, **1**, 50–60 [in Russian]. English Abstract in *Petroleum Geology*, **31** (1997), 162-164.

ABIDOV, A. A., TAL-VIRSKIY, B. B., BABADZHANOV, T. L., KHODZHAEV, A. R., LEPESHKIN, V.S. & BERBAEV, F. B. 2004. *Tectonic zoning map of the Bukhara-Khiva oil and gas region, 1: 500000*.Tashkent, in RADJABOV 2009.

AKRAMKHODJAEV, A. M., MIRKAMALOV, H. H., AHMEDOV, P. U., KORSUN, V. V. & ABDULLAEV, G. S. 1982. Stratigraphic and facial schemes of the Upper Jurassic carbonate unit in Western Uzbekistan. *Bulletin of the Moscow Society of Nature Explorers. Geological section*, **57** (20), 53-62 [in Russian].

ALEXEIEV, D. V., COOK, H. E., BUVTYSHKIN, V. M. & GOLUB L. Y. 2009. Structural evolution of the Ural–Tian Shan junction: A view from Karatau ridge, South Kazakhstan. *Comptes Rendus Geoscience*, **341**, 287–297.

ALIYEV, M. M., KRILOV, N. A., GENKINA, R. Z., GOFMAN, E. A., DUBROVSKAYA, E. N., TSATUROVA, A. A., AMMANOYAZOV, K. N., ALIMOV, K.N., MIRKAMALOV, H. H., MALTSEVA, A. K., PROZOROVSKAYA, E. L., ROSTOVTSEV, K. O. & SQXAROV, A. S. 1983. *Jurassic of the south USSR*. Nauka, Moscow, 208 p.

AMURSKII, G. I. 1966. Tectonics of Turkmenistan and adjacent territories. *In*: AGRANOVSKII L. E. & AMURSKII G. I. *Tectonics of Turkmenistan and neighboring areas.* Nauka Moscow, 6-32 [in Russian]. Accessed on March 8, 2017, at http://www.geokniga.org/books/7736

ANTROPOV, P. JA. (ed.) 1957. *Geology of the USSR. Volume 22-1 Geological description. Turkmen SSR*. Moscow, 658 p. [in Russian] Accessed on March 8, 2017, at http://www.geokniga.org/books/153

BA, J., HAO, Y., LI, J., YAN, X., ZHANG, X. & HE, X. 2015. Rock physics models and quantitative seismic prediction of heterogeneous gas reservoirs-A case study in Metejan area of Amu Darya Basin. *In*: BA, J., DU, Q., CARCIONE, J. M., ZHANG, H. & MÜLLER, T. (eds) *Seismic Exploration of Hydrocarbons in Heterogeneous Reservoirs: New theories, methods, and applications*. Elsevier, Amsterdam, 291-338.

BABADZHANOV, T. L. 2005. *The studying of the pre-Jurassic complexes of the southeastern part of the paleorift system in the Bukhara-Khiva region*. Uzbekgeofizika, report, Tashkent [in Russian].

BABADZHANOV, T. L. 2008. *Summarizing and re-interpretation of the data of the regional, searching and thematic geological-geophysical studies of pre-Jurassic complexes of the Bukhara-Khiva region, made in 1990-2004 years on the base of the modern geological ideas.* Uzbekgeofizika JSC, report, Tashkent, 364 p. [in Russian].

BABADZHANOV, T. L. 2012. *Studying of the structural features of the North-East oriented flexure-break zones and their influence on the character of the sedimentation of the cover, diffusion of the main structural-material complexes of the intermediate structural stage and spacing of the oil and gas deposits.* Uzbekgeofizika*,* Tashkent, 238 p. [in Russian].

BABADZHANOV, T. L. & ABDULLAEV, G. S. (eds) 2009. *The structure features and oil and gas perspectives of the pre-Jurassic complexes of the Bukhara-Khiva region (Western Uzbekistan).* Oil and Gas Institute, Tashkent, 120 p. [in Russian].

BABADZHANOV, T. L., KUNIN, N. Y. & LUK-ZILBERMAN, V. I. 1986. *Structure and petroleum potential of deeply buried complexes of Central Asia from geophysical data*. FAN, Tashkent, 188 p. [in Russian]. Accessed on March 22, 2017 at http://www.jurassic.ru/publ.htm

BABADZHANOV, T. L. & ZUNNUNOV, F. K. 1998. Lithosphere of Central Asia according to geophysics. *The Leading Edge*, **17**, 353-355. ANG

BABADZHANOV, T. L., MORDVINTSEV, O. P. & MORDVINTSEV, D. O. 2012. Deep geological structure as the basis for prediction of placement of mineral deposits in the Central Asia. Proceedings of the All-Russian conference on the genesis of deep oil, Moscow, CGE, 22-25 October 2012, 218-221 [in Russian]. Accessed on March 8, 2017, at www.asgeos.ru/data/Files/File/386.pdf

BABAYEV, A. G. 1976. *Formations, palaeotectonics and oil and gas interest of the Palaeozoic and Mesozoic of Turkmenistan*. Moscow, Nedra, 131 p. [in Russian].

BAKIROV, A. A. 1979. *Oil–gas Provinces and Regions of the USSR.* Nedra, Moscow, 456 p. [in Russian]

BARRIER, E. & VRIELYNCK, B. 2017. *Palaeotectonic maps of Middle East and Western Central Asia from the Middle Permian to the Pliocene.* Scale 1:17 000 000, 20 sheets. CGMW, Paris, ISBN: 9782917310304.

BELENITSKAYA, G. A., 1999. *Litho-geodynamic analysis of salt-bearing sedimentary basins*. Thesis, St Petersburg, 351 p. Accessed on March 11, 2016 at http://www.dissercat.com/content/litologo-geodinamicheskii-analiz-solenosnykh-osadochnykh-basseinov [in Russian]

BELENITSKAYA, G. A., 2000. Distribution pattern of hydrogen sulphide-bearing gas in the former Soviet Union. *Petroleum Geoscience*, **6**, 175–187.

BELENITSKAYA, G. A., 2013. Tectonic Aspects of Spatial and Temporal Allocation of Salt-bearing Basins of the World. *Electronic Scientific Edition Almanac Space and Time. Special Issue 'The Earth Planet System,*

4, 31 p. Accessed on March 8, 2017, at http://j-spacetime.com/actual%20content/t4v1/2227-9490e-aprovr_e-ast4-1.2013.22.php [in Russian].

BELIAYEVSKY, N. A., BORISOV, A. A., VOLVOVSKY, I. S. & SCHUKIN, YU. K. 1968. Transcontinental crustal sections of the U.S.S.R. and adjacent areas. *Canadian Journal of Earth Sciences*, **5**, 1067-1078. doi:10.1139/e68-103

BERRA, F. & ANGIOLINI, L. 2014. The Evolution of the Tethys Region throughout the Phanerozoic: A Brief Tectonic Reconstruction. *In*: MARLOW, L., KENDALL, C. & YOSE, L. (eds) *Petroleum systems of the Tethyan region*. AAPG Memoir **106**, 1–27.

BESNOSOV N. V. & MITTA V. V. 1995. *Upper Jurassic Ammonitids and black shales of Central Asia.* All-Russian Geological Oil Institute (VNIGNI), Moscow, 148 p. [in Russian] Accessed on March 8, 2017, at http://ashipunov.info/jurassic/j/Besnosov,Mitta,1993_Bt-bj_amm.pdf

BISKE YU. S. & SELTMAN R. 2010. Paleozoic Tian-Shan as a transitional region between the Rheic and Urals-Turkestan oceans. *Gondwana Research*, **17**, 602–613.

BISKE, YU. S., KONOPELKO, D. L. & SELTMANN, R. 2013. Geodynamics of Late Paleozoic magmatism in the Tien Shan and its framework. *Geotectonics*, **47**, 291–309.

BLACKBOURN, G. 2008. Enclosure 2—Amu Dar'ya Basin and surrounding areas: Generalised location map showing major structural elements, hydrocarbon provinces, hydrocarbon fields and well locations: Blackbourn Geoconsulting, scale 1:1,350,000. Accessed on February 24, 2017, at http://www.blackbourn.co.uk/reports/amu-darya.html

BOULILA, S., GALBRUN, B., HINNOV, L. A., COLLIN, P.-Y., OGG, J. G., FORTWENGLER, D. &MARCHAND, D. 2010. Milankovitch and sub-Milankovitch forcing of the Oxfordian (Late Jurassic) Terres Noires Formation (SE France) and global implications. *Basin Research*, **22**, 717–732. doi: 10.1111/j.1365-2117.2009.00429.x

BROOKFIELD, M. E. 2000. Geological development and Phanerozoic crustal accretion in the western segment of the southern Tien Shan (Kyrgyzstan, Uzbekistan and Tajikistan). *Tectonophysics*, **328**, 1–14.

BROOKFIELD, M. E. & HASHMAT, A. 2001. The geology and petroleum potential of the North Afghan platform and adjacent areas (northern Afghanistan, with parts of southern Turkmenistan, Uzbekistan and Tajikistan). *Earth-Science Reviews*, **55**, 41–71.

BRUNET M.-F. 1981. Etude quantitative de la subsidence du Bassin de Paris. Thesis 3e cycle Univ. Paris VI, Mém. Sci. Terre Univ. P. & M. Curie n° 81-21, 161 p.

BRUNET, M.-F., MCCANN, T. & SOBEL, E. R. (eds). 2017 *Geological Evolution of Central Asian Basins and the Western Tien Shan Range*. Geological Society, London, Special Publications, **427**.

BRUNET, M.-F., KOROTAEV, M. V., ERSHOV, A. V. & NIKISHIN, A. M. 2003. The South Caspian Basin: a review of its evolution from subsidence modelling. *In*: BRUNET M.-F. & CLOETINGH S. (eds), *Integrated Peri-Tethyan Basins Studies (Peri-Tethys Programme). Sedimentary Geology,* **156**, 119–148.

BRUNET, M.-F., SHAHIDI, A., BARRIER, E., MULLER, C. & SAÏDI, A. 2007. Geodynamics of the South Caspian Basin southern margin now inverted in Alborz and Kopet Dagh (Northern Iran). *In: Abstracts of the European Geosciences Union, General Assembly 2007, Vienna*. Geophysical Research Abstracts, 9, 08080, Accessed on March 8, 2017, at http://www.cosis.net/abstracts/EGU2007/08080/EGU2007-J-08080.pdf

BRUNET, M.-F., SHAHIDI, A., BARRIER, E., MULLER, C. & SAIDI, A. 2010. South Caspian Basin opening: inferences from subsidence analysis in Northern Iran. *In:* VINING, B.A. & PICKERING, S.C. (eds), *Petroleum Geology: From Mature Basins to New Frontiers—Proceedings of the 7th Petroleum Geology Conference*. The Geological Society of London, v. 7, interactive DVD, Poster 1. Accessed on March 8, 2017, at http://www2.geolsoc.org.uk/PGC7/Posters/Poster01Brunet.pdf

BURTMAN V. S. 2006. Tien Shan and high Asia. Tectonics and Geodynamics in the Paleozoic. GEOS, Moscow, 214.

CARMEILLE, M., BOURILLOT, R., BARRIER, E., FÜRSICH, F., THIERRY, J., PELLENARD, P., SCHNYDER, J., AUXIÈTRE, J.-L., MUNSCH, H., MORTVINTSEV, D. & SIDOROVA, I. 2014. Facies, architecture and diagenesis of middle to upper Jurassic carbonates in the Ghissar Range (Uzbekistan). Abstract EGU meeting, 27 April

– 02 May *2014*, Vienna. Accessed on March 8, 2017, at http://meetingorganizer.copernicus.org/EGU2014/EGU2014-12208.pdf

CARMEILLE, M., BOURILLOT, R., BRUNET, M.-F., BARRIER, E., PELLENARD, P., SCHNYDER, J., BLANPIED, C. & SIDOROVA, I. 2016. Facies, architecture and diagenesis of middle to upper Jurassic carbonates: an outcrop analogue for subsurface reservoir prediction (Ghissar - Uzbekistan). AAPG/SEG International Conference & Exhibition, Cancun, Mexico, 6-9 September 2016. Accessed on March 8, 2017, at http://www.searchanddiscovery.com/abstracts/html/2016/90260ice/abstracts/2474332.html

CECCA, F., MARTIN GARIN, B., MARCHAND, D., LATHUILIERE, B. & BARTOLINI, A. 2005. Paleoclimatic control of biogeographic and sedimentary events in Tethyan and peri-Tethyan areas during the Oxfordian (Late Jurassic). *Palaeogeography Palaeoclimatology Palaeoecology*, **222**, 10-32.

CLARKE, J. W. 1988. *Petroleum geology of the Amu-Dar'ya gas-oil province of Soviet Central Asia.* United States Geological Survey Publications Warehouse, Washington DC, United States Geological Survey, Open-File Report, **88–272**, 59. Accessed on March 8, 2017, at http://pubs.er.usgs.gov/publication/ofr88272

CLARKE, J. W. 1994. Petroleum potential of the Amu-Dar'ya Province, Western Uzbekistan and Eastern Turkmenistan. *International Geology Review,* **36**, 407-415.

CLARKE, J. W. & KLESHCHEV K. 1992. Dauletabad-Donmez Field–Commonwealth of Independent States (Former USSR) Amu-Dar'ya Basin, Turkmenistan/Uzbekistan. In: FOSTER, N. H. & BEAUMONT, E. (eds) *Stratigraphic Traps III, Treatise of Petroleum Geology, Atlas of Oil and Gas Fields*, AAPG Tulsa, 285-300.

COHEN, K. M., FINNEY, S. C., GIBBARD, P. L. & FAN, J.-X. 2013. The ICS International Chronostratigraphic Chart. *Episodes*, **36**, 199-204, updated 2016-12 Accessed on March 14, 2017, at http://www.stratigraphy.org/index.php/ics-chart-timescale

DARMAN, H. 2010. Evaporite Deposits in Central Asian Pricaspian and Amu Darya Basins - Stratigraphy, Salt Tectonics and the Potential as Petroleum Seal. Abstract Proceedings KazGeo 2010 – Where Geoscience Meets the Silk Road Almaty, Kazakhstan, 15-17 November 2010, EAGE, 5 p.

DIKENSHTEYN, G. H., ALIEV, I. M., ARZHEVSKIJ G. A., KIROV, V. A., KONTOROVICH, A. JE., MAKSIMOV S. P ET AL. (5 others) (eds) 1977. Petroleum provinces of the USSR. Nedra, Moscow, 328 p.

DOLGOPOLOVA, A., SELTMANN, R., KONOPELKO, D., BISKE, YU. S., SHATOV, V., ARMSTRONG, R., BELOUSOVA, E., PANKHURST, R., KONEEV, R., DIVAEV, F. 2016. Geodynamic evolution of the western Tien Shan, Uzbekistan: Insights from U-Pb SHRIMP geochronology and Sr-Nd-Pb-Hf isotope mapping of granitoids. *Gondwana Research*, doi: 10.1016/j.gr.2016.10.022

DOLITSKAYA, I. V., KUZNETSOVA, K. I. & FORTUNATOVA, N. K. 1984. The Upper Jurassic foraminifera of associations of reef massif at Gaurdak range (south-western Gissar). I*zvestiya Akademii Nauk SSSR, Seria Geologiceskaya A.*, **5**, 80-90 [in Russian].

EGAMBERDIEV, M. E. & ISHNIYAZOV, D. P. 1990. *Comparative lithologic and facial-paleogeographic characteristics of lower and middle Jurassic deposits of South Uzbekistan and North Afghanistan with hypothetical resources evaluation of coalfield.* Final Report (1986-1990) by the Institute of Geology & Geophysics of Academy of Sciences of Uzbekistan, Tashkent, 2 volumes [in Russian].

EVSEEVA, G. B. 2015a. Lithofacies features and reservoir properties of Jurassic terrigenous deposits of the Bukhara-Khiva oil and gas region. Socar Proceedings, **B2**, 4-10 [in Russian], accessed on March 8, 2017, at http://proceedings.socar.az/uploads/pdf/13/Evseeva-4-10.pdf

EVSEEVA, G. B. 2015b. Bukhara-Khiva oil and gas region-depositional environment of the Jurassic carbonate deposits and reservoir rock properties. *Neftegazovaya Geologiya. Teoriya I Praktika*, **10/2** [in Russian]. Accessed on March 8, 2017, at http://dx.doi.org/10.17353/2070-5379/15_2015

EVSEEVA, G. B. 2016. *Features of foraminiferal laws and their change in the context of the Jurassic carbonate formation in the Bukhara-Khiva region*. Unpublished IGIRNIGM report, Tashkent.

FANTI F., CONTESSI M., NIGAROV A. & ESENOV P. 2013. New Data on Two Large Dinosaur Tracksites from the Upper Jurassic of Eastern Turkmenistan (Central Asia). *Ichnos*, **20**, 54–71.

FILIPPOVA, I. B., BUSH, V. A. & DIDENKO, A. N. 2001. Middle Paleozoic subduction belts: The leading factor in the formation of the Central Asian fold-and-thrust belt. *Russian Journal of Earth Sciences,* **3/6**, 405–426.

FORTUNATOVA, N.K. 2000. *Sedimentological modeling of carbonate sedimentary complexes*. REFIA, Moscow, 239 p. [in Russian] Accessed on March 8, 2017, at http://lithology.ru/node/85

FORTUNATOVA, N. K. 2007. Sedimentation models of carbonate alluvial fans - New oil and gas exploration objects. Geologiya Nefti i Gaza, **2**, 61-68 [in Russian].

FÜRSICH, F. T., WILMSEN, M., SEYED-EMAMI, K. & MAJIDIFARD, M. R. 2009a. Lithostratigraphy of the Upper Triassic–Middle Jurassic Shemshak Group of Northern Iran. *In*: BRUNET, M.-F., WILMSEN, M. & GRANATH, J. W. (eds) *South Caspian to Central Iran Basins*. Geological Society, London, Special Publications, **312,** 129–160, http://doi.org/10.1144/SP312.6

FÜRSICH, F. T., WILMSEN, M., SEYED-EMAMI, K. & MAJIDIFARD, M. R. 2009b. The Mid-Cimmerian tectonic event (Bajocian) in the Alborz Mountains, Northern Iran: evidence of the break-up unconformity of the South Caspian Basin. *In*: BRUNET, M.-F., WILMSEN, M. & GRANATH, J. W. (eds) *South Caspian to Central Iran Basins*. Geological Society, London, Special Publications, **312**, 189–203, http://doi.org/ 10.1144/SP312.9

FÜRSICH, F. T., BRUNET, M.-F., AUXIETRE, J.-L. & MUNSCH, H. 2015. Lower-Middle Jurassic facies patterns in the NW Afghan-Tajik Basin of southern Uzbekistan and their geodynamic context. *In:* BRUNET, M.-F., MCCANN, T. & SOBEL, E. R. (eds) *Geological Evolution of Central Asian Basins and the Western Tien Shan Range*. Geological Society, London, Special Publications, **427**. First published online August 6, 2015. http://doi.org/10.1144/SP427.9

GARZANTI, E. & GAETANI, M. 2002. Unroofing history of Late Paleozoic magmatic arcs within the ‘‘Turan Plate’’ (Tuarkyr, Turkmenistan). *Sedimentary Geology*, **151**, 67–87 doi:10.1016/S0037-0738(01)00231-7

GAVRILCHEVA, L. G. & PASHAEV, M. S., 1993. Structure of Upper Jurassic deposits and extension of seismic reflectors in the Amu-Darya basin. *Geologiya Nefti i Gaza*, **11**, 15–20 [in Russian]. Accessed on March 8, 2017, at http://geolib.narod.ru/OilGasGeo/1993/11/Stat/stat04.html

GRACE 2012. G*ravity Recovery And Climate Experiment*. Accessed on March 8, 2017, at http://earthobservatory.nasa.gov/Features/GRACE/ and http://www.gfz-potsdam.de/grace/

GRADSTEIN, F. M., OGG, J. G., SCHMITZ, M. & OGG, G. 2012. *The Geologic Time Scale 2012*. Cambridge University Press, Cambridge.

HEUBECK C. 2001. Assembly of central Asia during the middle and late Paleozoic. In: Paleozoic and Mesozoic tectonic evolution of central Asia: from continental assembly to intracontinental deformation. *Geological society of America Memoir*, **194**, 1–22.

HOLT, P. J., ALLEN, M. B. & VAN HUNEN, J. 2015. Basin formation by thermal subsidence of accretionary orogens. *Tectonophysics,* **639**, 132-143.

HOUSE, M. R., MENNER, V. V., BECKER, R. T., KLAPPER, G., OVNATANOVA, N. S. & KUZ'MIN, V. 2000. Reef episodes, anoxia and sea-level changes in the Frasnian of the southern Timan (NE Russian platform). *In:* INSALACO, E., SKELTON, P. W. & PALMER, T. J. (eds) *Carbonate Platform Systems: components and interactions*. Geological Society, London, Special Publications, **178**, 147-176.

HUGHES, G.W. & NAJI, N. 2008. Sedimentological and micropalaeontological evidence to elucidate post-evaporitic carbonate palaeoenvironments of the Saudi Arabian latest Jurassic. *Volumina Jurassica*, **6**, 61-73.

ISAKSEN, G H. & KHALYLOV, M. 2007. Controls on hydrogen sulphide formation in a Jurassic carbonate play, Turkmenistan. *In*: YILMAZ, P.O. & ISAKSEN, G.H. (eds) *Oil and gas of the Greater Caspian area*. AAPG Studies in Geology, Tulsa, **55**, 133–149.

JABOYEDOFF, M., DERRON, M.-H. & MANBY, G. M., 2005. Note on seismic hazard assessment using gradient of uplift velocities in the Turan block (Central Asia). Natural Hazards and Earth System Sciences, **5**, 43–47.

JOLIVET, M. 2015. Mesozoic tectonic and topographic evolution of Central Asia and Tibet: a preliminary synthesis. *In:* BRUNET, M.-F., MCCANN, T. & SOBEL, E. R. (eds) *Geological Evolution of Central Asian Basins and the Western Tien Shan Range*. Geological Society, London, Special Publications, **427**. First published online September 21, 2015, http://doi.org/10.1144/SP427.2

KEMPE, U., GRAUPNER, T., REIMAR SELTMANN, R., HUGO DE BOORDER, H., DOLGOPOLOVA, A. & MAARTEN ZEYLMANS VAN EMMICHOVEN, M. 2016. The Muruntau gold deposit (Uzbekistan) - A unique ancient hydrothermal system in the southern Tien Shan. *Geoscience Frontiers* **7**, 495-528.

KHAIN, V. E., SOKOLOV, B. A., KLESHCHEV, K. A. & SHEIN, V. S. 1991, Tectonic and geodynamic setting of oil and gas basins of the Soviet Union. *American Association of Petroleum Geologists Bulletin,* **75**, 2, 313–325.

KHUDAYKULEYEV, KH. 1986. Structure of the Upper Jurassic halogen complex and its role in predicting buried reefs in the Amu-Dar'ya regional low. *Novyye dannyye po geologii solenosnykh basseynov Sovetskogo Soyuza*, Moscow, Nauka, 101–115 [in Russian]. English version in *Petroleum Geology*, **23**, (1988) 247–252.

KHUSANOV, S. T. 1984: Stratigraphical significance of Scleractinia in Upper Jurassic carbonates of southern and western Uzbekistan. *Uzbekskii Geologicheskii Zhurnal*, **6**, 53-59.

KHUSANOV, S. T. 1995. Stratigraphy and Scleractinia of Jurassic carbonate reefogenic formations in the South of Central Asia. Thesis Tashkent, 41 p. [in Russian] Accessed on March 8, 2017, at http://earthpapers.net/stratigrafiya-i-sklerati-karbonatnyh-rifogen-yuga-sredney-azii#ixzz433umytny

KIM, A. I., SALIMOVA, F. A., ABDUASIMOVA, I. M. & MESHCHANKINA, N. A. (eds) 2007. *Palaeontological Atlas of Phanerozoic faunas and floras of Uzbekistan. Volume II. Mesozoic and Cenozoic (Jurassic, Cretaceous, Palaeogene).* Republic of Uzbekistan, State committee on geology and mineral resources, Tashkent, 261 p.

KINGSTON, J. 1990. *The Undiscovered Oil and Gas of Afghanistan.* United States Geological Survey, Open-File Report, 90-401. 33 p. Accessed on March 8, 2017, at http://pubs.usgs.gov/of/1990/0401/report.pdf

KINGSTON, J. & CLARKE, J. W. 1995. Petroleum geology and resources of Afghanistan. *International Geology Review*, **37**, 111-127.

KLETT, T. R., ULMISHEK, G. F., WANDREY, C. J., AGENA, W. F. & U.S. GEOLOGICAL SURVEY-AFGHANISTAN MINISTRY OF MINES AND INDUSTRY JOINT OIL AND GAS RESOURCE ASSESSMENT TEAM. 2006. *Assessment of undiscovered technically recoverable conventional petroleum resources of northern Afghanistan. U*nited States Geological Survey, Open-File Report, **2006-1253**, 237 **p.** and 182 figures and plates. Accessed on March 8, 2017, at http://pubs.usgs.gov/of/2006/1253/

KLETT, T. R., SCHENK, C. J., WANDREY, C. J., CHARPENTIER R. R., BROWNFIELD, M. E., PITMAN, J. K., POLLASTRO, R. M., COOK, T. A. & TENNYSON, M. E. 2012. Assessment of Undiscovered Oil and Gas Resources of the Amu Darya Basin and Afghan–Tajik Basin Provinces, Afghanistan, Iran, Tajikistan, Turkmenistan, and Uzbekistan, 2011. United States Department of the Interior, United States Geological Survey, Fact Sheet **2011–3154**, January 2012. 4 p. Accessed on March 8, 2017, at http://pubs.usgs.gov/fs/2011/3154/

KNEPEL, M. N. 2010. *Current status and development trends of the oil and gas complex of Turkmenistan and other Central Asian countries of the near abroad.* Thesis, OAO "All-Russian Research Institute of Geology of Foreign Countries" Moscow, 285 p. [in Russian]

KNYAZEV, V. S. & MAVYYEV, N.Ch. 1974. Sediments underlying the platform cover in the southern part of the Murgab basin. *Doklady Akademii Nauk SSSR*, **215**, 78–81. [in Russian]

KONOPELKO, D., SELTMANN, R., MAMADJANOV, Y., ROMER, R. L., ROJAS-AGRAMONTE, Y., JEFFRIES, T., FIDAEV, D. & NIYOZOV, A. 2016. A geotraverse across two paleo-subduction zones in Tien Shan, Tajikistan. *Gondwana Research*, http://dx.doi.org/10.1016/j.gr.2016.09.010

KOSMINSKAYA, I. P., BELIAYEVSKY, N. A. & VOLVOVSKY, I. S. 1969. Explosionseismology in the U.S.S.R. *In*: Hart, P. J. (ed.). *The Earth's Crust and Upper Mantle*. American Geophysical Union, Washington, Geophysical Monograph Series, **8**, 195-208.

KRYMHOLTS, G. YA., MESEZHNIKOV, M. S. & WESTERMANN, G. E. G. (eds) 1988. The Jurassic ammonite zones of the Soviet Union. *Geological Society of America, Special Paper*, **223**, 1-116.

KRYLOV, N. A. & GRIZIK, A. YA. 2015. New Data on the Structure of Permian–Triassic Complex of the Ustyurt Plateau, Uzbekistan*, Geotectonics,* **49**, 4, 291–301.

LIU, Y.A, YANG, H.A, LIU, Y.A, ZHU, W.A & BIE, Q.B 2013. Characteristics and main controlling factors of the Oxfordian biohermal reservoirs in Girsan of Amu Darya Right Bank, Turkmenistan. *Natural Gas Industry*, **33(3)**, 10-14 [in Chinese with English abstract]. Accessed on March 8, 2017, at http://news.gasshow.com/News/SimpleNews.aspx?newsid=342529

LOUIS-SCHMID, B., RAIS, P., BERNASCONI, S. M., PELLENARD, P., COLLIN, P.-Y. & WEISSERT, H. 2007. Detailed record of mid-Oxfordian (Late Jurassic) positive carbon-isotope excursion in two hemipelagic sections (France and Switzerland): A plate tectonic trigger? *Palaeogeography Palaeoclimology Palaeoecology*, **248**, 459-472. doi:10.1016/j.palaeo.2007.01.001

LU, S.-K., BAO, Z.-H. & YANG, J.-S. 2013. Structural deformation of the Lower-middle Jurassic Series and their trap characteristics in the Amu-Dar'ya right bank area. *Geoscience*, **27**, 774–782 [in Chinese with English abstract].

LYBERIS, N. & MANBY, G. 1999. Oblique to orthogonal convergence across the Turan Block in the Post-Miocene. *American Association of Petroleum Geologists Bulletin*, **83**, 1135–1160.

MAKAROV, V. I., ABDRAKHMATOV, K., YE. ET AL. (45 Authors) 2005. Recent geodynamics of intracontinental areas of collision mountain building (Central Asia). Scientific world, Moscow, 400 p. [in Russian].

MAKSIMOV, S. P. 1987. Oil and gas deposits of the USSR. Moscow, Nedra. 2 volumes 304 p., 360 p. [in Russian]

MAKSIMOV, S. P. (ed.) 1992. Geological Structure of the USSR and patterns of distribution of Economic Minerals, vol 6, Kazakhstan and Central Asia, book 3, Sedimentary cover of Central Asia and south Kazakhstan (Turan plate and adjacent areas), Moscow, Nedra, 148 p. [in Russian]

MARTIN-GARIN, B., LATHUILIERE, B. & GEISTER, J. 2012. The shifting biogeography of reef corals during the Oxfordian (Late Jurassic). A climatic control? *Palaeogeography, Palaeoclimatology, Palaeoecology,* **365–366**, 136–153, http://dx.doi.org/10.1016/j.palaeo.2012.09.022

MAUS, S., BARCKHAUSEN, U., BERKENBOSCH, H., BOURNAS, N., BROZENA, J., CHILDERS, V., DOSTALER, F., FAIRHEAD, J. D., FINN, C., VON FRESE, R. R. B., GAINA, C., GOLYNSKY, S., KUCKS, R., LÜHR, H., MILLIGAN, P., MOGREN, S., MÜLLER, R. D,. OLESEN, O., PILKINGTON, M., SALTUS, R., SCHRECKENBERGER, B., THÉBAULT, E. & CARATORI TONTINI, F. 2009. EMAG2: A 2-arc minute resolution Earth Magnetic Anomaly Grid compiled from satellite, airborne, and marine magnetic measurements. *Geochemistry Geophysics Geosystems*, **10**, 12p. doi:10.1029/2009GC002471 https://produktcenter.bgr.de/terraCatalog/

MCCANN, T. 2016a. The Jurassic of the Western Tien Shan: the Central Kyzylkum region, Uzbekistan. *In:* BRUNET, M.-F., MCCANN, T. & SOBEL, E. R. (eds). *Geological Evolution of Central Asian Basins and the Western Tien Shan Range*. Geological Society, London, Special Publications, **427**. First published online March 31, 2016. http://doi.org/10.1144/SP427.13

MCCANN, T. 2016b. The Cretaceous of the South Kyzylkum and Nuratau region, Western Tien Shan, Central Uzbekistan. *In:* BRUNET, M.-F., MCCANN, T. & SOBEL, E. R. (eds). *Geological Evolution of Central Asian Basins and the Western Tien Shan Range*. Geological Society, London, Special Publications, **427**. First published online April 29, 2016. http://doi.org/10.1144/SP427.14

MELIKHOV, V. N. 2000. Geological framework and ways of implementing the oil and gas potential of the South Turan Plate. Doctor Dissertation, Moscow, 253 p. [in Russian]. Accessed on March 8, 2017, at http://earthpapers.net/geologicheskaya-osnova-i-puti-realizatsii-potentsiala-gazoneftenosnosti-yuga-turanskoy-plity-1

MELIKHOV, V. N. 2008. Oil and gas of the Scythian plate and the adjacent part of the Turan plate. In: BLYUMAN, B. A., KRASNYJ, L. I., PETROV, O. V. & MOROZOV, A. F. (eds), *Tom "Minerageny" Book 2. Mineral resources, geology of mineral deposits over the world, their passive margins, the active zones of transition continent-ocean and ocean continents and passive margins Eurasia Europe, Lesser and Middle Asia and Middle East*. The Planet Earth, the encyclopaedic reference book. VSEGEI, St Petersburg [in Russian].

MELIKHOV, V. N. 2013. Resource potential and exploration prospects of cross-border oil and gas basins of southeastern Turkmenistan, southern Uzbekistan and Tajikistan, northern Afghanistan and northeastern Iran. *Neftegazovaya Geologiya. Teoriya I Praktika,* **8**/1, 28 p. [in Russian]. Accessed on March 8, 2017, at http://www.ngtp.ru/rub/6/6_2013.pdf

MELIKHOV, V. N. 2017. *Geology and oil and gas potential of the Karakum province. Evaluation of oil and gas perspective zones, direction of exploration in the platform part of Turkmenista*. Publishing house of Polytechnic University, St Petersburg [in Russian].

MESEZHNIKOV, M.S. 1988. Oxfordian. In: KRYMHOLTS, G. YA., MESEZHNIKOV, M. S. & WESTERMANN, G. E. G. (eds). The Jurassic ammonite zones of the Soviet Union. *Geological Society of America, Special Paper*, **223**, 39-45.

MIRKAMALOV, H. H., ABDULLAEV, G. S., EVSEEVA, G. B., SUDAREVA, E. U., AHMEDOVA, M. R., HANEEVA, F. R. & MURATOVA, L. M. 2005. *Studying the Jurassic sediments of the Beshkent trough and nearby areas to precise its lithological-facial and stratigraphic structure and to determine its relations with the pre-Mesozoic complexes.* Unpublished report, Oil and Gas Institute, Tashkent, 111 p. [in Russian].

MITTA, V. V. & BESNOSOV, N. V. 2007. Jurassic system Cephalopods. *In*: KIM, A. I., SALIMOVA, F. A., ABDUASIMOVA, I. M. & MESHCHANKINA, N. A. (eds) *Palaeontological Atlas of Phanerozoic faunas and floras of Uzbekistan. Volume II, Mesozoic and Cenozoic*. Republic of Uzbekistan State Committee on Geology and Mineral Resources, Tashkent, 26–41.

MONTENAT, C. 2009. The Mesozoic of Afghanistan. *GeoArabia*, **14**, **1**, 147-210.

MOORE, C. H. & WADE, W. J. 2013. *Carbonate Reservoirs, Porosity and diagenesis in a sequence stratigraphic framewor*k. 2nd Edition. Elsevier, Amsterdam, 392 p.

MORDVINTSEV, D. 2015. *Tectono-stratigraphic evolution of the northern margin of the Amu-Darya basin in Uzbekistan (Bukhara-Khiva and Southwestern Gissar regions)*. PhD Thesis, University P. & M. Curie, Paris, 277 p.

MORDVINTSEV, D., BARRIER, E., BRUNET, M.-F., BLANPIED, C. & SIDOROVA, I. 2017. Structure and evolution of the Bukhara-Khiva region during the Mesozoic: the northern margin of the Amu-Darya Basin (southern Uzbekistan). *In:* BRUNET, M.-F., MCCANN, T. & SOBEL, E. R. (eds) *Geological Evolution of Central Asian Basins and the Western Tien Shan Range*. Geological Society, London, Special Publications, **427**. First published online May 3, 2017, http://doi.org/10.1144/SP427.16

MORDVINTSEV, O. P. 2004. Deep geological structure of the Western Uzbekistan. Thesis, Uzbekgeofizika, Tashkent, 290 p. [in Russian].

MORDVINTSEV, O. P. 2008. *Map of the pre-Jurassic relief of the Bukhara-Khiva region, 1:200 000*. Uzbekgeofizika, Tashkent.

MORDVINTSEV O. P. & MORDVINTSEV D. O. 2011. Nature of the 'anti Tien-Shan' flexure-fault zones and their role in the Central Asia-Kazakhstan region geological structure. Geology and mineral resources, **6**, 41-46, Tashkent [in Russian].

MOROZOV, I. B., MOROZOVA, E. A., SMITHSON, S. B. & LIPOVETSKY, I.A. 2006. Deep seismic sounding profiles for seismic calibration of northern Eurasia. Proceedings of the 28th Seismic Research Review: Ground-Based Nuclear Explosion Monitoring Technologies. Orlando, FL (Sept 19 – 21 2006). Accessed on March 8, 2017, at http://www.ldeo.columbia.edu/res/pi/Monitoring/Doc/Srr_2006/PAPERS/01-16.PDF for data https://ds.iris.edu/

MORTAVAZI, M., MOUSSAVI-HARAMI, R. & MAHBOUBI A. 2013. Detrital Mode and Geochemistry of the Shurijeh Formation (Late Jurassic-Early Cretaceous) in the Central and Western Parts of the Intracontinental Kopet-Dagh Basin, NE Iran: Implications for Provenance, Tectonic Setting and Weathering Processes. *Acta Geologica Sinica*, **87**, 1058-1080.

MOTAVALLI ANBARAN, S. H., ZEYEN, H., BRUNET, M.-F. & ARDESTANI, V. E. 2011. Crustal and lithospheric structure of the Alborz Mountains, Iran, and surrounding areas from integrated geophysical modeling. Tectonics, **30**, doi:10.1029/2011TC002934, 16 pages.

MÜLLER, R. D., SDROLIAS, M., GAINA, C., STEINBERGER, B. & HEINE, C. 2008. Long-term sea-level fluctuations driven by ocean Basin dynamics. *Science*, **319**, 1357–1362.

MUTTONI, G., GAETANI, M., KENT, D. V., SCIUNNACH, D., ANGIOLINI, L., BERRA, F., GARZANTI, E. & ZANCHI, A. 2009. Opening of the Neo-tethys ocean and the Pangea A to Pangea B transformation during the Permian. *Geoarabia*, **14**, 17-48.

NATAL'IN, B. A. & ŞENGÖR, A. M. C. 2005. Late Palaeozoic to Triassic evolution of the Turan and Scythian platforms: The pre-history of the Palaeo-Tethyan closure. *Tectonophysics*, **404**, 175–202 tecto.2005.04.011.

NIE, M., WU, L., SUN, L. & GAO, A. 2013a. Salt-related fault characteristics and their petroleum geological significance in Zarzhu terrace and its adjacent areas, the Amu Darya Basin. *Oil & Gas Geology*, **34**, 803-808 [in Chinese with English abstract] Accessed on July 21, 2014, at http://ogg.pepris.com/EN/abstract/abstract11140.shtml

NIE, M., WU, L., XU, S. & LIU, B. 2013b. Genetic mechanism and exploration significance of tectonic action in the Bieshikent Depression and its adjacent area in the Amu-Darya Basin. *Natural Gas Industry*, **33**(11), 45-50, [in Chinese with English abstract].

NIE, M., XU, S., WU, L., HE, J., MING, H. & ZHANG, R. 2015. Features of gas reservoirs in subsalt faulted reef complex in the right bank of the Amu Darya River, Turkmenistan, and their significance in exploration: A case study of the BP gas reservoir. *Natural Gas Industry*, **35**(6), 24-29, [in Chinese].

NIE, M., TONG, X., LIU, Q., XU, S., WU, L., CHEN, X. & ZHUO, X. 2016. Types of pre-salt carbonate gas reservoirs and hydrocarbon enrichment factors of Amu Darya right bank area in Turkmenistan. Petroleum geology & experiment, **38**, 70-75, doi:10.11781/ sysydz 201601070 [in Chinese with English abstract].

NIKISHIN, A. M., CLOETINGH, S., LOBKOVSKY, L. I., BUROV, E. B. & LANKREIJER, A. C. 1993. Continental lithosphere folding in Central Asia (Part I): constraints from geological observations. *Tectonophysics,* **226**, 59–72.

NIKISHIN, A. M., BRUNET, M.-F., CLOETINGH, S. & ERSHOV, A. V. 1997. Northern Peri-Tethyan Cenozoic intraplate deformations: influence of the Tethyan collision belt on the Eurasian continent from Paris to Tian-Shan. *Comptes Rendus de l'Académie des Sciences Paris*, **324**, 49–57.

NIKOLAEV, V. G. 2002. Afghan–Tajik depression: Architecture of sedimentary cover and evolution. *Russian Journal of Earth Sciences*, **4**, 399–421.

NUGMANOV, A. H. 2010. Laws of formation of traps and oil and gas fields, oil and gas potential of the northern side of the Amu-Darya syncline. Thesis Geology geophysics Institute, Tashkent, Uzbekistan, 48 p. [in Russian]. Accessed on March 8, 2017, at http://uz.denemetr.com/docs/769/index-329222-1.html

NURTAEV B., KHARIN V., MCCANN T. & VALDIVIA-MANCHEGO M. 2013. The North Nuratau Fault Zone, Uzbekistan—Structure and evolution of Palaeozoic Suture Zone. *Journal of Geodynamics*, **64**, 1–14.

NURTAEV, B.S. 2015. Paleozoic sutures, position and role in geological history of South Tien Shan. Geology and mineral resources, **2**, 3-9 [in Russian]. Accessed on March 14, 2017, at gpniimr.uz/press/2_2015.pdf

OGG J. G., HINNOV, L. A. & HUANG, C. 2012. Jurassic. *In*: GRADSTEIN, F. M., OGG J. G., SCHMITZ M. D. & OGG G. M. (eds) *The Geologic Time Scale.* Elsevier, Boston, Chapter 26, 731-791.

OTTO, S. C. 1997. Mesozoic–Cenozoic history of deformation and petroleum systems in sedimentary basins of Central Asia: implications of collisions on the Eurasian margin. *Petroleum Geoscience*, **3**, 327–341.

PASHAYEV, M. S., GAVRIL'CHEVA, L. G. & REDZHEPOV, K. A. 1993. Structure and facies zonality of Lower Cretaceous salt, formation of non-anticlinal traps in southeast Turkmenistan. *Geologiya Nefti i Gaza*, **5**, 15–18, [in Russian] Accessed on March 14, 2017, at http://geolib.narod.ru/Journals/OilGasGeo/1993/05/Stat/04/stat04.html English abstract in *Petroleum Geology,* **28,** (1994) 263–266.

PAVLENKOVA, N. I. 1996. Crust and upper mantle structure in Northern Eurasia from seismic data. In: R. DMOWSKA & B. SALTZMAN (eds). *Advances in Geophysics*, Academic Press, Inc., **37**, 1–133.

PRODEHL, C. & MOONEY, W. D. 2012. *Exploring the Earth's Crust- History and Results of Controlled-source Seismology.* The Geological Society of America Memoir **208**, Boulder, Colorado, USA 764 p.

RADJABOV, S. 2009. Structure and lateral heterogeneity of the Jurassic section of Bukhara-Khiva region supported by the geophysical data. Thesis, National University of Uzbekistan, Tashkent, 293 p. [in Russian]

ROBERT, A. M. M., FERNANDEZ, M., JIMENEZ-MUNT, I. & VERGES, J. 2015. Lithospheric structure in Central Eurasia derived from elevation, geoid anomaly and thermal analysis. In: Brunet, M.-F., McCann, T. & Sobel, E. R. (eds) *Geological Evolution of Central Asian Basins and the Western Tien Shan Range*.

Geological Society, London, Special Publications, **427**. First published online September 7, 2015, http://doi.org/10.1144/SP427.10

ROBERT, A. M. M., LETOUZEY, J., KAVOOSI, M. A., SHERKATI, S., MÜLLER, C., VERGÉS, J. & AGHABABAEI, A. 2014. Structural evolution of the Kopeh Dagh fold-and-thrust-belt (NE Iran) and interactions with the South Caspian Sea Basin and Amu Darya Basin. *Marine and Petroleum Geology*, **57,** 68–87.

RYABOY, V. Z. 1967. Structure of Earth's crust and upper mantle along deep seismic profile (Kopet-Dag to Aral Sea). *International Geology Review*, **9**, 296-299.

RYABOY, V. 1968. Structure of the Earth's crust and upper mantle in the central regions of Turkmenia according to deep seismic sounding data (DSS). *In*: E. BISZTRICSÁNY (ed.), *Proceedings of the Eighth Assembly of the European Seismological Commission*, Akadémiai Kiadó, Budapest, 216-221.

SAINTOT A., BRUNET M.-F., YAKOVLEV F., SÉBRIER M., STEPHENSON R., ERSHOV A., CHALOT-PRAT F. & MC CANN R. 2006. The Mesozoic-Cenozoic tectonic evolution of the Greater Caucasus. In: R. A. STEPHENSON & D. G. GEE Eds, European Lithosphere Dynamics, Geological Society of London Memoirs, **32**, 277-289.

SARG, J. F. 2001. The sequence stratigraphy, sedimentology, and economic importance of evaporite–carbonate transitions: a review. *Sedimentary Geology*, **140**, 9-42.

SELTMANN, R., KONOPELKO, D., BISKE, G., DIVAEV, F. & SERGEEV, S. 2011. Hercynian postcollisional magmatism in the context of Paleozoic magmatic evolution of the Tien Shan orogenic belt. *Journal of Asian Earth Sciences,* **42**, 821–838.

SEREGIN, A. M., BURLIN, YU. K. & SOKOLOV, B. A. 1979. Kara Kum Basin. *Petroleum Geology*, **16,** 46-50, English abstract of Russian paper, Osnovy regional'noy neftegazonosnosti SSSR: Moscow, *Izdvestia Moskovskogo Universiteta*, 101–111, 1977.

ŞENGÖR A.M.C., NATAL'IN B., VAN DER VOO R. & SUNAL G. 2014. A new look at the Altaids: A superorogenic complex in northern and central Asia as a factory of continental crust. Part II: palaeomagnetic data, reconstructions, crustal growth and global sea-level. *Austrian Journal of Earth Sciences*, **107/2**, 131–181.

SHAHIDI, A. 2008. Evolution Tectonique du nord de l'Iran (Alborz et Kopet Dagh) depuis le Mésozoïque. PhD Thesis Univ P. and M. Curie, Paris, 500 p.

SHAYAKUBOV, T. SH. (ed.) 1998. *Geological map of Uzbekistan, Scale 1:500 000*. State Committee for Geology and Mineral Resources of the Republic of Uzbekistan, Tashkent.

SHAYAKUBOV, T. SH. & DALIMOV, T. N. (eds) 1998. *Geology and mineral resources of the Republic of Uzbekistan*. National University of Uzbekistan, Tashkent, 723 [in Russian].

SHEIKH-ZADE, E. R., 1996. Results of seismic reflection profiling in the Turanian Platform. *Tectonophysics,* **264**, 123–135.

SIDOROVA, I. P. & GOLOVKO, E. A. 2015. Deep structure of the lithosphere in Uzbekistan. Proceedings of the Conference "Actual problems of geology, geophysics and metallogeny" 5-6 May 2015, Tashkent, 49-53 [in Russian] Accessed on March 14, 2017, at http://ingeo.uz/library/ScientificConference/Actual%20problems%20of%20geology,%20geophysics%20and%20metallogeny.pdf

SIEHL, A. 2015. Structural setting and evolution of the Afghan orogenic segment – a review. In: Brunet, M.-F., McCann, T. & Sobel, E. R. (eds) *Geological Evolution of Central Asian Basins and the Western Tien Shan Range*. Geological Society, London, Special Publications, **427**. First published online August 3, 2015, http://doi.org/10.1144/SP427.8

SLIKIN, V. A. 1966. New data on the structure of the main structural elements of central Turkmenistan. *In*: AGRANOVSKII L. E. & AMURSKII G. I., *Tectonics of Turkmenistan and neighboring areas*. Nauka, Moscow, 77-81 [in Russian]. Accessed on March 22, 2017, at http://www.geokniga.org/books/7736

SMIT, J. H. W., CLOETINGH, S. A. P. L., BUROV, E., TESAURO, M., SOKOUTIS, D., & KABAN, M. 2013. Interference of lithospheric folding in western Central Asia by simultaneous Indian and Arabian plate indentation. *Tectonophysics,* **602,** 176–193. http://doi.org/10.1016/j.tecto.2012.10.032

STECKLER, M. S. & WATTS, A. B. 1978. Subsidence of the atlantic-type continental margin off New York. *Earth and Planetary Science Letters*, **41**, 1–13.

TAHERI, J., FÜRSICH, F. T. & WILMSEN, M. 2009. Stratigraphy, depositional environments and geodynamic significance of the Upper Bajocian-Bathonian Kashafrud Formation, NE Iran. *In*: BRUNET, M.-F., WILMSEN, M. & GRANATH, J. W. (eds) *South Caspian to Central Iran Basins*. *Geological Society, London, Special Publications*, **312**, 205–218.

TEVELEV, A. V. & GEORGIEVSKII, B. V. 2012. Deformation history and hydrocarbon potential of the Southwestern Gissar Range (Southern Uzbekistan). *Moscow University Geology Bulletin*, **67**, 340–352.

THOMAS, J.-C., COBBOLD, P. R., SHEIN, V. S. & LE DOUARAN, S. 1999a. Sedimentary record of late Paleozoic to Recent tectonism in central Asia – analysis of subsurface data from the Turan and south Kazak domains. *Tectonophysics,* **313**, 243–263.

THOMAS, J. C., GRASSO, J. R., BOSSU, R., MARTINOD, J. & NURTAEV, B. 1999b. Recent deformation in the Turan and South Kazakh platforms, western central Asia, and its relation to Arabia-Asia and India-Asia collisions. *Tectonics*, **18**, 201-214.

TORRES, M.A. 2007. The Petroleum Geology of Western Turkmenistan: The Gograndag-Okarem Province. *In*: YILMAZ, P.O. & ISAKSEN, G.H. (eds). *Oil and gas of the Greater Caspian area*. AAPG Studies in Geology, Tulsa, **55**, 109–132.

TROITSKY, V. I., 2012 Oceanic basins and fold system of the Middle and High Asia. LAP, Lambert Academic Publishing, 262 p. [in Russian].

ULMISHEK, G. F. 2004. Petroleum Geology and Resources of the Amu-Darya Basin, Turkmenistan, Uzbekistan, Afghanistan, and Iran. *United States Geological Survey Bulletin*, **2201–H**, 32 p. Accessed on March 8, 2017, at http://pubs.usgs.gov/bul/2201/H/

VNIGNI & BEICIP FRANLAB, 1992. Petroleum potential of Central Asia. Beicip Franlab, Rueil-Malmaison, 2 vol.

VOL'VOVSKIY, I. S., GARETSKIY, R. G., SHLEZINGER, A. E. & SHRAYBMAN, V. I. 1966. Tectonics of the Turan plate. Nauka, Moscow. 287 p. [In Russian, Table of Contents in English].

WANG, H.-F., CHEN, H.-L., WANG, W.-B., YAO, W.-J., SUN, L., WANG, Z.-F. & WEN, T. 2014a. Controlling factors of the oil and gas differential distribution in the East of Amu-Darya Basin of Northern Afghanistan. *Natural Gas Geoscience*, **25**, 860-866 (in Chinese with English abstract).

WANG, Q., YAN, X., XU, W.-L, ZHENG, R.-C, LI, F.-J., WANG, X.-Z. & WU, L. 2014b. Sequence-paleogeographic characteristics and evolution of Callovian-Oxfordian in Amu Darya Basin, Turkmenistan. *Geology and Exploration*, **50**, 795-804 [in Chinese with English abstract].

WEN, H., GONG, B., ZHENG, R., LIU, H. WU, L., CHEN, R., LI, S. & CHEN, S. 2012. Deposition and Diagenetic System of Carbonate in Callovian-Oxfordian of Samandepe Gasfield, Turkmenistan. Journal of Jilin University (Earth Science Edition), **42**, 991-1002 [in Chinese with English abstract].

WILMSEN, M., FÜRSICH, F. T., SEYED-EMAMI, K. & MAJIDIFARD, M. R. 2009. An overview of the stratigraphy and facies development of the Jurassic System on the Tabas Block, east-central Iran. *In*: BRUNET, M.-F., WILMSEN, M. & GRANATH, J. W. (eds) *South Caspian to Central Iran Basins*. Geological Society, London, Special Publications, **312**, 323–343, http://doi.org/ 10.1144/SP312.15

WYNN, J., ORRIS, G. J., DUNLAP, P., COCKER, M. D. & BLISS, J. D. 2016. Geology and undiscovered resource assessment of the potash-bearing Central Asia Salt Basin, Turkmenistan, Uzbekistan, Tajikistan, and Afghanistan. United States Geological Survey Scientific Investigations Report **SIR 2010–5090–AA**, 106 p., and spatial data. Accessed on March 8, 2017, at *http://dx.doi.org/10.3133/sir20105090AA*

XU, W., ZHENG, R., FEI, H., WANG, Q. & WU, L. 2012. The sedimentary facies of Callovian-Oxfordian stage in Amu Darya Basin, Turkmenistan. *Geology in China*, **39**, 954-964 [in Chinese with English abstract].

YAKUBCHUK, A., COLE, A., SELTMANN, R. & SHATOV, V. 2002. Tectonic setting, characteristics, and regional exploration criteria for gold mineralization in the Altaid orogenic collage: the Tien Shan province as a key example. *Society of Economic Geologists Special Publication* **9**, 177-201.

YEGORKIN, A. V. & MATUSHKIN, B. A. 1970. Crustal structure of the Caucasus and Western Central Asia based on geophysical sounding data. *International Geology Review*, **12,** 281–290.

ZAKIROV A. SH. 2011. Results of the application of multi-level technology studies of the deep structure of Central Asia. Proceedings of the Russian State University of Oil and Gas, **2(263)**, 5-12. Accessed on March 8, 2017, at http://article.gubkin.ru/ru/archive/2

ZANCHETTA, S., BERRA, F., ZANCHI, A., BERGOMI, M., CARIDROIT, M., NICORA, A. & HEIDARZADEH, G. 2013. The record of the Late Palaeozoic active margin of the Palaeotethys in NE Iran: Constraints on the Cimmerian orogeny. *Gondwana Research*, **24**, 1237–1266. http://dx.doi.org/10.1016/j.gr.2013.02.013

ZANCHI, A., ZANCHETTA, S., BALINI, M. & GHASSEMI, M. R. 2016. Oblique convergence during the Cimmerian collision: Evidence from the Triassic Aghdarband Basin, NE Iran. *Gondwana Research,* **38**, 149-170. http://dx.doi.org/10.1016/j.gr.2015.11.008

ZHENG, R., LI, Y., WU, L., WU, X, LI, F. & NIU, G. 2011. Geochemical Characteristics of Callovian–Oxfordian carbonates in Samandepe gas field, Amu Darya Basin, Turkmenistan. *Petroleum Science*, **8**, 371–381. doi:10.1007/s12182-011-0155-8

ZHENG, R., PAN, Y., ZHAO, C., WU, L., CHEN, R. & YANG, R. 2013. Carbon and Oxygen Isotope Stratigraphy of the Oxfordian Carbonate Rocks in Amu Darya Basin. *Journal of Earth Science*, **24**, 42–56.

ZHENG, R., CHEN, H., WANG, Q., CUI, C., FEI, H. & XU, W. 2014. The reservoir characteristics and their controlling factors of Callovian-Oxfordian carbonates in Amu Darya Basin. *Acta Petrologica Sinica*, **30,** 779-788 [in Chinese with English abstract].

Figures captions

Fig. 1. Location map of major structures of the Amu Darya and Afghan-Tajik basins.
Compiled from Melikhov (2000), Brookfield & Hashmat (2001), Abidov *et al.* (2004), Blackbourn (2008), Siehl (2015), Kempe *et al.* (2016), Zanchi *et al.* (2016). Background. Topography: USGS SRTM; Colours on geological map: blue Jurassic, green Cretaceous, red and reddish-blue magmatic, volcanic rocks, yellow Cenozoic. Scale bar at 36° latitude. Projection world Mercator, conformal projection preserving angles but not distances.
Inset map shows location of Figure 1 in western Central Asia region. Afgh: Afghanistan; ATB: Afghan-Tajik Basin; Cauc: Caucasus; KD: Kopet-Dagh; Kyr: Kyrgyzstan; Tad: Tajikistan; Tur: Turkmenistan; Uzb: Uzbekistan.
Ornamented blue-green line: contours of the Amu Darya and Afghan-Tajik basins (after Melikhov 2000; modified). Green solid line with dark dashes: political boundaries; light brown areas: main swells and uplift zones at depth. Thin black dotted lines: boundaries of some sub-areas, more details can be found in Blackbourn (2008) and Melikhov (2013). Red lines or dotted lines show approximate location of main structures: flexure zones, thrusts or faults without indication of movement. For simplification they are drawn very schematically with long continuous lines although some are actually segmented, only a few faults are drawn in the mountainous areas to show the general trend. Red large dashed lines show approximate location of the Turkestan suture to the north and Palaeo-Tethys suture to the south; the location is often not well determined.
Colour of names: darkest blue or yellow: mountains or highs; middle dark blue: step/bench, homocline/slope; light blue: depression, trough; dark brown: high/arch inside the basins; light brown: swell/ zone of uplift; red: faults/zone of flexure.
.
ADF, Amu Darya Fault; Agh, Aghdarband; Andkhoy U., Andkhoy zone of uplifts; Au, Auminzatau; B, Basin; Ba, Bagadzha swell; BaF, Bagadzha Fault; Bay, Bayramali field and swell; BuF, Bukhara Fault; D, Dep, Depression; DaD, Dauletabad Donmez field and high; De, Dengizkul Arch; F, Fault; Ga, Gaurdak; Gaz, Gazli field and high; Gg, Gagarin field and swell; GB, Great Balkhan; Io, Iolotan field and swell (= part of Galkynysh); Ka, Kagan Arch; Kd, Kandym-Alat Arch; KF, Karshi Fault; Kg, Kugitang Mts; Kh, Khiva; Ki, Kirpichili swell; KML, Khiva-Murgab Lineament; Ku, Kuldzhuktau Mts; Kushka U., Kushka zone of uplift; Ky, Kyzylkum Trough =(Karakul rift, Kimerek graben for one part); Ma, Mary-Serakhs uplift zone; Mts, Mountains; Mu, Mubarek Arch; MuF, Murgab Fault; Os, Osman field and swell; R, Range; RF, Repetek Fault; RKU, Repetek-Kelif zone of uplifts; Rom, Rometan Trough; SG, Sultan Sandzhar Gugurtli Arch; Sh, Shatlyk field and swell; Su, Sultanuizdag Mts; T, Trough; TFF, Talas Fergana Fault; Tu, Tubegatan; U, Uplift ; Uc, Uchkyr Arch; UKFFZ, Uchbash-Karshi Flexure Fault Zone; Ya, Yashlar field and swell; Ye, Yelan field and swell; Yg, Yangikazgan Arch.

Fig. 2. Synthetic lithostratigraphic column of the Amu Darya Basin, highlighting main unconformities and tectonic events (after VNIGNI & Beicip Franlab 1992; Melikhov 2000; Klett et al. 2006; Nugmanov 2010; Knepel 2010; Evseeva 2015b; Jolivet 2015; Siehl 2015). The lithologies are simplified into clastics, carbonates and evaporites. Some names of formations of the Bukhara-Khiva and Murgab regions are indicated. Possible hiatus are only displayed for the Triassic to Middle Jurassic.

Fig. 3. Representative outcrops of Jurassic units in the Southwestern Gissar Mountains.
(a) Locations are indicated on the geological map of Uzbekistan 1:500 000 (Shayakubov 1998); Jurassic rocks are shown in blue.
(b) Lower Jurassic siliciclastic unit in Boysun (Uzbekistan) (pen for scale);
(c) upper Middle-Upper Jurassic carbonate unit in Derbent (Uzbekistan);
(d) upper Middle-Upper Jurassic carbonate unit in the southwest of Kugitang Mountains (Turkmenistan). R, reef build-up;
(e) Upper Jurassic Gaurdak evaporites in Langar (Uzbekistan) (hammer for scale).

Fig. 4. Magnetic and gravimetric anomalies in the Amu Darya and Afghan-Tajik basins.
Anomalies are overlaid on the shaded relief (SRTM) map; main names, faults and contour of areas are indicated to aid identification of locations, see caption of Fig. 1 for nomenclature.
Scale bar at 36° latitude. Projection world Mercator, conformal projection preserving angles but not distances.
Ornamented blue green line: contours of the Amu Darya and Afghan-Tajik basins; green line: political boundaries; red lines schematized faults; thin black dotted lines: boundaries of some sub-areas. Red large dashed lines show approximate location of suture zones.

(a) Magnetic anomalies from Emag2 (Maus *et al.* 2009). VBK, Valerianov- Beltau-Kurama arc (Yakubchuk *et al.* 2002)
(b) Gravity anomalies from GRACE (Gravity Recovery And Climate Experiment) satellite mission (GRACE 2012; http://www.gfz-potsdam.de/grace/)

Fig. 5. Depth-structure map to the basement, pre-Upper Carboniferous or Permian; modified after Melikhov (2000) for the Turkmenistan and western Uzbekistan parts; modified from O. Mordvintsev, in Babadzhanov (2008), for eastern Uzbekistan.
Depth-structure map represents depth below mean sea-level, implying that altitude must be added to get the real depth from the surface of the ground.
Scale bar at 36° latitude. Projection world Mercator, conformal projection preserving angles but not distances.
Blue green line with black dots: contour of the Amu Darya and Afghan-Tajik basins; green lines with black dashes: political boundaries; red lines schematized faults. See Figure 1 for meaning of acronyms.

Fig. 6. Depth-structure maps to some important stratigraphic horizons (modified after Melikhov 2000, 2017). Depths are shown below mean sea-level, implying that altitude must be added to get the real depth from the surface of the ground. Scale bar at 36° latitude. Projection world Mercator, conformal projection preserving angles but not distances.
Blue green line with black dots: contour of the Amu Darya and Afghan-Tajik basins; green lines with black dashes: political boundaries; red lines schematized faults. See Fig. 1 for meaning of acronyms.
(a) Base of the Jurassic. Intermediate isolines every 500 m down to 8 km. The deepest areas and corresponding contours are rather hypothetical as few deep seismic lines are available.
(b) Top of the upper Middle-Upper Jurassic carbonates (i.e. base of the Gaurdak Formation). Age between latest Oxfordian and Late Kimmeridgian. Additional isolines represent the shape of the depocentres.
Dashed pink line: boundary of salt in the Gaurdak Upper Jurassic Formation. Cross hatched area, upper Middle-Upper Jurassic carbonate unit absent; simple hatched area, carbonate unit partly eroded.
(c) Base of the Cretaceous (top of the Karabil Formation, Berriasian?). Dashed blue line: boundary of the stratigraphic pinch out of Upper Jurassic; dashed pink line: boundary of salt in the Gaurdak Upper Jurassic Formation.
(d) Top of the Palaeocene. Black dashed line: Palaeo-Amu Darya incised River valley and erosion of the Bayramali high. Intermediate isolines within the color ranges every 200 m except the isolines x600 m that are instead replaced by the color boundaries at x500 m.

Fig. 7. Isopach maps of selected sedimentary sequences in the Amu Darya Basin (modified after Melikhov 2000, 2017). The maps generally do not display thicknesses on the Bukhara and Chardzhou steps in Uzbekistan as they were drawn with data from Turkmenistan; only the map of the Lower-Middle Jurassic covers the southern part of the Chardzhou Step and the Beshkent Depression.
Scale bar at 36° latitude. Projection world Mercator, conformal projection preserving angles but not distances.
Blue green line with black dots: contour of the Amu Darya and Afghan-Tajik basins; green lines with black dashes: political boundaries. See Fig. 1 for meaning of acronyms.
(a) Lower to Middle Jurassic siliciclastic unit. The Lower Callovian siliciclastic layer is excluded because of the progressive enrichment in carbonate, it is grouped with the overlying carbonate unit.
(b) upper Middle-Upper Jurassic carbonate unit. Age Lower Callovian to Oxfordian or Kimmeridgian, see text for explanation; dashed pink line: boundary of salt in the Gaurdak Upper Jurassic Formation; purple areas: main oil-gas fields inside the Callovian-Oxfordian carbonate reservoirs sealed by the Gaurdak evaporites.
(c) Upper Jurassic to Berriasian series. This isopach map includes the Gaurdak carbonates-evaporites Formation, from latest Oxfordian? or Kimmeridgian to Tithonian or Tithonian only, see text for explanation, the Karabil red sequence of Late Tithonian? to Berriasian age; and a carbonate layer in the south and northwest of the ADB; dashed pink line: boundary of salt in the Gaurdak Upper Jurassic Formation; cross hatched area: deposits absent.
(d) Berriasian? or Valanginian to Lower Barremian. Purple small areas: main reservoirs of hydrocarbon fields present only in this series. Green dashed line: boundary of Hauterivian salt and sandstones, which blocks hydrocarbons migration.
(e) Upper Barremian-Aptian
(f) Albian-Cenomanian
(g) Turonian-Maastrichtian
(h) Paleocene
(i) Eocene-Oligocene

(j) Neogene-Quaternary. Black dashed line: Palaeo-Amu Darya incised River valley and erosion of the Bayramali high.

Fig. 8. 2-D backstripping along three general cross-sections of the Amu Darya Basin showing basin evolution during Mesozoic through the Present. Compaction of sediments, flexural loading and effect of estimated water depth are taken into account.
(a) Location map: depth contour map (below mean sea-level) of the basement (shown in Fig. 5, see Fig. 1 for meaning of acronyms).
(b) Cross-section 1: NNE-SW-trending, from Gazli on the Bukhara Step to the pre-Kopet-Dagh Foredeep (data modified from Bakirov 1979; Brookfield & Hashmat 2001; Isaksen & Khalylov 2007). In light purple, the Palaeozoic sub-basins of Chardzhou and Bagadzha steps are shown (modified from Thomas *et al.* 1999a and Melikhov 2000).
(c) Cross-section 2: NE-S-trending, from the Bukhara Step to the Kalaymor Trough (data modified from VNIGNI & Beicip Franlab 1992).
(d) Cross-section 3: WNW-ESE-trending, from the Central Karakum Arch to the Beshkent Depression (data modified from VNIGNI & Beicip Franlab 1992).

Fig. 9. Cross-sections through the mains parts of the Amu Darya Basin, drawn at the same scale, simplified from Melikhov (2000, 2008, 2017). Location of the boreholes used for construction is indicated by vertical thin black lines down to the depths reached. Location map: depth contour map (below mean sea-level) of the basement (shown in Fig. 5).
ADF, Amu Darya Fault; AFGH, Afghanistan; Alb, Albian; Apt, Aptian; Bar, Barremian; Berr, Berriasian; Bt, Bathonian; C, Cretaceous; Call, Callovian; F, Fault; Fm, Formation; H, High; Km, Kimmeridgian; l, lower; m, middle; N, Neogene; Ox, Oxfordian; Q, Quaternary; RF, Repetek Fault; SW, Southwestern; T, Trough; Tt, Tithonian; TURKM, Turkmenistan; u, upper; UKFFZ, Uchbash-Karshi Flexure Fault Zone; UZBEK, Uzbekistan; Val, Valanginian.

Fig. 10. Structures and cross-sections along the northeastern margin of the Amu Darya Basin.
(a) Synthetic map showing the main orientation of structural features and a literature-based model for the deposition of the carbonates during the late Middle-Late Jurassic. The carbonate build-up contours are compiled according to the "barrier reef model" (barrier reef in dark blue, basinal part in light blue, isolated reefal build-ups in light purple) of Fortunatova (2007) in Turkmenistan, G. Evseeva in Babadzhanov (2012) and Evseeva (2015b) for the Uzbekistan part, Wang *et al.* (2014b) for the Amu Darya right bank in Turkmenistan. The inset map shows the location of the main map on the northeastern margin of the ADB.
Dashed green-black line: Uzbekistan-Turkmenistan political border. Dotted black lines: contours of Beshkent Trough, Karabekaul Trough, Uchadzhi-Kurama Arch and Obruchev Trough.
Locations of cross-sections. The solid orange line locates the part of the section shown in part (b). Orange line (solid and dashed): part of the cross-section 4 of Figure 9; green line: part of the cross-section H-H' shown in Mordvintsev *et al.* (2017). Four lettered, black solid lines mark location of seismic lines of Lu *et al.* (2013) shown in part (c).
The faults, in red, are compiled from Blackbourn (2008), Melikhov (2008, 2017), Lu *et al.* (2013), Mordvintsev (2014), Mordvintsev *et al.* (2017), Nie *et al.* (2016). F1 to F5 refer to faults shown on the seismic lines in part (c) of this figure.
Ak, Akkumulyam; Aka, Akayri; BB, Bereketli-Bota; Be, Beshkent; Dug, Dugoba; El, El'dzhik; Far, Farab; Gau, Gaurdak; Gir, Girsan; Ka, Kamashi; Ko, Kokdumalak; N-Ur, North Urtabulak; Pa, Pamuk; Met, Metedzhan; N-Al, North Alan; N-Ni, North Nishan; Sam, Samantepe; Sak, Sakar; Sh, Shurtan; Ta, Tangikuduk; Tu, Tubegatan; TURK, Turkmenistan; UKFFZ, Uchbash Karshi Flexure Fault Zone; Ur, Urtabulak; UZB, Uzbekistan; Ya, Yankui; Ze, Zevardi.
(b) Detailed portion of cross-section 7 shown in Figure 9 (modified after Melikhov 2000, 2008, 2017); same colour key as in Figure 9. In the Gaurdak series, the three levels of anhydrite are drawn in dark pink and the two salt levels in pink. The uppermost level of the Jurassic succession (upper anhydrite) is differentiated from the Lower Cretaceous Karabil level.
(c) Examples of seismic lines (in ms TWT) showing the steps delineated by normal faults (modified from Lu *et al.* 2013, by courtesy of Dr Shi Kuo Lu). The lines are calibrated by the wells Samantepe 24 (Sam 24) on the line AA', and Metedzhan 2 (Met 2) on the line DD', the upper, Cenozoic part is not shown.
Labeled reflectors and color code: T5, top K2 (Upper Cretaceous in light green); T7, top Cenomanian; T8, top K1 (Lower Cretaceous in dark green); T9, top Aptian; T11, top J3 (Upper Jurassic mainly Gaurdak Formation

in pink); T14, top Callovian-Oxfordian (carbonate formation in light blue); T16, top J2; T16-1, J2 top of the lower sequence boundary (siliciclastic formation in dark blue); T16', Top J1; Tg, Top of the Palaeozoic basement. F1-5 faults located on map (a); ADF, probable location of Amu Darya Fault.

Fig. 11. Features of the northeastern margin of the Amu Darya Basin during the Jurassic. Dashed green-black line: Uzbekistan-Turkmenistan political border.
(a) Isopach map of the Lower to Middle Jurassic siliciclastic succession, excluding the Lower Callovian; see Fig. 7a for the full map (modified after Melikhov 2000, 2017). Main orientation of structural features (in red) and contour of carbonate build-ups (in light grey) from Fig. 10a (after Fortunatova 2007; Blackbourn 2008; Melikhov 2008, 2017; Lu *et al.* 2013; Mordvintsev 2014; Wang *et al.* 2014b; G. Evseeva in Babadzhanov 2012; Evseeva 2015b; Nie *et al.* 2016; Mordvintsev *et al.* 2017). See Fig. 1 for meaning of acronyms.
(b) Composite map. In northern portion, depth-structure map (below mean sea-level) to the base of the Jurassic in part of Uzbekistan (modified after Mordvintsev *et al.* 2017 from Mordvintsev 2008). Colour caption is in the top right corner. Main structural features are shown in red. Magnetic anomalies from Emag2 (Maus *et al.* 2009) are superimposed on SRTM topography in the remaining parts of Uzbekistan and Turkmenistan. Dotted black lines: outlines of Beshkent Trough, Karabekaul Trough, Uchadzhi-Kurama Arch and Obruchev Trough.

Fig. 12. Subsidence evolution of deep parts of the Amu Darya Basin. (a) Location map: depth-structure map (below mean sea-level) of the basement (shown in Fig. 5, see Fig. 1 for meaning of acronyms). B, Bayramali pseudo-well; I, Izgant pseudo-well; Ki, well Kimerek 4; Ku, East Kulach pseudo-well. Location of the points are also indicated on the cross-sections in Fig. 9.
(b) Subsidence curves. Colour of name of each well/pseudo-well matches colour of associated curves. Top curve, tectonic subsidence in free air; bottom curve, total subsidence, corrected for compaction, sea-level and bathymetry. Subsidence curves of Kimerek 4 well are modified after Mordvintsev (2015).
(c) Comparison of the tectonic subsidence rates.
General parameters used for subsidence calculations: International Chronostratigraphic Chart of 2016 (Cohen *et al.* 2013 updated), eustatic sea-level variations are the first order curves of Haq (2014; in Sengör *et al.* 2014), but calibrated with a maximum of 170 m during the Late Cretaceous transgression (maximum average value of Müller *et al.*, 2008). The assumed density of the mantle for local Airy isostatic compensation is 3.2 g/cm^3. Porosity/depth laws and grain densities are modified from Brunet (1981).

Fig. 13. Legend for the maps shown in Figs. 14 and 15 (modified after Barrier and Vrielynck 2017).

Fig. 14. The Amu Darya Basin in the geodynamic context of western Central Asia at different stages from the Late Permian to the Middle Aptian. Modified after palaeotectonic maps of Barrier and Vrielynck (2017). Legend: see Fig. 13.
ADB, Amu Darya Basin; ArP, Arabian Platform; ATB, Afghan Tajik Basin; BB, Band-e Bayan block; CIr, Central Iran; CP, Central Pamir block; He, Helmand block; HK, Hindu Kush arc; KD, Kopet-Dagh; Kh, Kandahar arc; Kk, Karakoram block; KTuL, Kugitang-Tunka line; Lh, Lhasa block; NIr Alb, North Iran Alborz block; NP, North Pamir block; PB; Pamir Basin; Qi, Qiantang block; SC, South Caspian Basin; SP, South Pamir block; TaB, Tarim Basin; TFF, Talas Fergana Fault; WP, Waras-Panjaw ocean then suture.

Fig. 15. Deposition of evaporites during Late Jurassic times on the southern and northern margins of the Neo-Tethys (modified after the palaeotectonic map of Barrier and Vrielynck 2017). Legend: see Fig. 13; evaporites are shown in pink. ADB, Amu Darya Basin; ArP, Arabian Platform; ATB, Afghan Tajik Basin; Ca, Great Caucasus Basin; CiI, Central Iran; CP, Central Pamir block; Ga, Gaurdak Formation; He, Helmand block; Hi, Hith Formation; Kb, Kabul block; KD, Kopet-Dagh; Kh, Kandahar arc; Kk, Karakoram block; KTuL, Kugitang-Tunka line; Lh, Lhasa block; PB, Pamir Basin; Qi, Qiantang block; SC, South Caspian Basin; SP, South Pamir block; TaB, Tarim Basin; WP, Waras-Panjaw suture.

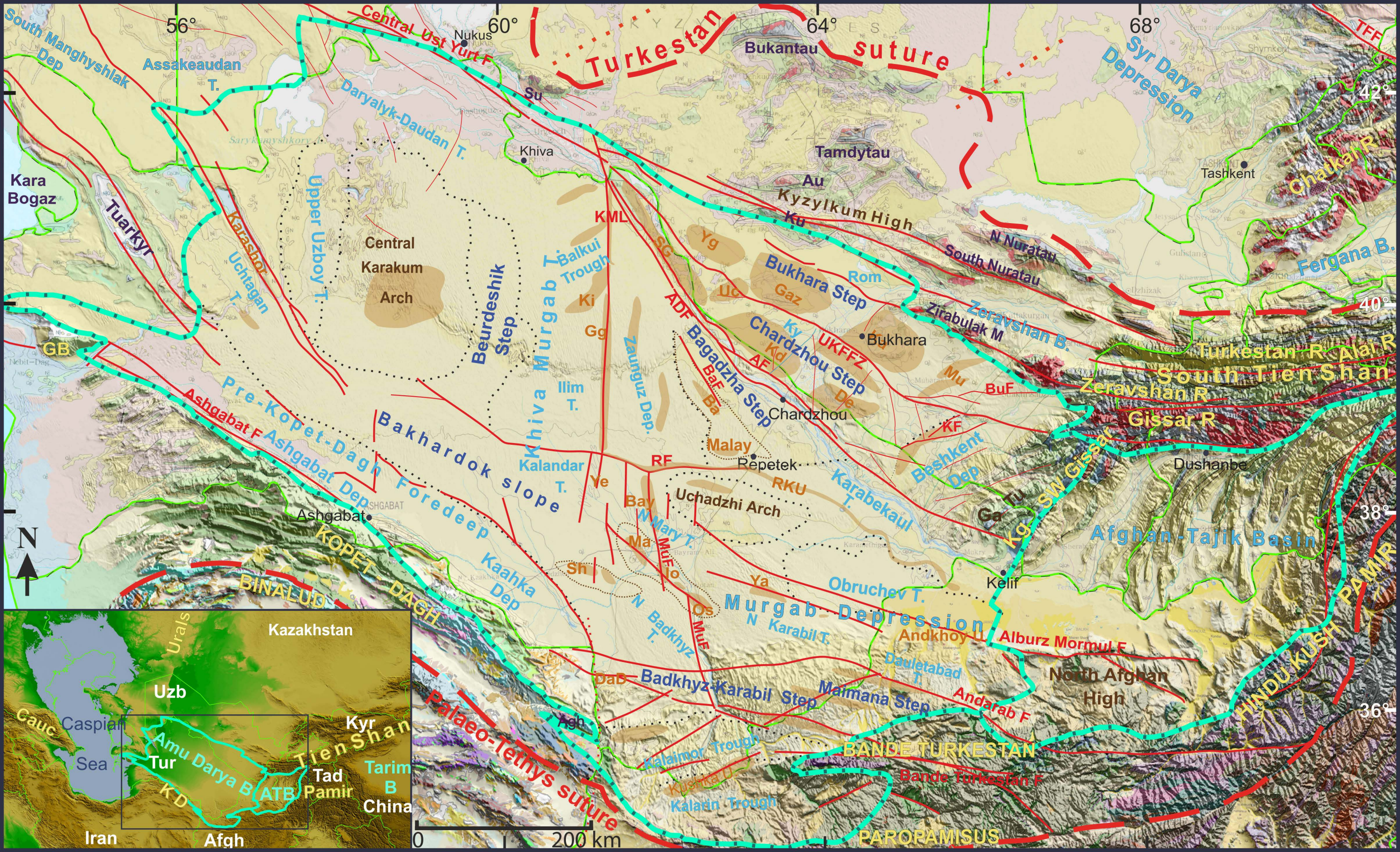

56°
60°
64°
68°
42°
40°
38°
36°
Central Ust Yurt F
Nukus
Turkestan
suture
Bukantau
TFF
South Manghyshlak Dep
Assakeaudan T.
Syr Darya Depression
Su
Daryalyk-Daudan T.
Khiva
Tamdytau
Tashkent
Kara Bogaz
Au
Chatkal R
Tuarkyr
Kyzylkum High
Ku
N Nuratau
South Nuratau
Fergana B.
Karashor
Uchtagan T.
Upper Uzboy T.
Central Karakum Arch
KML
Balkui Trough
Yg
SG
Bukhara Step
Rom
UC
Gaz
Zirabulak M
Zeravshan B.
Beurdeshik Step
Khiva Murgab T.
Ki
Gg
ADF
Ky
Bukhara
UKFFZ
Chardzhou Step
Turkestan R
Alai R
South Tien Shan
Zeravshan R
GB
Zaunguz Dep.
Bagadzha Step
Kd
AF
BaF
Ba
De
Mu
BuF
Chardzhou
Gissar R
Ashgabat F
Pre-Kopet-Dagh Foredeep
Ilim T.
KF
Bakhardok slope
Ashgabat Dep
Kalandar T.
RF
Malay
Repetek
Beshkent Dep
SW Gissar
Dushanbe
Ye
RKU
Bay
Uchadzhi Arch
Karabekaul T.
Ga
Tu
Kg
Ashgabat
N Mary T.
Ma
MuF
Jo
Afghan-Tajik Basin
KOPET DAGH
Kaahka Dep
Sh
Ya
Obruchev T.
Kelif
BINALUD
N Badkhyz T.
Os
Murgab Depression
N Karabil T.
Andkhoy U
Alburz Mormul F
PAMIR
HINDU KUSH
N
DaB
Badkhyz-Karabil Step
Dauletabad T.
Maimana Step
North Afghan High
Andarab F
Agh
Kalaimor Trough
BANDE TURKESTAN
Palaeo-Tethys suture
Kushka U
Bande Turkestan F
Kalarin Trough
PAROPAMISUS
0
200 km
Urals
Kazakhstan
Uzb
Cauc
Caspian
Sea
Kyr
Tien Shan
Amu Darya B
Tur
Tad
Tarim B
ATB
Pamir
KD
China
Iran
Afgh

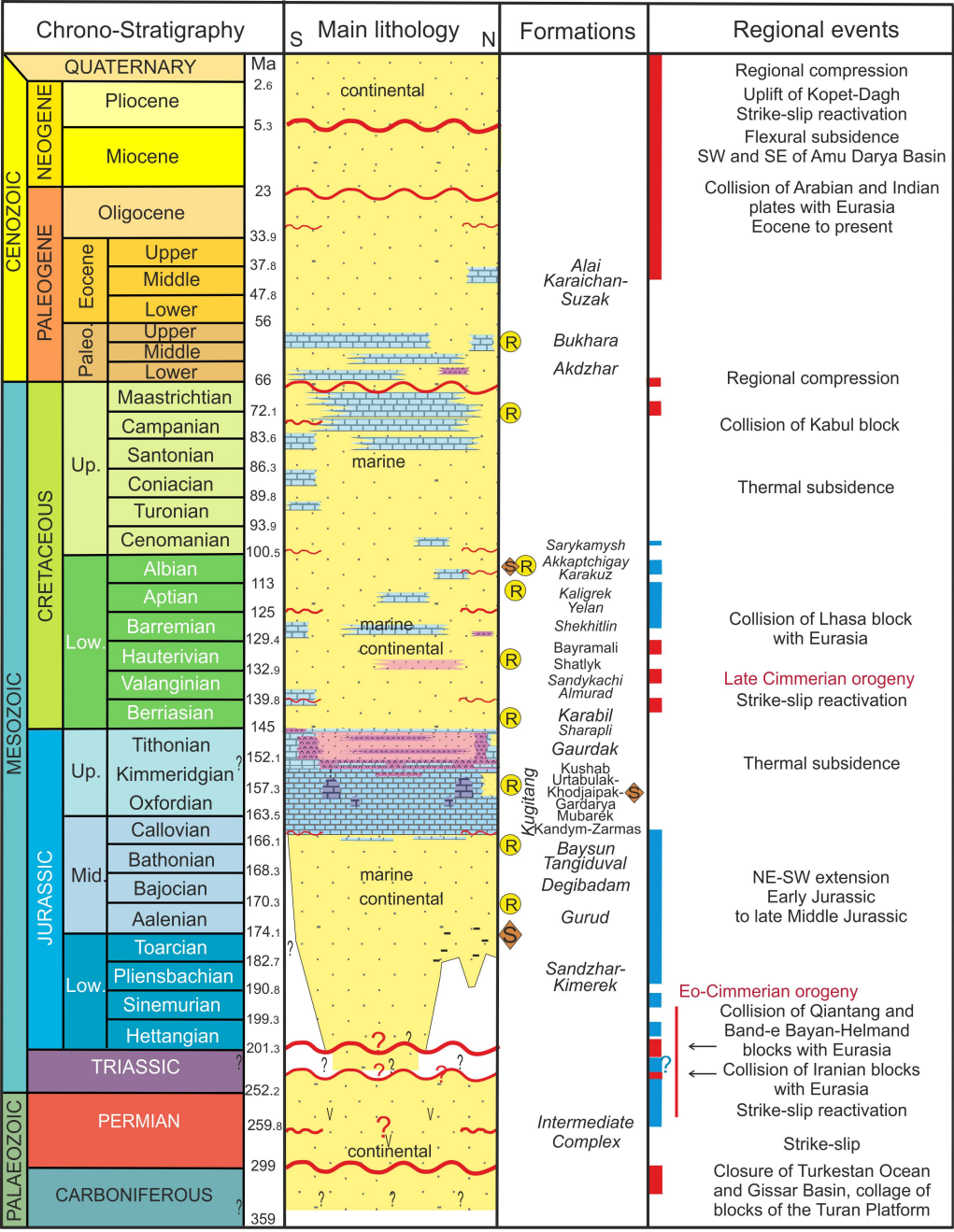
Chrono-Stratigraphy
Main lithology
S
N
Formations
Regional events
QUATERNARY
NEOGENE
PALEOGENE
CENOZOIC
MESOZOIC
PALAEOZOIC
Pliocene
Miocene
Oligocene
Eocene
Paleo.
Upper
Middle
Lower
CRETACEOUS
JURASSIC
TRIASSIC
PERMIAN
CARBONIFEROUS
Up.
Low.
Mid.
Maastrichtian
Campanian
Santonian
Coniacian
Turonian
Cenomanian
Albian
Aptian
Barremian
Hauterivian
Valanginian
Berriasian
Tithonian
Kimmeridgian
Oxfordian
Callovian
Bathonian
Bajocian
Aalenian
Toarcian
Pliensbachian
Sinemurian
Hettangian
Ma
2.6
5.3
23
33.9
37.8
47.8
56
66
72.1
83.6
86.3
89.8
93.9
100.5
113
125
129.4
132.9
139.8
145
152.1
157.3
163.5
166.1
168.3
170.3
174.1
182.7
190.8
199.3
201.3
252.2
259.8
299
359
continental
marine
continental
marine
continental
marine
continental
continental
Alai
Karaichan-
Suzak
Bukhara
Akdzhar
Sarykamysh
Akkaptchigay
Karakuz
Kaligrek
Yelan
Shekhitlin
Bayramali
Shatlyk
Sandykachi
Almurad
Karabil
Sharapli
Gaurdak
Kushab
Urtabulak-
Khodjaipak-
Gardarya
Mubarek
Kandym-Zarmas
Kugitang
Baysun
Tangiduval
Degibadam
Gurud
Sandzhar-
Kimerek
Intermediate
Complex
R
S
Regional compression
Uplift of Kopet-Dagh
Strike-slip reactivation
Flexural subsidence
SW and SE of Amu Darya Basin
Collision of Arabian and Indian
plates with Eurasia
Eocene to present
Regional compression
Collision of Kabul block
Thermal subsidence
Collision of Lhasa block
with Eurasia
Late Cimmerian orogeny
Strike-slip reactivation
Thermal subsidence
NE-SW extension
Early Jurassic
to late Middle Jurassic
Eo-Cimmerian orogeny
Collision of Qiantang and
Band-e Bayan-Helmand
blocks with Eurasia
Collision of Iranian blocks
with Eurasia
Strike-slip reactivation
Strike-slip
Closure of Turkestan Ocean
and Gissar Basin, collage of
blocks of the Turan Platform
Extension
Main
compression
Unconformity
Erosion
Volcanics
Carbonates
Build-ups
Clastics
Coal
Anhydrite-gypsum
Salt
Source Rock
Reservoir


(e)

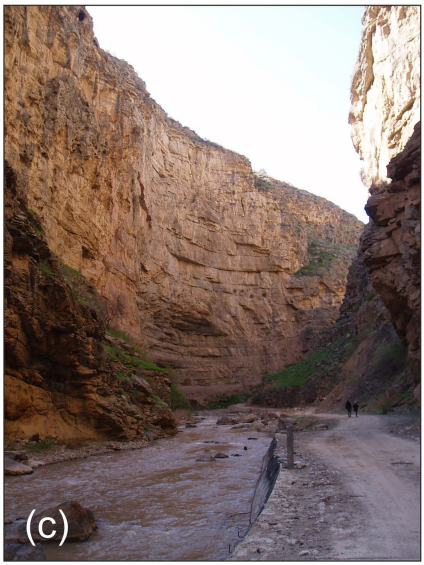
(c)

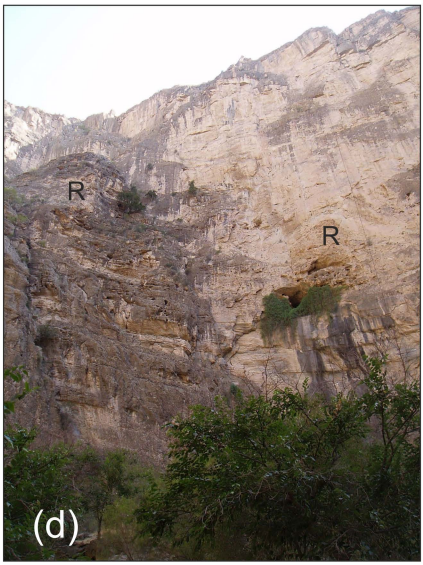
R
R
(d)

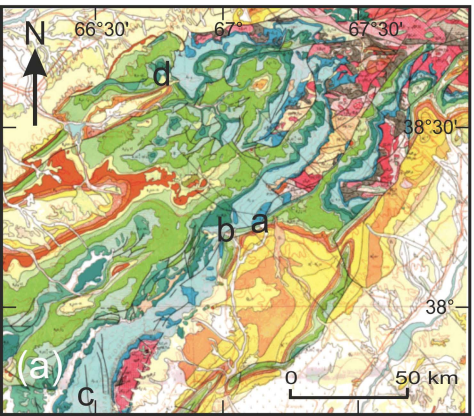
N
66°30'
67°
67°30'
38°30'
38°
d
b
a
c
(a)
0
50 km


(b)

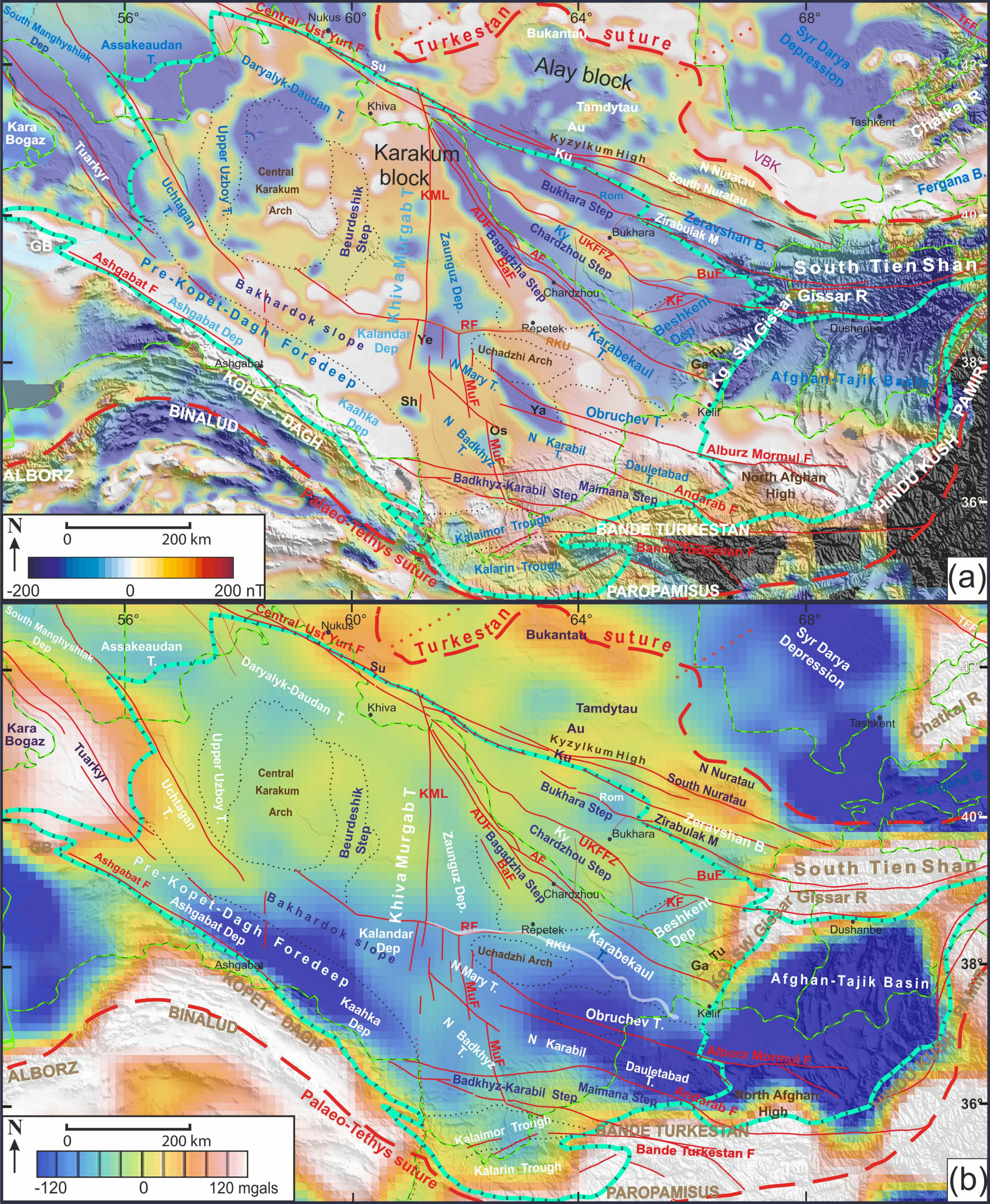

56°
60°
64°
68°
42°
40°
38°
36°
Central Ust Yurt F
Nukus
Turkestan
suture
Bukantau
Alay block
Syr Darya Depression
TFF
South Manghyshlak Dep
Assakeaudan T.
Su
Daryalyk-Daudan T.
Khiva
Tamdytau
Au
Tashkent
Chatkal R
Kara Bogaz
Tuarkyr
Upper Uzboy T.
Central Karakum Arch
Karakum block
Kyzylkum High
Ku
VBK
N Nuratau
South Nuratau
Fergana B.
Uchtagan T.
Beurdeshik Step
KML
Khiva Murgab T
Zaunguz Dep.
ADF
Bagadzha Step
Bukhara Step
Rom
Ky
UKFFZ
Bukhara
Zirabulak M
Zeravshan B.
Chardzhou Step
AF
BaF
GB
Ashgabat F
Pre-Kopet-Dagh Foredeep
Ashgabat Dep
Bakhardok slope
Chardzhou
BuF
South Tien Shan
Gissar R
KF
Beshkent Dep
SW Gissar
Kalandar Dep
Ye
RF
Repetek
RKU
Karabekaul T.
Dushanbe
Uchadzhi Arch
Ga
Tu
Kg
Afghan-Tajik Basin
Ashgabat
KOPET - DAGH
N Mary T.
MuF
Kaahka Dep
Sh
Ya
Kelif
Obruchev T.
PAMIR
BINALUD
N Badkhyz T.
Os
N Karabil T.
Alburz Mormul F
HINDU KUSH
ALBORZ
Dauletabad T.
Andarab F
North Afghan High
Badkhyz-Karabil Step
Maimana Step
N
0
200 km
Palaeo-Tethys suture
Kalaimor Trough
BANDE TURKESTAN
Bande Turkestan F
Kalarin Trough
PAROPAMISUS
-200
0
200 nT
(a)
-120
0
120 mgals
(b)

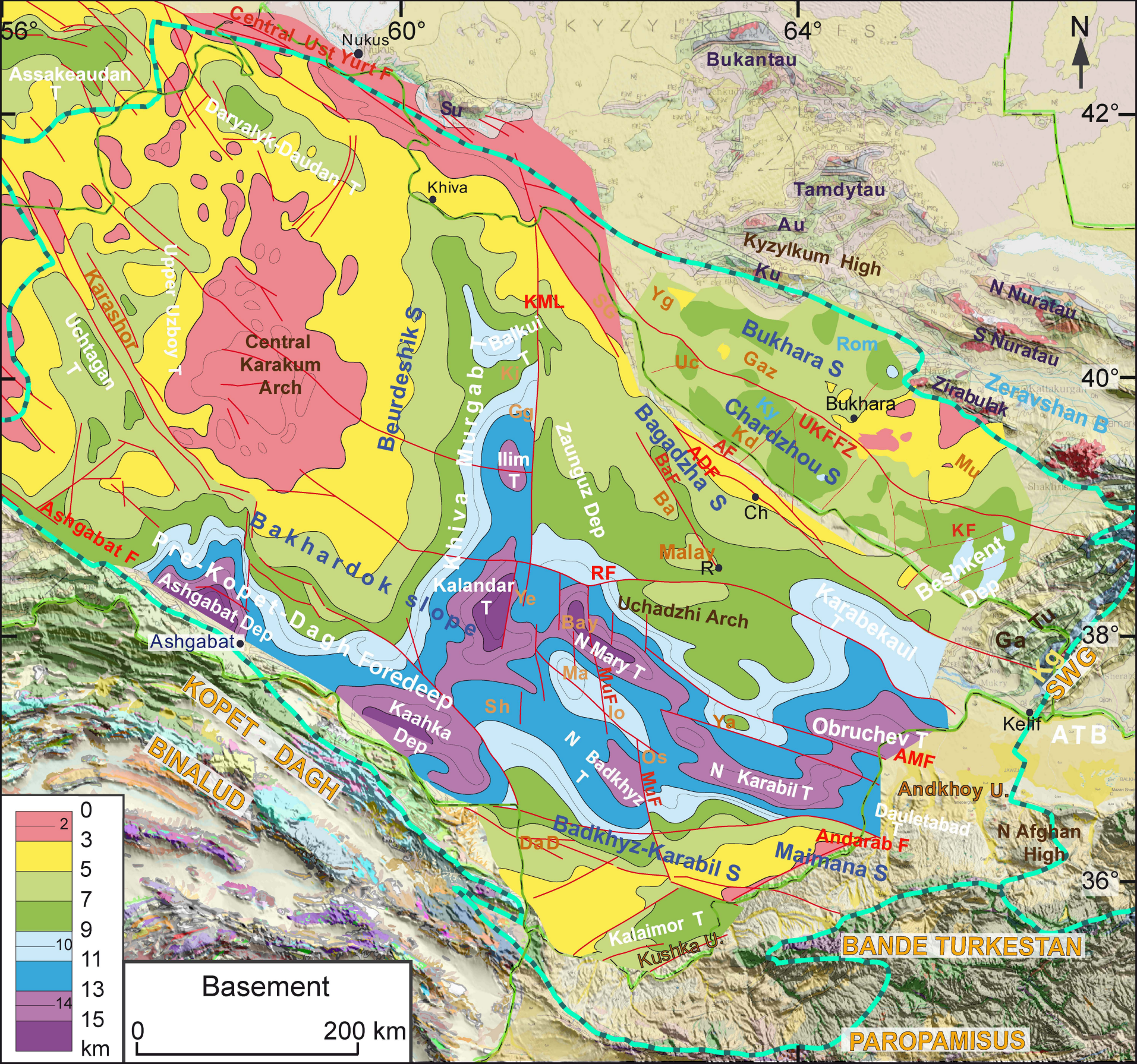
56°
60°
64°
N
42°
40°
38°
36°
Nukus
Khiva
Bukantau
Tamdytau
Au
Kyzylkum High
Ku
N Nuratau
S Nuratau
Zirabulak
Zeravshan B
Bukhara
Ch
Kelif
ATB
Andkhoy U.
Dauletabad
N Afghan High
Assakeaudan T
Central Ust Yurt F
Daryalyk-Daudan T
Karashor
Uchtagan T
Upper Uzboy T
Central Karakum Arch
Beurdeshik S
Khiva Murgab T
Balkui T
KML
SG
Yg
Bukhara S
Rom
Uc
Gaz
Ky
Chardzhou S
UKFFZ
Kd
AF
ADF
Mu
Bagadzha S
BaF
Ba
Ilim T
Gg
Kt
Zaunguz Dep
Ashgabat F
Bakhardok Slope
Pre Kopet Dagh Foredeep
Ashgabat Dep
Kalandar T
Ye
RF
Malay R
Uchadzhi Arch
Karabekaul T
Beshkent Dep
KF
Tu
Ga
Kg
SWG
Bay
N Mary T
Ma
MuF
Sh
Kaahka Dep
Lo
Ya
Obruchev T
AMF
Os
MvF
N Badkhyz T
N Karabil T
Badkhyz-Karabil S
DaD
Andarab F
Maimana S
Kalaimor T
Kushka U.
KOPET - DAGH
BINALUD
BANDE TURKESTAN
PAROPAMISUS
Basement
0
200 km
0
2
3
5
7
9
10
11
13
14
15
km

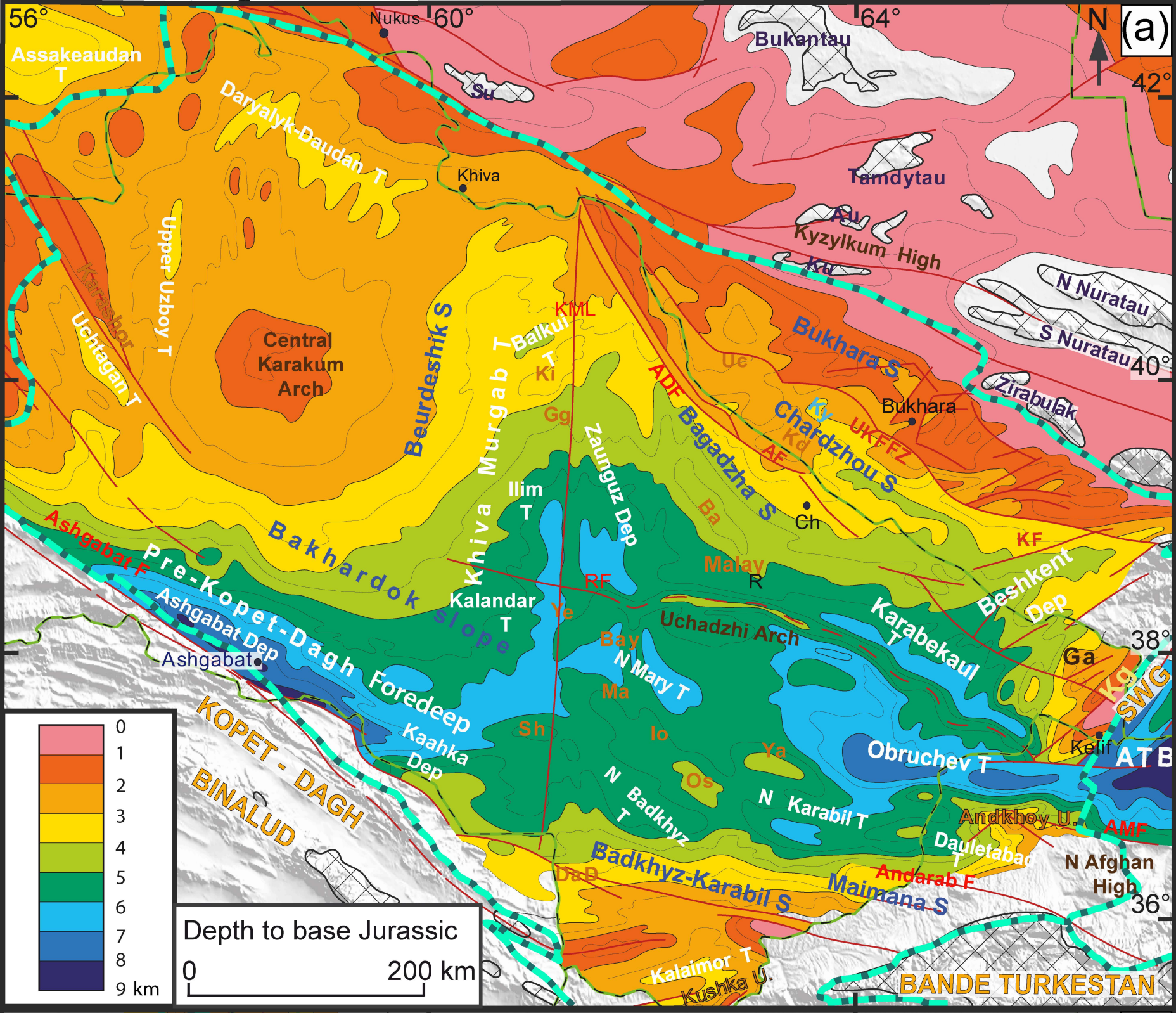
(a)
N
56°
60°
64°
42°
40°
38°
36°
Nukus
Khiva
Bukantau
Tamdytau
Au
Kyzylkum High
Ku
N Nuratau
S Nuratau
Zirabulak
Bukhara
Ch
Assakeaudan T
Daryalyk-Daudan T
Upper Uzboy T
Kareshor
Uchtagan T
Central Karakum Arch
Beurdeshik S
Khiva Murgab T
Balkui T
KML
Ki
Gg
Uc
Kd
Ky
ADF
AF
UKFFZ
Bukhara S
Chardzhou S
Bagadzha S
Ba
Ilim T
Zaunguz Dep
Bakhardok slope
Ashgabat F
Pre-Kopet-Dagh Foredeep
Ashgabat Dep
Ashgabat
Kalandar T
RF
Ye
Malay R
KF
Beshkent Dep
Karabekaul T
Uchadzhi Arch
Bay
N Mary T
Ma
Sh
Io
Ya
Os
Ga
Ka
SWG
Kelif
ATB
Obruchev T
N Karabil T
N Badkhyz T
Andkhoy U.
AMF
Dauletabad T
Andarab F
N Afghan High
Badkhyz-Karabil S
Maimana S
DaD
Kaahka Dep
KOPET - DAGH
BINALUD
Kalaimor T
Kushka U.
BANDE TURKESTAN
0
1
2
3
4
5
6
7
8
9 km
Depth to base Jurassic
0
200 km

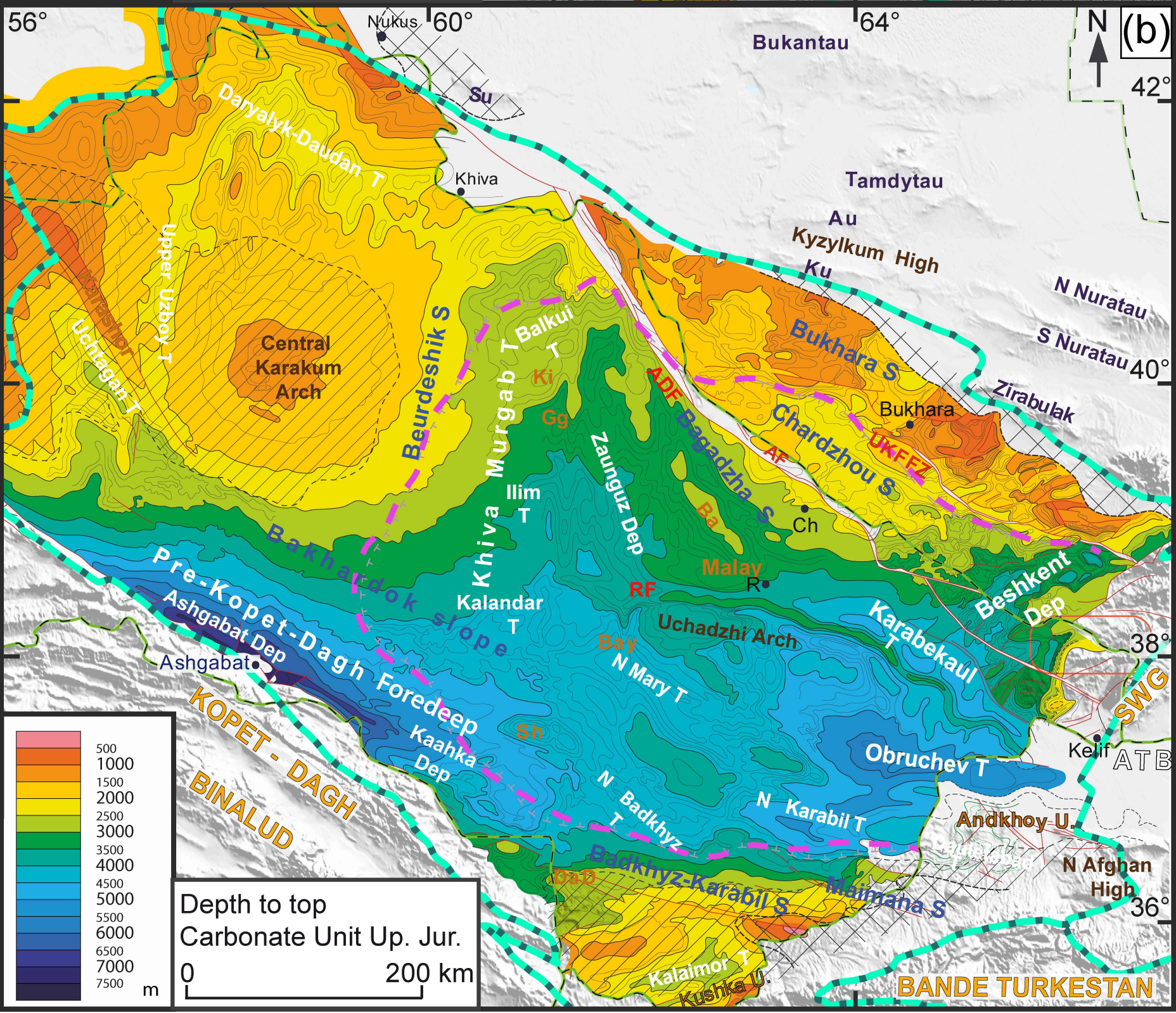
(b)
N
56°
60°
64°
42°
40°
38°
36°
Nukus
Khiva
Bukantau
Tamdytau
Au
Kyzylkum High
Ku
N Nuratau
S Nuratau
Zirabulak
Bukhara
Ch
Daryalyk-Daudan T
Upper Uzboy T
Kareshor
Uchtagan T
Central Karakum Arch
Beurdeshik S
Khiva Murgab T
Balkui T
Ki
Gg
ADF
AF
UKFFZ
Bukhara S
Chardzhou S
Bagadzha S
Ba
Ilim T
Zaunguz Dep
Bakhardok slope
Pre-Kopet-Dagh Foredeep
Ashgabat Dep
Ashgabat
Kalandar T
RF
Malay R
Beshkent Dep
Karabekaul T
Uchadzhi Arch
Bay
N Mary T
Sh
SWG
Kelif
ATB
Obruchev T
N Karabil T
N Badkhyz T
Andkhoy U.
N Afghan High
Badkhyz-Karabil S
Maimana S
DaD
Kaahka Dep
KOPET - DAGH
BINALUD
Kalaimor T
Kushka U.
BANDE TURKESTAN
500
1000
1500
2000
2500
3000
3500
4000
4500
5000
5500
6000
6500
7000
7500
m
Depth to top
Carbonate Unit Up. Jur.
0
200 km

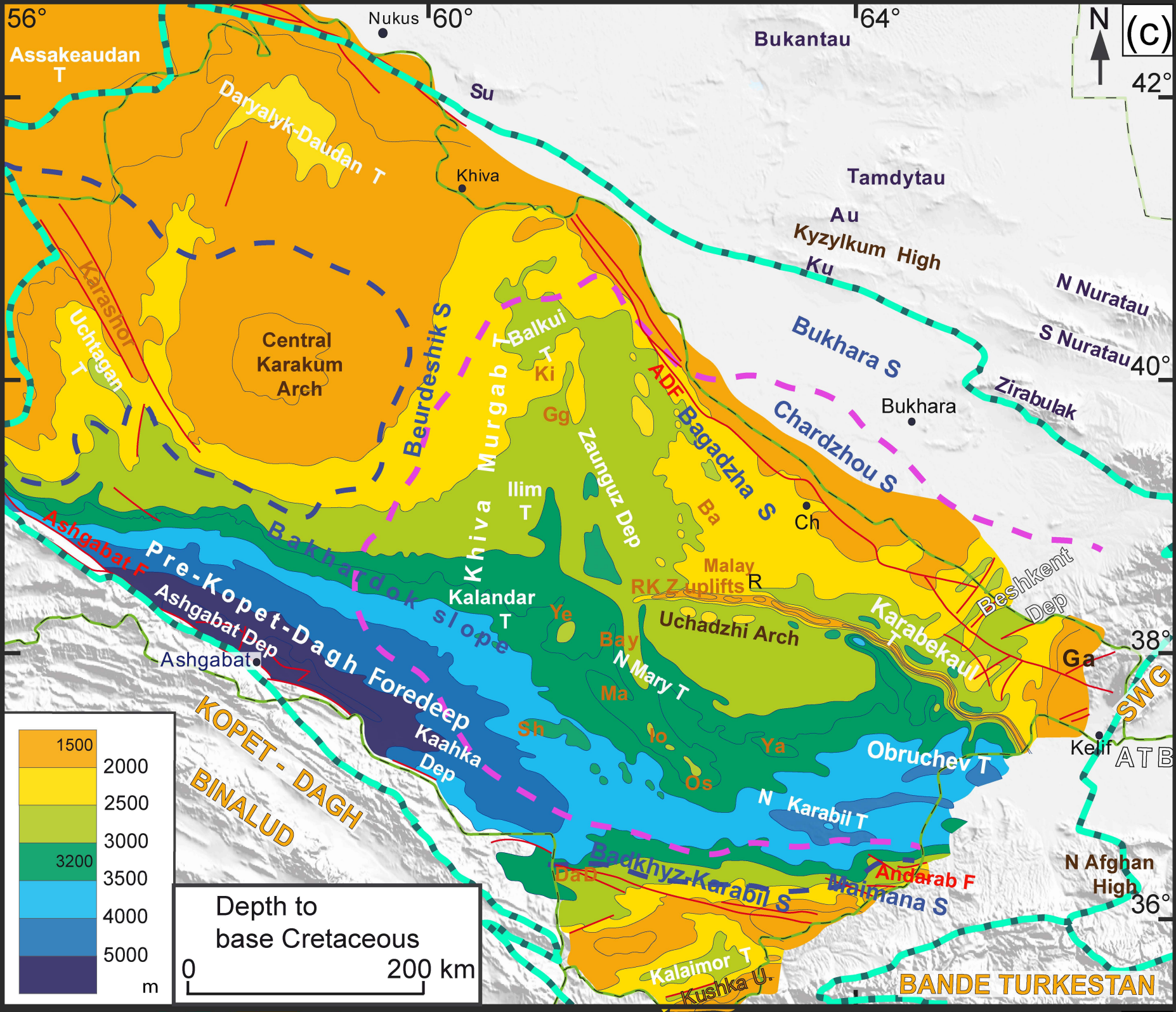
(c)
N
56°
60°
64°
42°
40°
38°
36°
Nukus
Khiva
Bukantau
Tamdytau
Au
Kyzylkum High
Ku
N Nuratau
S Nuratau
Zirabulak
Bukhara
Ch
Kelif
Assakeaudan T
Daryalyk-Daudan T
Su
Karashor
Uchtagan T
Central Karakum Arch
Beurdeshik S
Khiva
Murgab T
Balkui T
Ki
Gg
Zaunguz Dep
Ilim T
ADF
Bagadzha S
Chardzhou S
Bukhara S
Ba
Malay R
RK Z uplifts
Uchadzhi Arch
Karabekaul T
Beshkent Dep
Ga
SWG
ATB
Ashgabat F
Bakhardok slope
Pre-Kopet-Dagh Foredeep
Ashgabat Dep
Ashgabat
Kalandar T
Ye
Bay
N Mary T
Ma
Sh
Io
Os
Ya
Obruchev T
N Karabil T
Kaahka Dep
KOPET - DAGH
BINALUD
Badkhyz-Karabil S
DaD
Andarab F
Maimana S
N Afghan High
Kalaimor T
Kushka U.
BANDE TURKESTAN
1500
2000
2500
3000
3200
3500
4000
5000
m
Depth to base Cretaceous
0
200 km

(d)
N
56°
60°
64°
42°
40°
38°
36°
Nukus
Khiva
Bukantau
Tamdytau
Au
Kyzylkum High
Ku
N Nuratau
S Nuratau
Zirabulak
Bukhara
Ch
Kelif
Daryalyk-Daudan T
Su
Karashor
Uchtagan T
Upper Uzboy T
Central Karakum Arch
Beurdeshik S
Khiva
Murgab T
Balkui T
Ki
Gg
KML
Zaunguz Dep
Ilim T
Bagadzha S
Chardzhou S
Bukhara S
Ba
Malay R
Uchadzhi Arch
Karabekaul T
Beshkent Dep
Palaeo Amu Darya River
Ashgabat F
Bakhardok slope
Pre-Kopet-Dagh Foredeep
Ashgabat Dep
Ashgabat
Kalandar T
Bay
N Mary T
Ma
Sh
Io
Os
Ya
Obruchev T
N Karabil T
Kaahka Dep
KOPET - DAGH
BINALUD
N Badkhyz T
Badkhyz-Karabil S
DaD
Andkhoy U.
AMF
Dauletabad T
Andarab F
Maimana S
N Afghan High
Kalaimor T
Kushka U.
BANDE TURKESTAN
SWG
ATB
0
500
1000
1500
2000
2500
3000
3500
m
Depth to top Paleocene
0
200 km

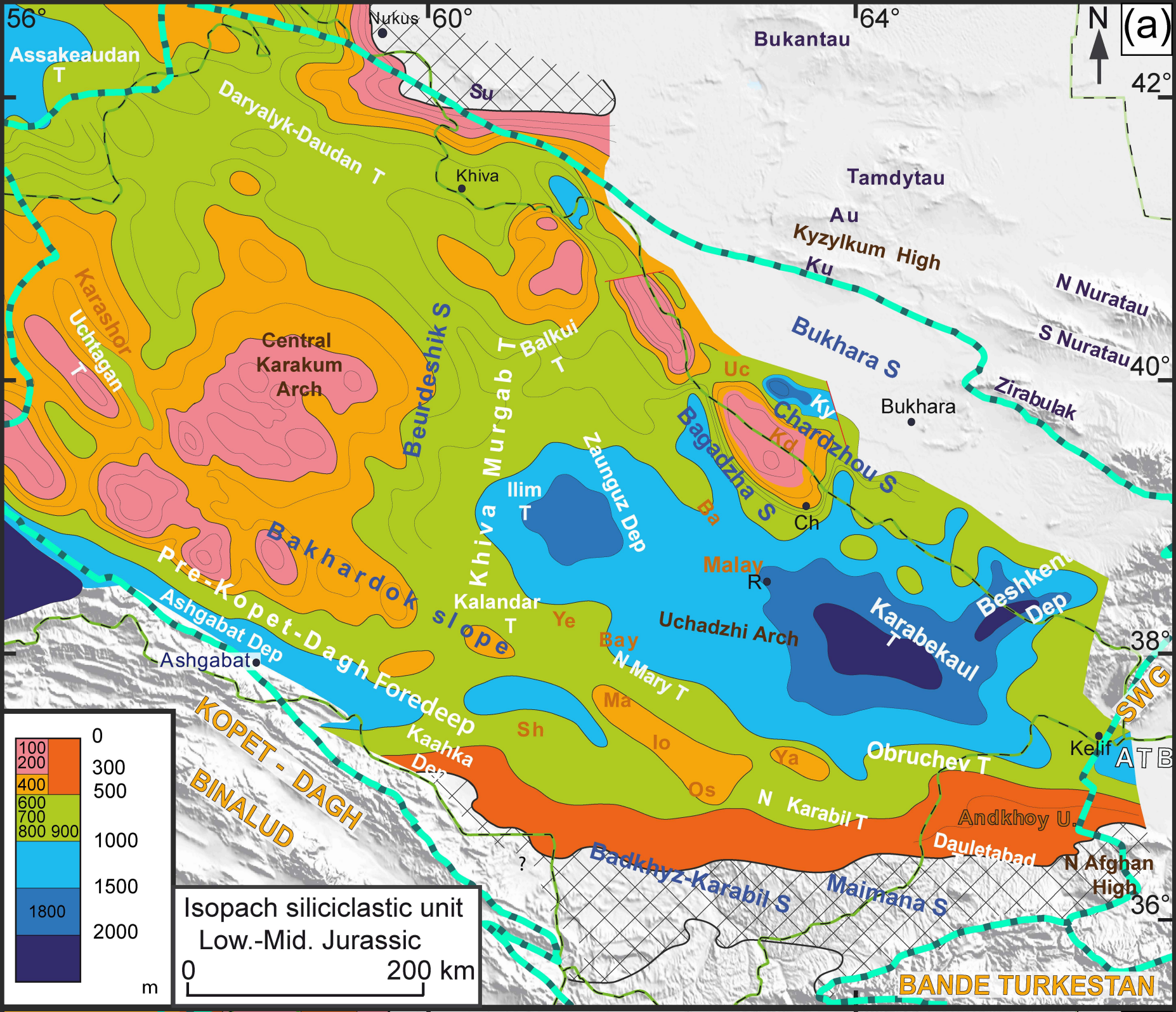
(a)
N
56°
60°
64°
42°
40°
38°
36°
Nukus
Khiva
Bukantau
Tamdytau
Au
Kyzylkum High
Ku
N Nuratau
S Nuratau
Zirabulak
Bukhara
Ch
Assakeaudan T
Daryalyk-Daudan T
Su
Karashor Uchtagan T
Central Karakum Arch
Beurdeshik S
Khiva Murgab T
Balkui T
Bukhara S
Uc
Ky
Kd
Chardzhou S
Bagadzha S
Ba
Ilim T
Zaunguz Dep
Malay R
Bakhardok slope
Pre-Kopet-Dagh Foredeep
Ashgabat Dep
Ashgabat
Kalandar T
Ye
Bay
N Mary T
Uchadzhi Arch
Karabekaul T
Beshkent Dep
Ma
Sh
Io
Ya
Os
Kaahka Dep
Obruchev T
N Karabil T
Andkhoy U.
Dauletabad T
N Afghan High
Badkhyz-Karabil S
Maimana S
KOPET - DAGH
BINALUD
BANDE TURKESTAN
SWG
ATB
Kelif
?
0
100
200
300
400
500
600
700
800
900
1000
1500
1800
2000
m
Isopach siliciclastic unit
Low.-Mid. Jurassic
0
200 km

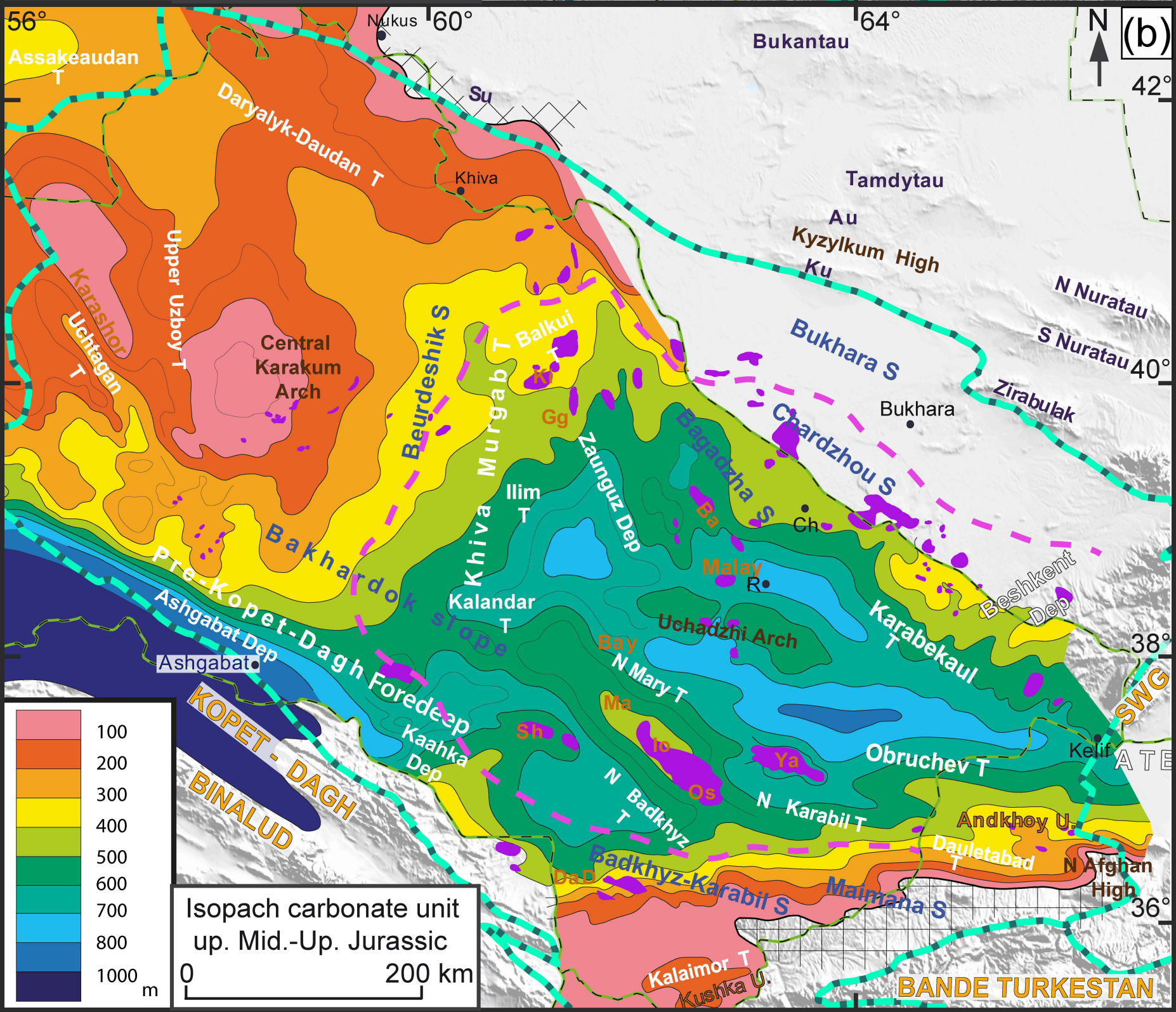
(b)
N
56°
60°
64°
42°
40°
38°
36°
Nukus
Khiva
Bukantau
Tamdytau
Au
Kyzylkum High
Ku
N Nuratau
S Nuratau
Zirabulak
Bukhara
Ch
Assakeaudan T
Daryalyk-Daudan T
Su
Upper Uzboy T
Karashor Uchtagan T
Central Karakum Arch
Beurdeshik S
Khiva Murgab T
Balkui T
Ki
Gg
Bukhara S
Chardzhou S
Bagadzha S
Ba
Ilim T
Zaunguz Dep
Malay R
Bakhardok slope
Pre-Kopet-Dagh Foredeep
Ashgabat Dep
Ashgabat
Kalandar T
Bay
N Mary T
Uchadzhi Arch
Karabekaul T
Beshkent Dep
Ma
Sh
Io
Ya
Os
Kaahka Dep
Obruchev T
N Badkhyz T
N Karabil T
Andkhoy U.
Dauletabad T
N Afghan High
Da D
Badkhyz-Karabil S
Maimana S
Kalaimor T
Kushka U.
KOPET - DAGH
BINALUD
BANDE TURKESTAN
SWG
ATE
Kelif
100
200
300
400
500
600
700
800
1000
m
Isopach carbonate unit
up. Mid.-Up. Jurassic
0
200 km

56°
60°
64°
Nukus
Bukantau
Su
Khiva
Tamdytau
Au
Kyzylkum High
Ku
N Nuratau
S Nuratau
42°
40°
38°
36°
N
(c)
Daryalyk-Daudan T
Central Karakum Arch
Beurdeshik S
Khiva Murgab T
Balkui T
Ilim T
Zaunguz Dep
Bagadzha S
Ba
Ch
Bukhara S
Chardzhou S
Bukhara
Zirabulak
Bakhardok slope
Pre-Kopet-Dagh
Ashgabat Dep
Ashgabat
Foredeep
Kaahka Dep
Kalandar T
Malay R
Uchadzhi Arch
Karabekaul T
Beshkent Dep
Bay
N Mary T
Ma
Io
Ya
Os
N Badkhyz T
N Karabil T
Obruchev T
Andkhoy U.
Daulet T
Badkhyz-Karabil S
Maimana S
N Afghan High
SWG
Kelif
ATB
KOPET - DAGH
BINALUD
BANDE TURKESTAN
100
300
400
200
500
750
1000
1250
1500
1750
m
Isopach evaporite unit
+ equiv. Up. Jur. to Berr.?
0
200 km

56°
60°
64°
Nukus
Bukantau
Su
Khiva
Tamdytau
Au
Kyzylkum High
Ku
N Nuratau
S Nuratau
42°
40°
38°
36°
N
(d)
Daryalyk-Daudan T
Upper Uzboy T
Karashor
Uchtagan T
Central Karakum Arch
Beurdeshik S
Khiva Murgab T
Balkui T
Ki
Gg
Zaunguz Dep
Bagadzha S
Ba
Ch
Bukhara S
Chardzhou S
Bukhara
Zirabulak
Bakhardok slope
Pre-Kopet-Dagh
Ashgabat Dep
Ashgabat
Foredeep
Kaahka Dep
Ilim T
Kalandar T
Ye
Malay R
Uchadzhi Arch
Karabekaul T
Bay
N Mary T
Ma
Sh
Io
Ya
Os
N Badkhyz T
N Karabil T
Obruchev T
Andkhoy U.
Badkhyz-Karabil S
Maimana S
N Afghan High
SWG
Kelif
ATB
KOPET - DAGH
BINALUD
BANDE TURKESTAN
100
150
200
300
400
500
600
700
800
900
1000
1500
m
Isopach Berriasian?
to Lower Barremian
0
200 km

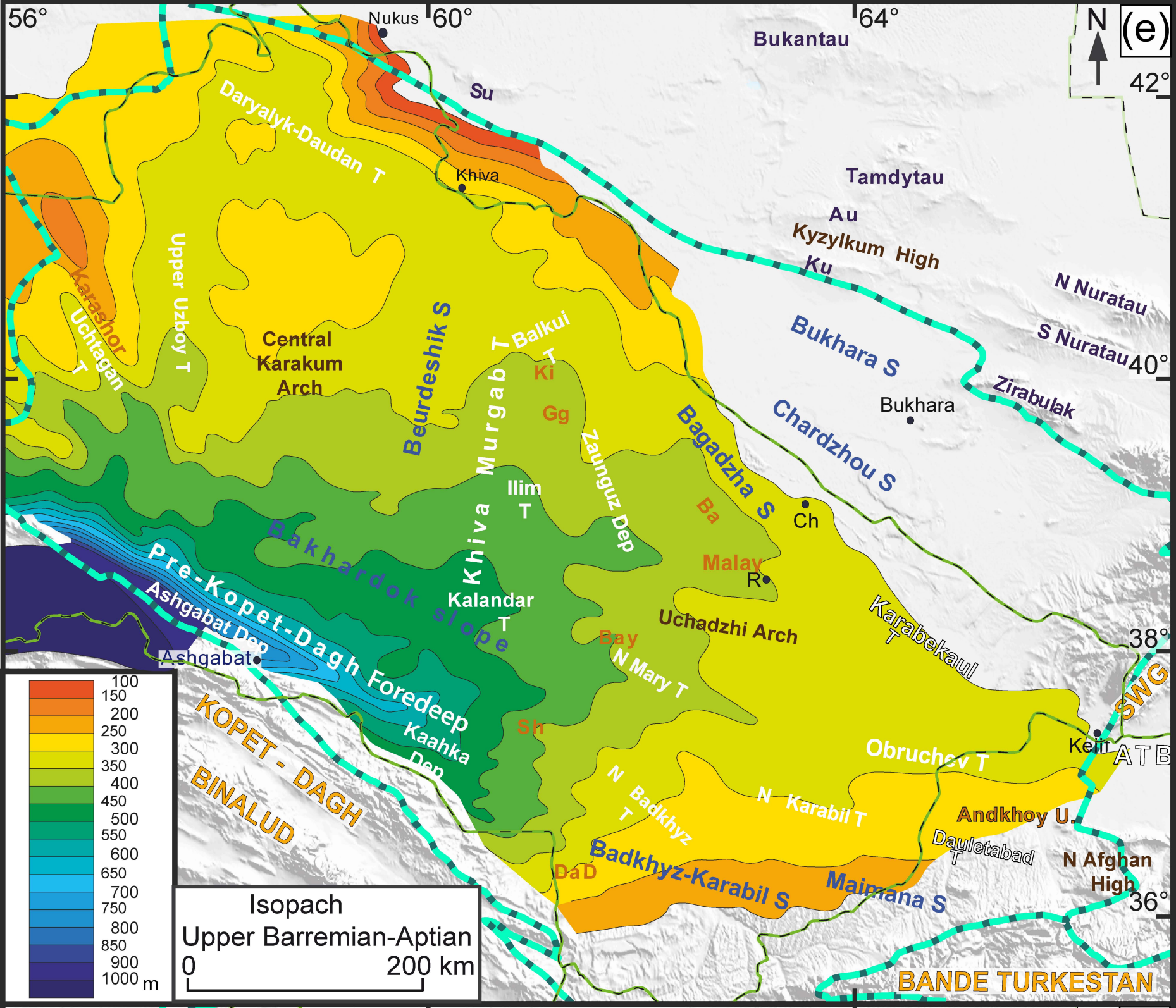
56°
60°
64°
42°
40°
38°
36°
Nukus
Khiva
Bukantau
Tamdytau
Au
Kyzylkum High
Ku
N Nuratau
S Nuratau
Zirabulak
Bukhara
Ch
Malay
R
Ashgabat
Kelif
Su
Daryalyk-Daudan T
Karashor
Uchtagan
T
Upper Uzboy T
Central
Karakum
Arch
Beurdeshik S
Khiva
Murgab T
Balkui
T
Ki
Gg
Ilim
T
Zaunguz Dep
Bagadzha S
Ba
Chardzhou S
Bakhardok slope
Kalandar
T
Pre-Kopet-Dagh Foredeep
Ashgabat Dep
Kaahka
Dep
Sh
Bay
N Mary T
Uchadzhi Arch
Karabekaul
T
Obruchev T
N Badkhyz
T
N Karabil T
Andkhoy U.
Dauletabad
T
Badkhyz-Karabil S
DaD
Maimana S
N Afghan
High
KOPET - DAGH
BINALUD
SWG
ATB
BANDE TURKESTAN
100
150
200
250
300
350
400
450
500
550
600
650
700
750
800
850
900
1000
m
Isopach
Upper Barremian-Aptian
0
200 km
N
(e)

56°
60°
64°
42°
40°
38°
36°
Nukus
Khiva
Bukantau
Tamdytau
Au
Kyzylkum High
Ku
N Nuratau
S Nuratau
Zirabulak
Bukhara
Ch
Malay
R
Ashgabat
Kelif
Su
Daryalyk-Daudan T
Karashor
Uchtagan
T
Upper Uzboy T
Central
Karakum
Arch
Beurdeshik S
Khiva
Murgab T
Balkui
T
Ki
Gg
Ilim
T
Zaunguz Dep
Bagadzha S
Ba
Chardzhou S
Bakhardok slope
Kalandar
T
Pre-Kopet-Dagh Foredeep
Ashgabat Dep
Kaahka
Dep
Sh
Ye
Bay
N Mary T
Ma
Io
Os
Ya
Uchadzhi Arch
Karabekaul
T
Obruchev T
N Badkhyz
T
N Karabil T
Andkhoy U.
Badkhyz-Karabil S
DaD
Maimana S
N Afghan
High
Kalaimor T
Kushka U.
KOPET - DAGH
BINALUD
SWG
ATB
BANDE TURKESTAN
200
300
400
500
600
650
700
800
1000
1500
m
Isopach
Albian-Cenomanian
0
200 km
N
(f)

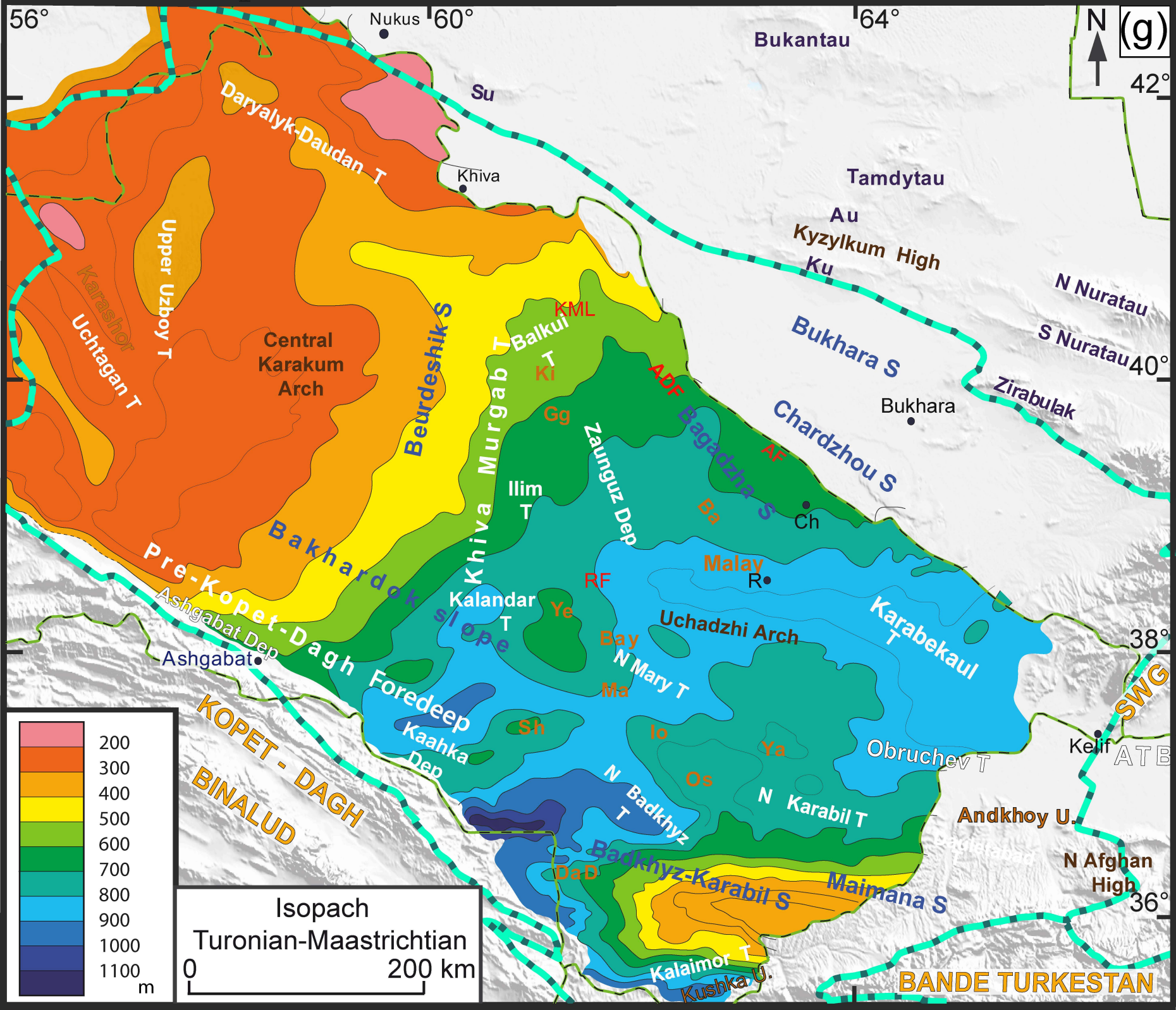
(g)
N
56°
60°
64°
42°
40°
38°
36°
Nukus
Khiva
Su
Bukantau
Tamdytau
Au
Kyzylkum High
Ku
N Nuratau
S Nuratau
Zirabulak
Bukhara
Bukhara S
Chardzhou S
Bagadzha S
Ch
Daryalyk-Daudan T
Upper Uzboy T
Karashor
Uchtagan T
Central
Karakum
Arch
Beurdeshik S
Khiva Murgab T
Balkui T
KML
Ki
Gg
ADF
AF
Ba
Ilim
T
Zaunguz Dep
Bakhardok slope
Pre-Kopet-Dagh Foredeep
Ashgabat Dep
Ashgabat
Kalandar
T
Ye
RF
Malay
R
Bay
N Mary T
Ma
Uchadzhi Arch
Karabekaul
T
Kaahka
Dep
Sh
Io
Ya
Os
Obruchev T
N Badkhyz
T
N Karabil T
Badkhyz-Karabil S
DaD
Maimana S
Andkhoy U.
N Afghan
High
Kelif
ATB
SWG
KOPET - DAGH
BINALUD
Kalaimor T
Kushka U.
BANDE TURKESTAN
200
300
400
500
600
700
800
900
1000
1100
m
Isopach
Turonian-Maastrichtian
0
200 km

(h)
N
56°
60°
64°
42°
40°
38°
36°
Nukus
Khiva
Su
Bukantau
Tamdytau
Au
Kyzylkum High
Ku
N Nuratau
S Nuratau
Zirabulak
Bukhara
Bukhara S
Chardzhou S
Bagadzha S
Ch
Assakeaudan
T
Daryalyk-Daudan T
Upper Uzboy T
Karashor
Uchtagan T
Central
Karakum
Arch
Beurdeshik S
Khiva Murgab T
Balkui T
Ki
Gg
Ba
Ilim
T
Zaunguz Dep
Bakhardok slope
Pre-Kopet-Dagh Foredeep
Ashgabat Dep
Ashgabat
Kalandar
T
Ye
Malay
R
Bay
N Mary T
Ma
Uchadzhi Arch
Karabekaul
T
Kaahka
Dep
Sh
Io
Ya
Os
Obruchev T
N Badkhyz
T
N Karabil T
Badkhyz-Karabil S
DaD
Maimana S
Andkhoy U.
N Afghan
High
Kelif
ATB
SWG
KOPET - DAGH
BINALUD
Kalaimor T
Kushka U.
BANDE TURKESTAN
50
100
150
200
250
300
350
400
450
500
550
m
Isopach Paleocene
0
200 km

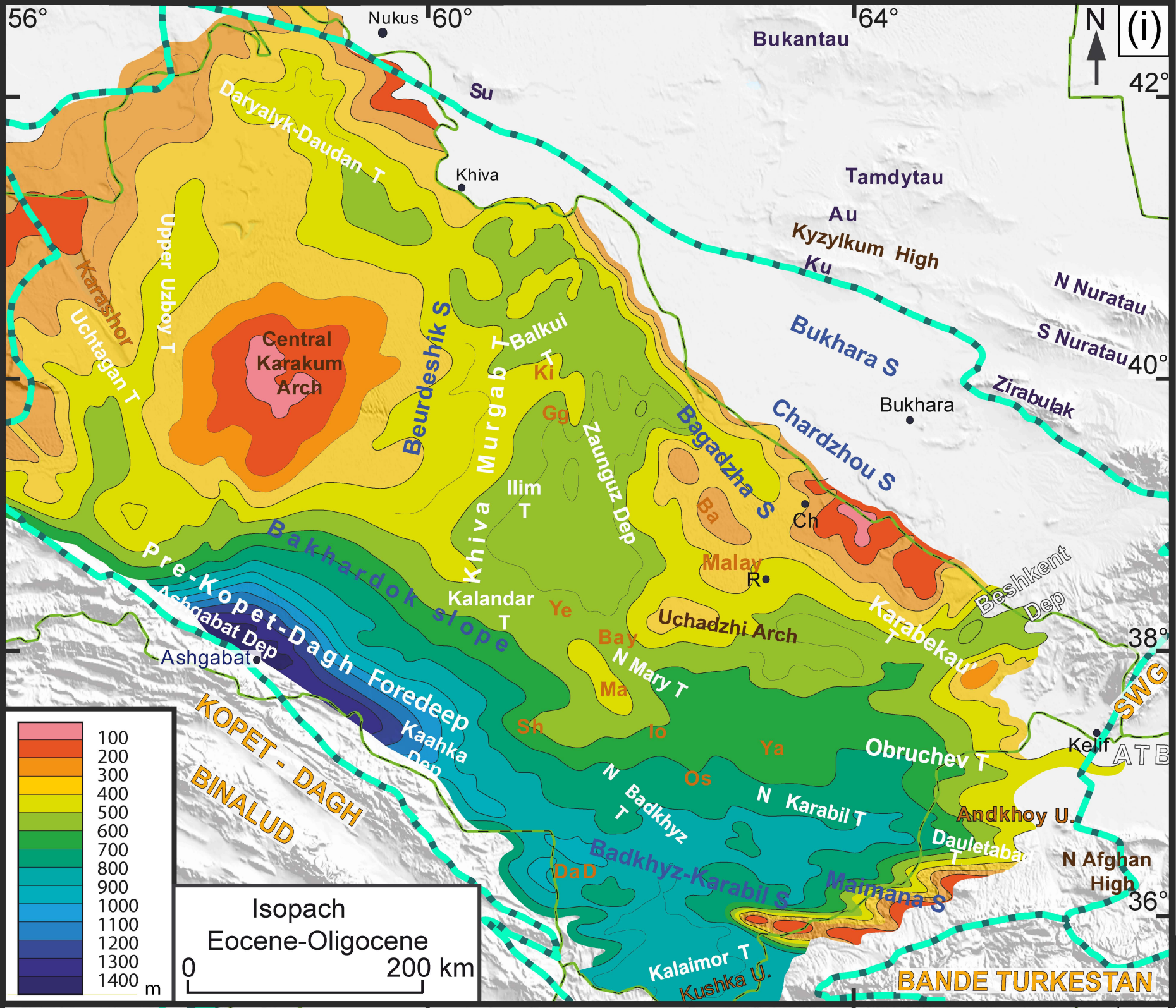
56°
Nukus
60°
64°
Bukantau
N
(i)
42°
Su
Daryalyk-Daudan T
Khiva
Tamdytau
Au
Kyzylkum High
Ku
N Nuratau
S Nuratau
40°
Bukhara S
Zirabulak
Bukhara
Chardzhou S
Karashor
Uchtagan T
Upper Uzboy T
Central
Karakum
Arch
Beurdeshik S
Khiva
Murgab T
Balkui T
Ki
Gg
Zaunguz Dep
Ilim
T
Bagadzha S
Ba
Ch
Malay
R
Bakhardok slope
Pre-Kopet-Dagh Foredeep
Ashgabat Dep
Kalandar
T
Ye
Uchadzhi Arch
Karabekaul
T
Beshkent
Dep
38°
Ashgabat
Bay
N Mary T
Ma
Sh
Io
Ya
Obruchev T
Kelif
SWG
ATB
Kaahka
Dep
KOPET - DAGH
BINALUD
N Badkhyz
T
Os
N Karabil T
Andkhoy U.
Dauletabad
T
N Afghan
High
Badkhyz-Karabil S
DaD
Maimana S
36°
Kalaimor T
Kushka U.
BANDE TURKESTAN
100
200
300
400
500
600
700
800
900
1000
1100
1200
1300
1400
m
Isopach
Eocene-Oligocene
0
200 km

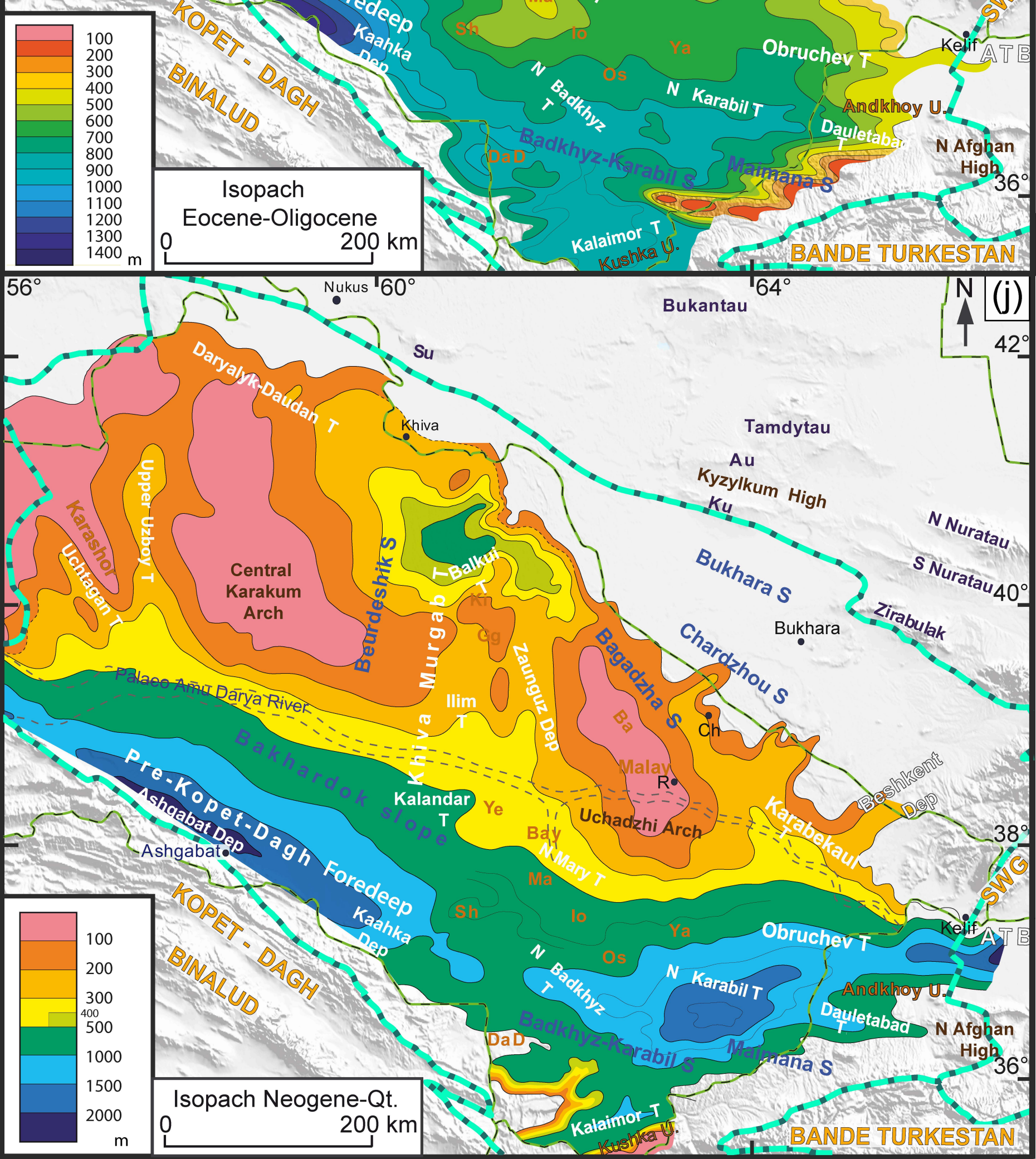
56°
Nukus
60°
64°
Bukantau
N
(j)
42°
Su
Daryalyk-Daudan T
Khiva
Tamdytau
Au
Kyzylkum High
Ku
N Nuratau
S Nuratau
40°
Bukhara S
Zirabulak
Bukhara
Chardzhou S
Karashor
Uchtagan T
Upper Uzboy T
Central
Karakum
Arch
Beurdeshik S
Khiva
Murgab T
Balkui T
Ki
Gg
Zaunguz Dep
Ilim
T
Bagadzha S
Ba
Ch
Malay
R
Palaeo Amu Darya River
Bakhardok slope
Pre-Kopet-Dagh Foredeep
Ashgabat Dep
Kalandar
T
Ye
Uchadzhi Arch
Karabekaul
T
Beshkent
Dep
38°
Ashgabat
Bay
N Mary T
Ma
Sh
Io
Ya
Obruchev T
Kelif
SWG
ATB
Kaahka
Dep
KOPET - DAGH
BINALUD
N Badkhyz
T
Os
N Karabil T
Andkhoy U.
Dauletabad
T
N Afghan
High
Badkhyz-Karabil S
DaD
Maimana S
36°
Kalaimor T
Kushka U.
BANDE TURKESTAN
100
200
300
400
500
1000
1500
2000
m
Isopach Neogene-Qt.
0
200 km

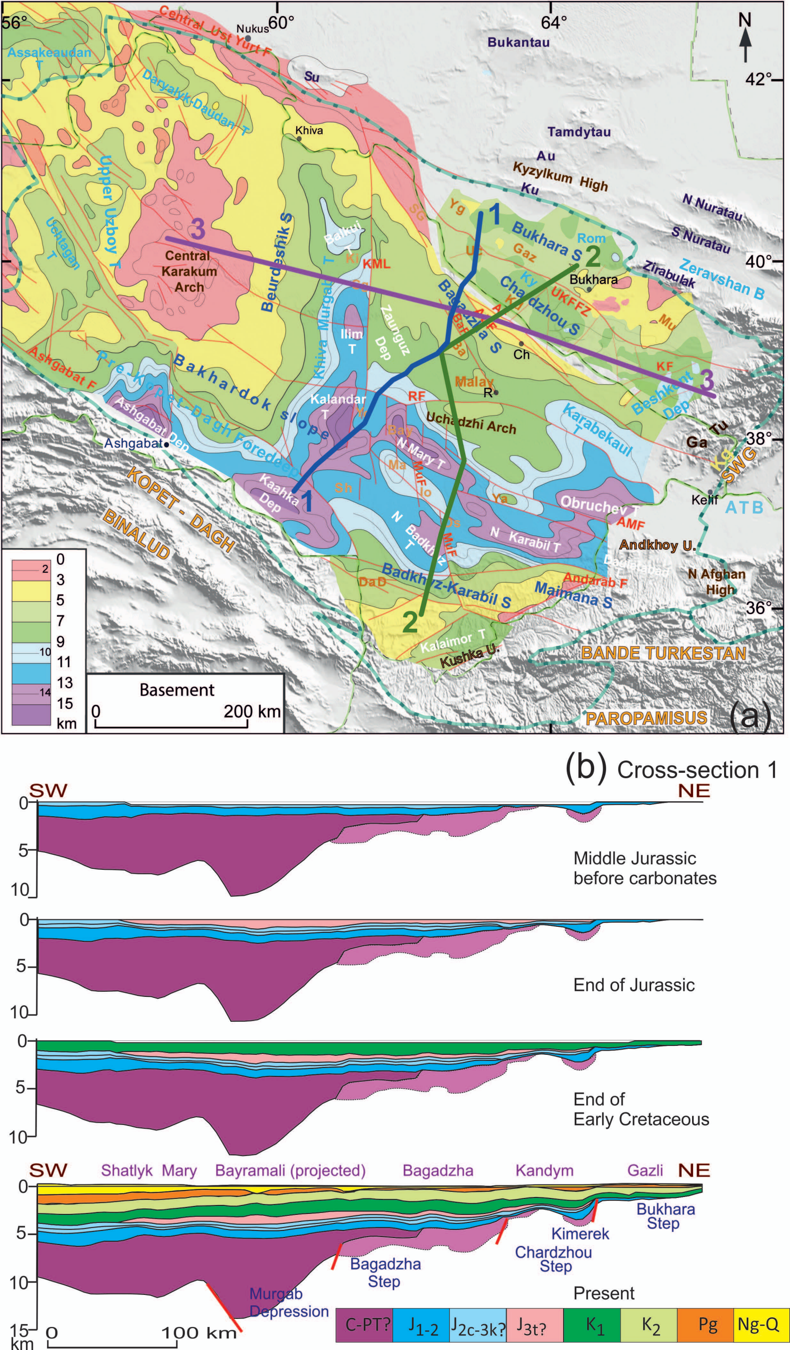
Central Ust Yurt F
Nukus
Assakeaudan T
Su
Daryalyk-Daudan T
Khiva
Bukantau
Tamdytau
Au
Kyzylkum High
Ku
N Nuratau
S Nuratau
Zirabulak
Zeravshan B
Upper Uzboy T
Uchtagan T
Central Karakum Arch
Beurdeshik S
Balkui T
KML
Bukhara S
Rom
Gaz
Bukhara
Chardzhou S
UKFFZ
Bagadzha S
Ch
Zaunguz Dep
Ilim T
Khiva Murgab T
Bakhardok slope
Pre-Kopet-Dagh Foredeep
Ashgabat F
Ashgabat Dep
Ashgabat
Kalandar T
RF
Malay
R
Uchadzhi Arch
Karabekaul T
Beshkent Dep
KF
Ga
Tu
SWG
Kelif
ATB
N Mary T
Kaahka Dep
KOPET - DAGH
BINALUD
Obruchev T
AMF
N Karabil T
N Badkhyz T
Andkhoy U.
N Afghan High
Andarab F
Badkhyz-Karabil S
Maimana S
Kalaimor T
Kushka U.
BANDE TURKESTAN
PAROPAMISUS
0
2
3
5
7
9
10
11
13
14
15
km
Basement
0 200 km
(a)
56°
60°
64°
42°
40°
38°
36°
N
1
2
3
(b) Cross-section 1
SW
NE
Middle Jurassic before carbonates
End of Jurassic
End of Early Cretaceous
Present
Shatlyk Mary Bayramali (projected) Bagadzha Kandym Gazli
Bukhara Step
Kimerek
Chardzhou Step
Bagadzha Step
Murgab Depression
0 100 km
km
C-PT? J1-2 J2c-3k? J3t? K1 K2 Pg Ng-Q

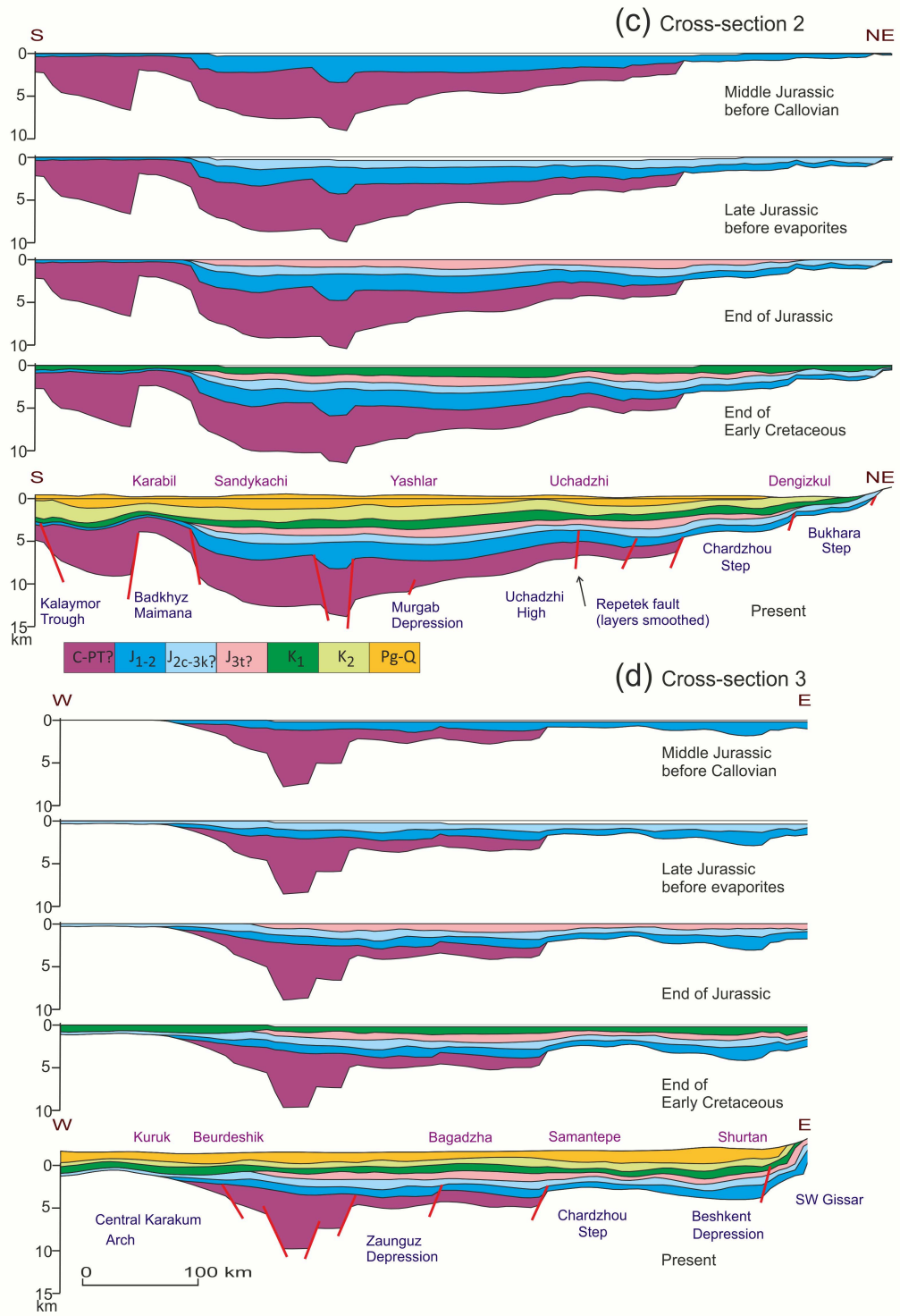
(c) Cross-section 2
S
NE
0
5
10
Middle Jurassic
before Callovian
Late Jurassic
before evaporites
End of Jurassic
End of
Early Cretaceous
S
NE
Karabil
Sandykachi
Yashlar
Uchadzhi
Dengizkul
Bukhara
Step
Chardzhou
Step
Kalaymor
Trough
Badkhyz
Maimana
Murgab
Depression
Uchadzhi
High
Repetek fault
(layers smoothed)
Present
15
km
C-PT?
J1-2
J2c-3k?
J3t?
K1
K2
Pg-Q
(d) Cross-section 3
W
E
Middle Jurassic
before Callovian
Late Jurassic
before evaporites
End of Jurassic
End of
Early Cretaceous
W
E
Kuruk
Beurdeshik
Bagadzha
Samantepe
Shurtan
SW Gissar
Central Karakum
Arch
Zaunguz
Depression
Chardzhou
Step
Beshkent
Depression
Present
0
100 km
15
km

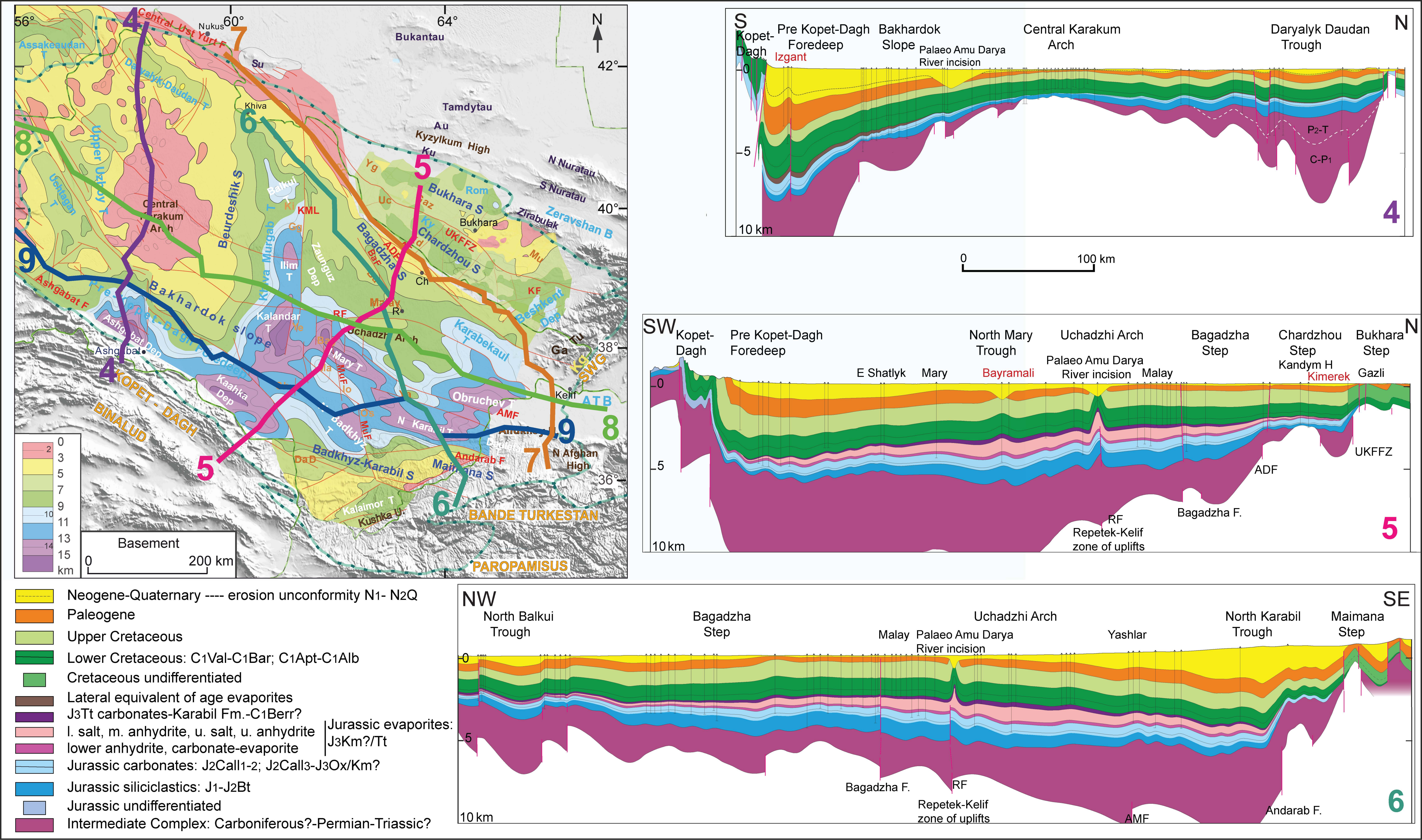

Neogene-Quaternary ---- erosion unconformity N1- N2Q
Paleogene
Upper Cretaceous
Lower Cretaceous: C1Val-C1Bar; C1Apt-C1Alb
Cretaceous undifferentiated
Lateral equivalent of age evaporites
J3Tt carbonates-Karabil Fm.-C1Berr?
l. salt, m. anhydrite, u. salt, u. anhydrite
lower anhydrite, carbonate-evaporite
Jurassic evaporites: J3Km?/Tt
Jurassic carbonates: J2Call1-2; J2Call3-J3Ox/Km?
Jurassic siliciclastics: J1-J2Bt
Jurassic undifferentiated
Intermediate Complex: Carboniferous?-Permian-Triassic?
Basement
0 200 km
km
N
Central Ust Yurt F
Nukus
Bukantau
Assakeaudan T
Daryalyk Daudan T
Su
Khiva
Tamdytau
Kyzylkum High
Upper Uzboy T
Ushtagan T
Central Karakum Arch
Beurdeshik S
Balkui T
KML
Bukhara S
Bukhara
N Nuratau
S Nuratau
Zirabulak
Zeravshan B
Chardzhou S
UKFFZ
Bagadzha S
Ilim T
Zaunguz Dep
ADF
KF
Beshkent Dep
Ashgabat F
Bakhardok slope
Pre-Kopet-Dagh Foredeep
Kalandar T
RF
Uchadzhi Arch
Karabekaul T
Ashgabat Dep
Ashgabat
Mary T
Kaahka Dep
Obruchev T
AMF
KOPET - DAGH
BINALUD
N Karabil T
Badkhyz T
Andarab F
N Afghan High
Badkhyz-Karabil S
Maimana S
Kalaimor T
Kushka U.
BANDE TURKESTAN
PAROPAMISUS
Kelif
ATB
SWG
S
Kopet-Dagh
Pre Kopet-Dagh Foredeep
Izgant
Bakhardok Slope
Palaeo Amu Darya River incision
Central Karakum Arch
Daryalyk Daudan Trough
P2-T
C-P1
10 km
0 100 km
SW
Pre Kopet-Dagh Foredeep
E Shatlyk
Mary
North Mary Trough
Bayramali
Uchadzhi Arch
Palaeo Amu Darya River incision
Malay
Bagadzha Step
Chardzhou Step
Kandym H
Kimerek
Bukhara Step
Gazli
UKFFZ
ADF
Bagadzha F.
RF
Repetek-Kelif zone of uplifts
NW
SE
North Balkui Trough
Bagadzha Step
Malay
Uchadzhi Arch
Palaeo Amu Darya River incision
Yashlar
North Karabil Trough
Maimana Step
Bagadzha F.
RF
Repetek-Kelif zone of uplifts
AMF
Andarab F.

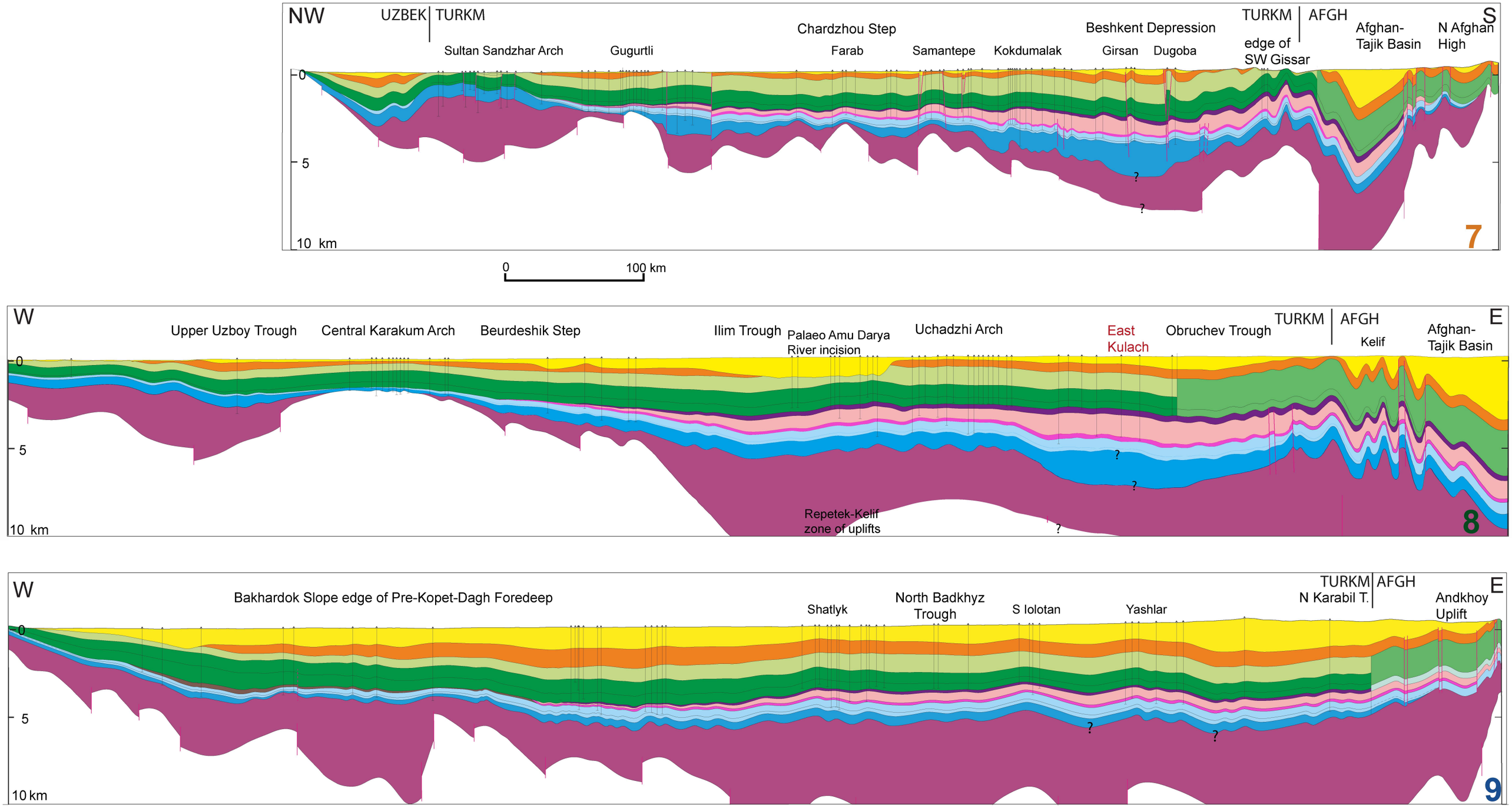
NW
UZBEK
TURKM
Sultan Sandzhar Arch
Gugurtli
Chardzhou Step
Farab
Samantepe
Kokdumalak
Beshkent Depression
Girsan
Dugoba
TURKM
AFGH
edge of
SW Gissar
Afghan-
Tajik Basin
N Afghan
High
S
0
5
10 km
7
0
100 km
W
Upper Uzboy Trough
Central Karakum Arch
Beurdeshik Step
Ilim Trough
Palaeo Amu Darya
River incision
Uchadzhi Arch
East
Kulach
Obruchev Trough
TURKM
AFGH
Kelif
Afghan-
Tajik Basin
E
0
5
10 km
Repetek-Kelif
zone of uplifts
8
W
Bakhardok Slope edge of Pre-Kopet-Dagh Foredeep
Shatlyk
North Badkhyz
Trough
S Iolotan
Yashlar
TURKM
AFGH
N Karabil T.
Andkhoy
Uplift
E
0
5
10 km
9

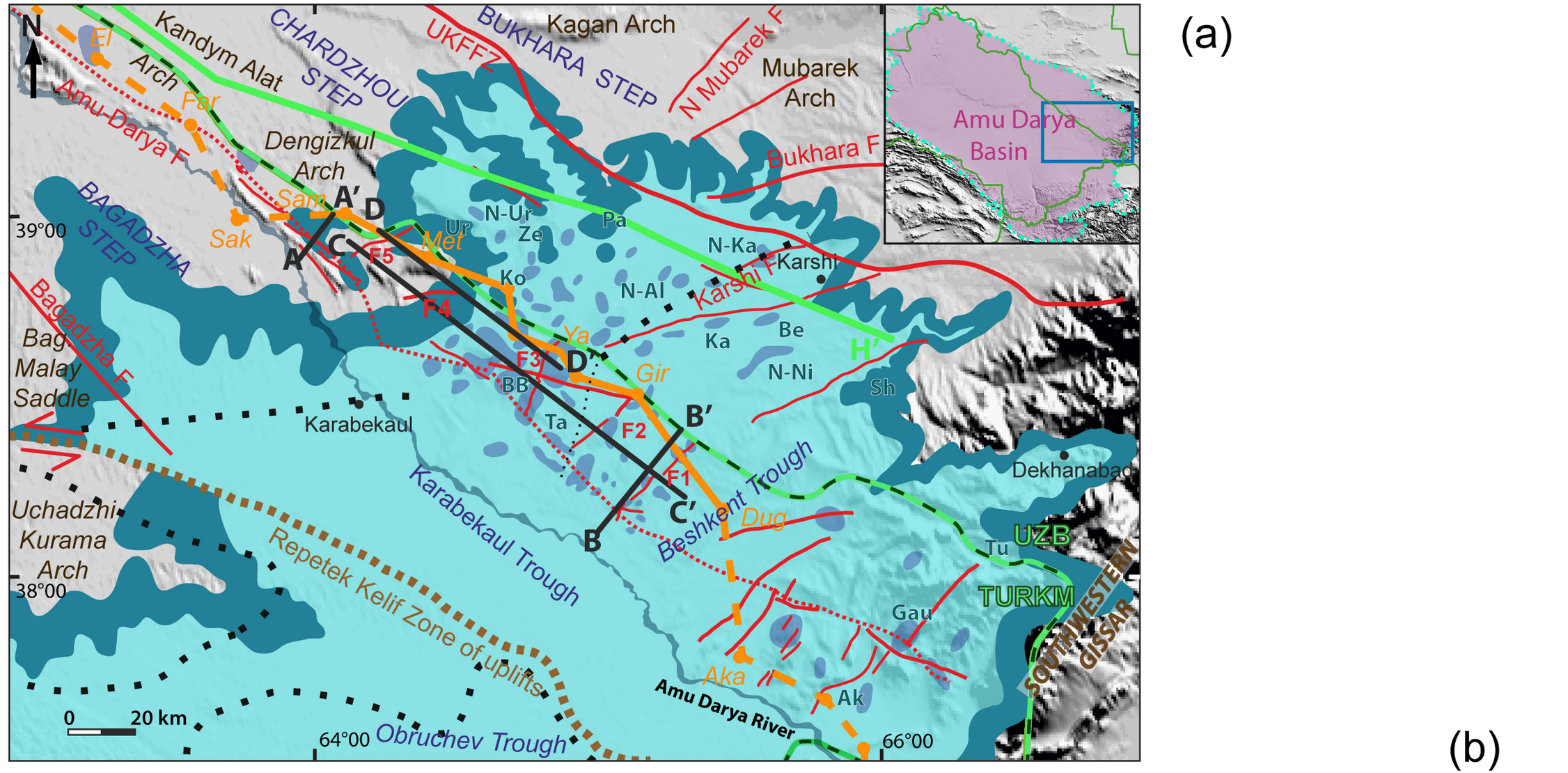
(a)
N
El Arch
Kandym Alat
CHARDZHOU STEP
UKFFZ
BUKHARA STEP
Kagan Arch
N Mubarek F
Mubarek Arch
Far
Amu-Darya F
Dengizkul Arch
Bukhara F
Amu Darya Basin
BAGADZHA STEP
Sam
A′
D
A
C
Sak
F5
Met
Ur
N-Ur
Ze
Pa
N-Ka
Karshi
Karshi F
39°00
F4
Ko
N-Al
Ya
F3
D′
Gir
Ka
Be
H′
Bag Malay Saddle
Bagadzha F
BB
N-Ni
Sh
Karabekaul
Ta
B′
F2
F1
C′
B
Karabekaul Trough
Beshkent Trough
Dekhanabad
Uchadzhi Kurama Arch
Dug
Tu
UZB
TURKM
SOUTHWESTERN GISSAR
Repetek Kelif Zone of uplifts
Gau
38°00
Aka
Ak
0
20 km
64°00
Obruchev Trough
Amu Darya River
66°00
(b)
NW
SE
SAMANTEPE
METEDZHAN
KOKDUMALAK
TANGIKUDUK
YANKUI
CHACHKUI
GIRSAN
TUILLEKUI
DUGOBA
0
F5
F3
F1
F4
5 km
0
20 km
?
5
km

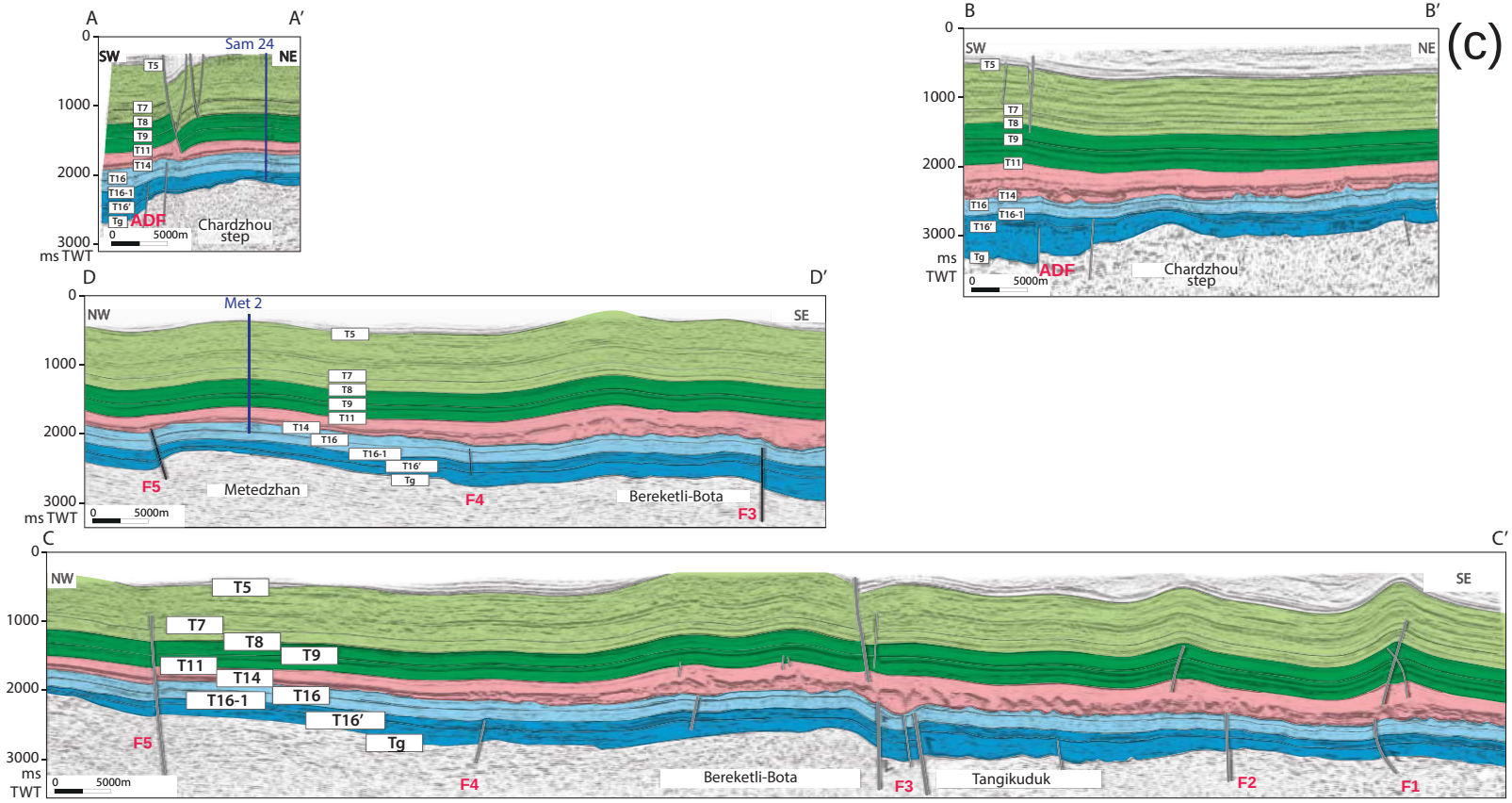
A
A′
Sam 24
SW
NE
0
1000
2000
3000
ms TWT
T5
T7
T8
T9
T11
T14
T16
T16-1
T16′
Tg
ADF
Chardzhou step
0
5000m
B
B′
(c)
SW
NE
ADF
Chardzhou step
D
D′
Met 2
NW
SE
F5
Metedzhan
F4
Bereketli-Bota
F3
C
C′
NW
SE
Bereketli-Bota
Tangikuduk
F5
F4
F3
F2
F1

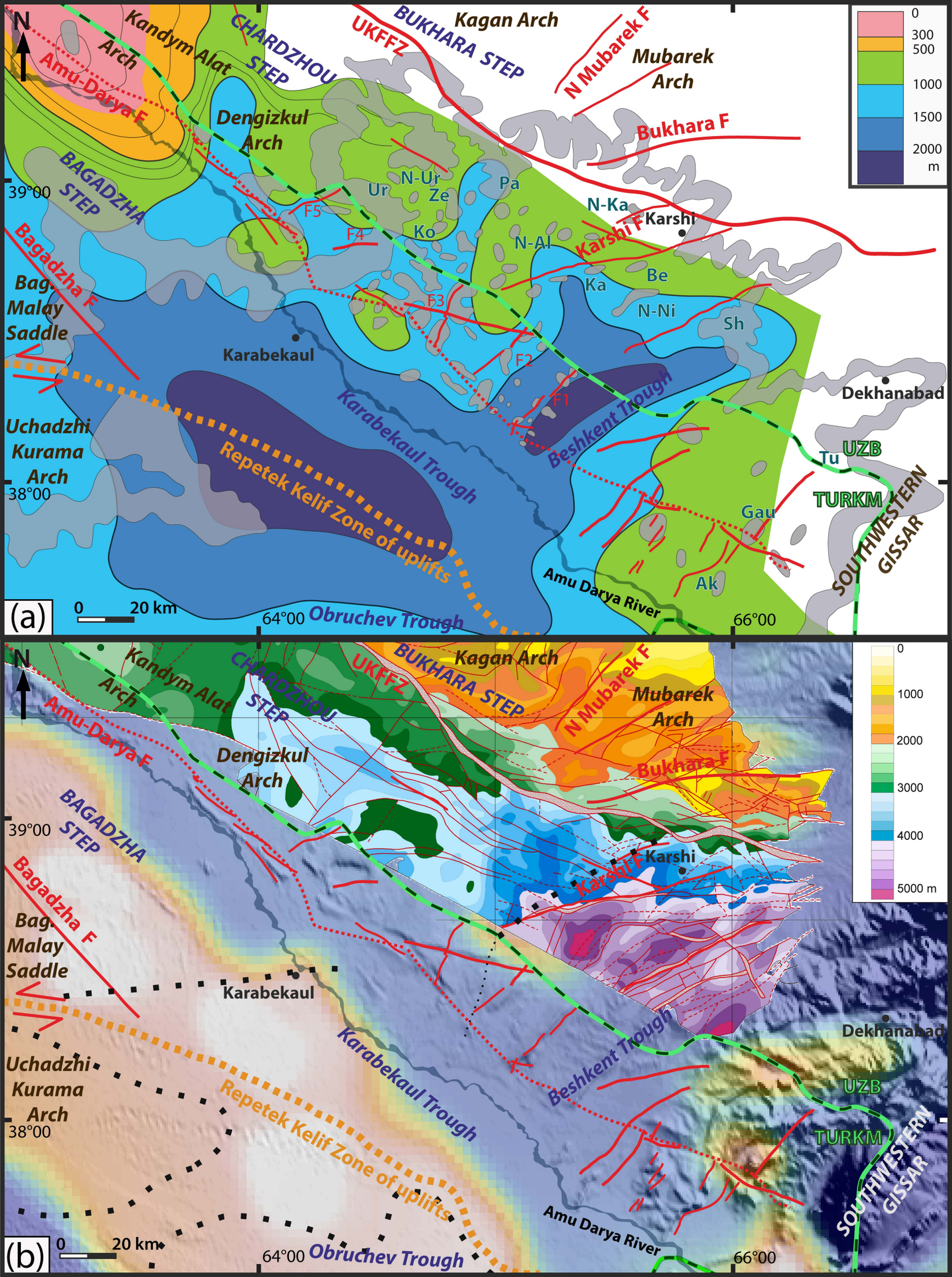
N
Kandym Alat Arch
Amu-Darya F
CHARDZHOU STEP
UKFFZ
BUKHARA STEP
Kagan Arch
N Mubarek F
Mubarek Arch
Bukhara F
Dengizkul Arch
BAGADZHA STEP
39°00
Bagadzha F
Bag. Malay Saddle
F5
F4
Ur
N-Ur
Ze
Ko
Pa
N-Ka
Karshi
Karshi F
N-Al
Ka
Be
N-Ni
Sh
F3
F2
F1
Karabekaul
Karabekaul Trough
Beshkent Trough
Dekhanabad
Uchadzhi Kurama Arch
38°00
Repetek Kelif Zone of uplifts
UZB
Tu
TURKM
Gau
SOUTHWESTERN GISSAR
Ak
Amu Darya River
0
20 km
(a)
64°00
Obruchev Trough
66°00
0
300
500
1000
1500
2000
m
1000
2000
3000
4000
5000 m
(b)

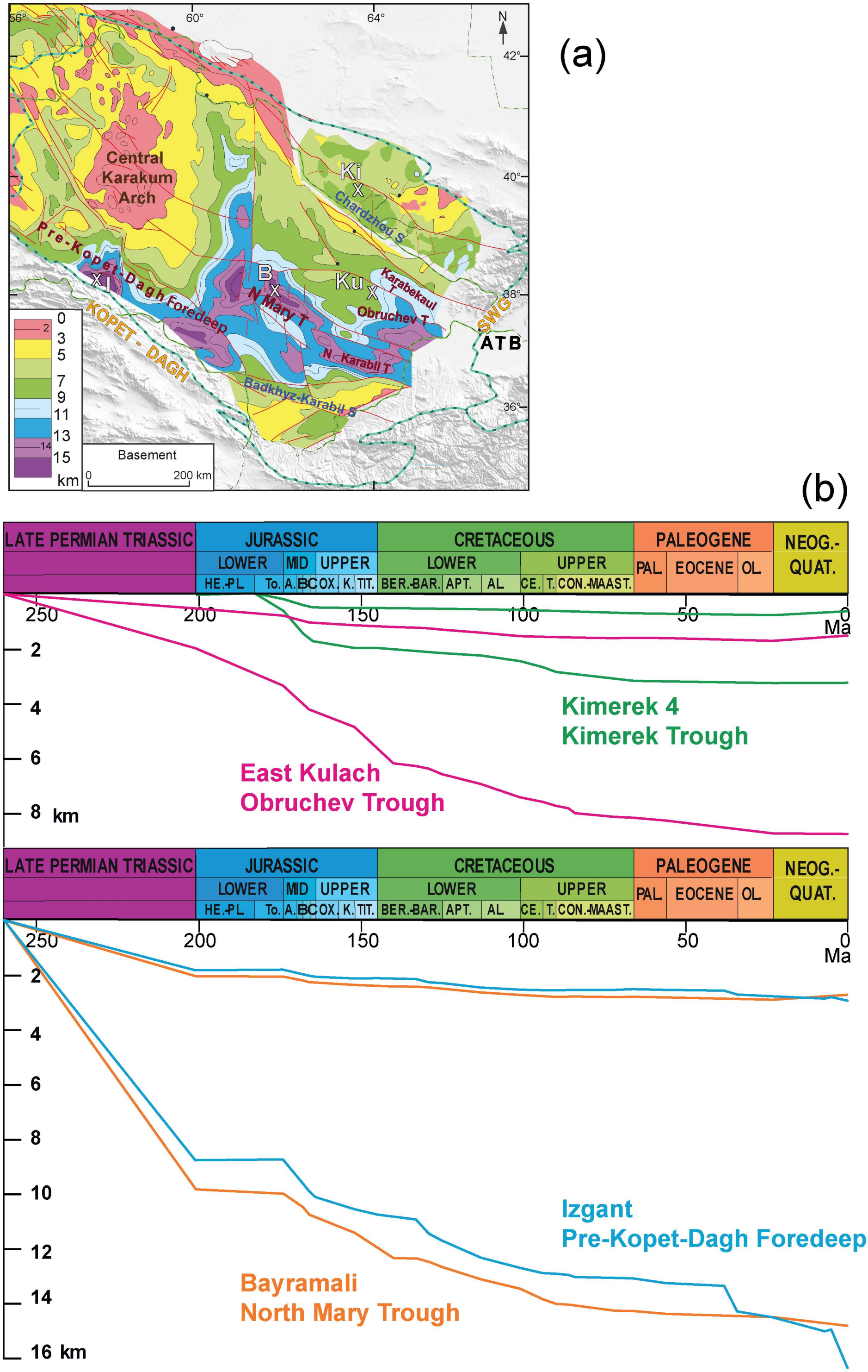

(a)
56°
60°
64°
N
42°
40°
38°
36°
Central Karakum Arch
Ki
Chardzhou S
Pre-Kopet-Dagh Foredeep
I
B
N Mary T
Ku
Karabekaul T
Obruchev T
N Karabil T
Badkhyz-Karabil S
KOPET - DAGH
SWG
ATB
0
2
3
5
7
9
11
13
14
15
km
Basement
0
200 km
(b)
LATE PERMIAN TRIASSIC
JURASSIC
LOWER
MID
UPPER
HE.-PL
To.
A.
B.
C.
OX.
K.
TIT.
CRETACEOUS
LOWER
UPPER
BER.-BAR.
APT.
AL
CE.
T.
CON.-MAAST.
PALEOGENE
PAL
EOCENE
OL
NEOG.-QUAT.
250
200
150
100
50
0
Ma
2
4
6
8 km
Kimerek 4
Kimerek Trough
East Kulach
Obruchev Trough
10
12
14
16 km
Izgant
Pre-Kopet-Dagh Foredeep
Bayramali
North Mary Trough

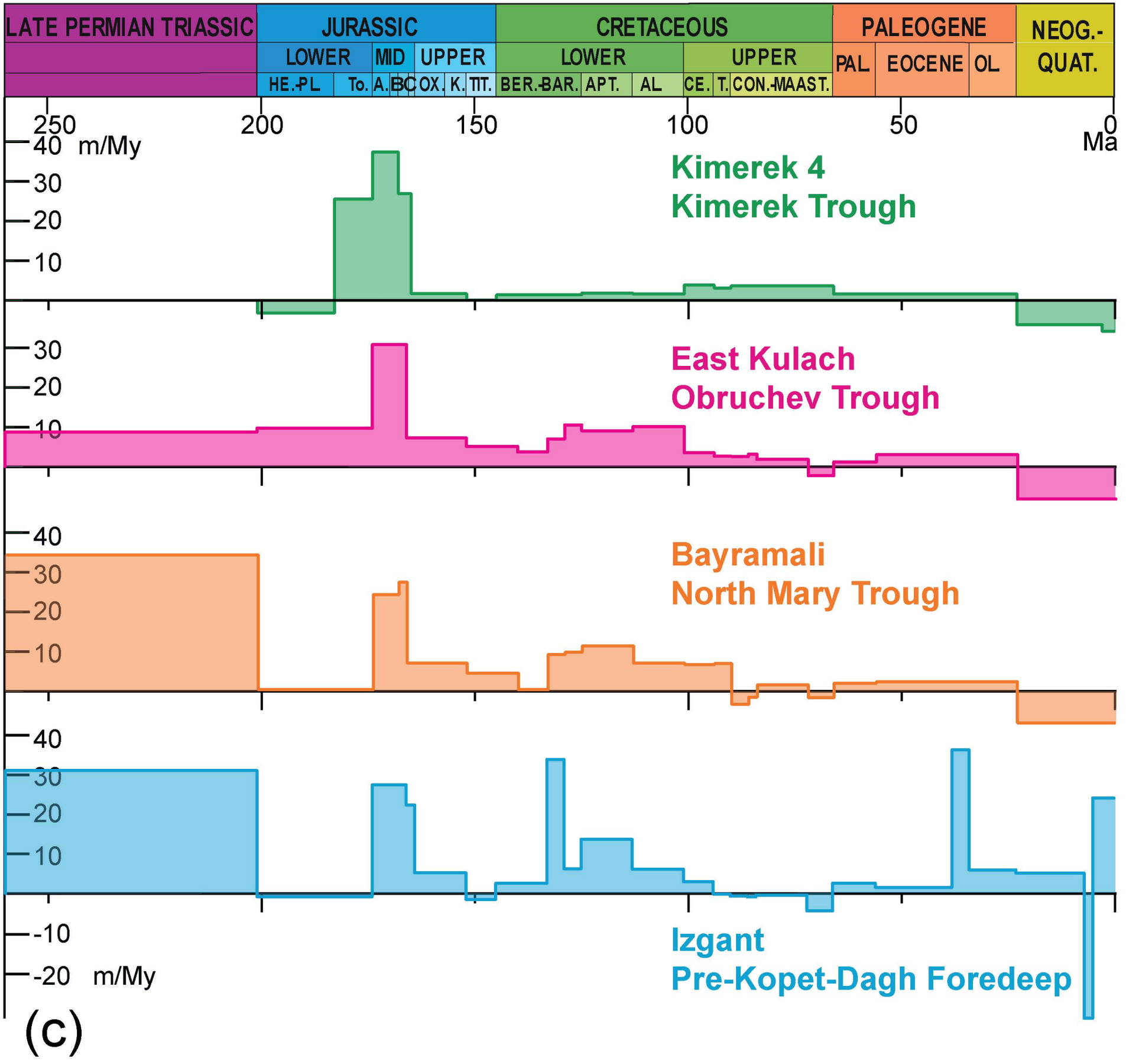
LATE PERMIAN TRIASSIC
JURASSIC
CRETACEOUS
PALEOGENE
NEOG.-QUAT.
LOWER
MID
UPPER
LOWER
UPPER
PAL
EOCENE
OL
HE.-PL.
To.
A.
BC
OX.
K.
TIT.
BER.-BAR.
APT.
AL.
CE.
T.
CON.-MAAST.
250
200
150
100
50
0
Ma
40 m/My
30
20
10
Kimerek 4
Kimerek Trough
30
20
10
East Kulach
Obruchev Trough
40
30
20
10
Bayramali
North Mary Trough
40
30
20
10
-10
-20 m/My
Izgant
Pre-Kopet-Dagh Foredeep
(c)

- LITHOLOGY -

- CONTINENTAL -

EXPOSED LAND - NO DEPOSITION

High-moderate mountains
Active mountain range

Low mountains and plateau

Lowland erosional plain

DEPOSITS

Fluvio-lacustrine, Alluvial plain

Large scale lacustrine deposits

Continental molasse -
Intramountain basin deposits

- TRANSITIONAL -

Flooded lowland/Marginal marine
Coastal plain/Shallow mixed shelf

Deltaic - Fan

Hypersaline - Evaporites

- VOLCANISM -

Undifferenciated volcanics

Volcaniclastics: Continental

- MARINE -

PLATFORM - SHALLOW SHELF

Reef platform - Carbonate build-up

Carbonate platform

Terrigenous platform
Coarse & fine clastics

DEEPER SHELF - SLOPE - BASIN

Slope/Basinal deeper
marine carbonates

Slope/basinal deeper
marine clastics

DEEP MARINE

Deep marine sediments

- SYMBOL -

Sediment influx

- TECTONIC ELEMENTS -

Accretionary complex
Tectonic melange

- OCEANIC DOMAIN -

Active subduction zone

Active oceanic spreading center
and transform

Oceanic/continental crust boundary
(observed and inferred)

- CONTINENTAL DOMAIN -

Major thrust fault

Major normal fault

Major strike-slip/wrench fault


KTuL
TaB
ADB
NP
Palaeo-Tethys
N
0
1000 km
Permian
KTuL
SC
TaB
ADB
ATB
Nlr Alb
PB
HK
NP
Clr
BB
Neo-Tethys
CP
He
Norian
TFF
KTuL
SC
TaB
ADB
ATB
Nlr Alb
PB
NP
Clr
BB
CP
He
SP
Qi
Neo-Tethys
Kk
Middle Toarcian
TFF
KTuL
SC
TaB
ADB
KD
ATB
Nlr Alb
PB
BB
NP
Clr
WP
CP
SP
He
Qi
Neo-Tethys
Kk
Callovian-Oxfordian
KTuL
SC
TaB
ADB
KD
ATB
Nlr Alb
PB
BB
WP
Clr
CP
He
SP
Qi
Neo-Tethys
Kh
Kk
Tithonian
KTuL
SC
TaB
ADB
KD
ATB
Nlr Alb
PB
BB
Clr
CP
SP
He
Qi
Kh
Neo-Tethys
Kk
Lh
Middle Aptian

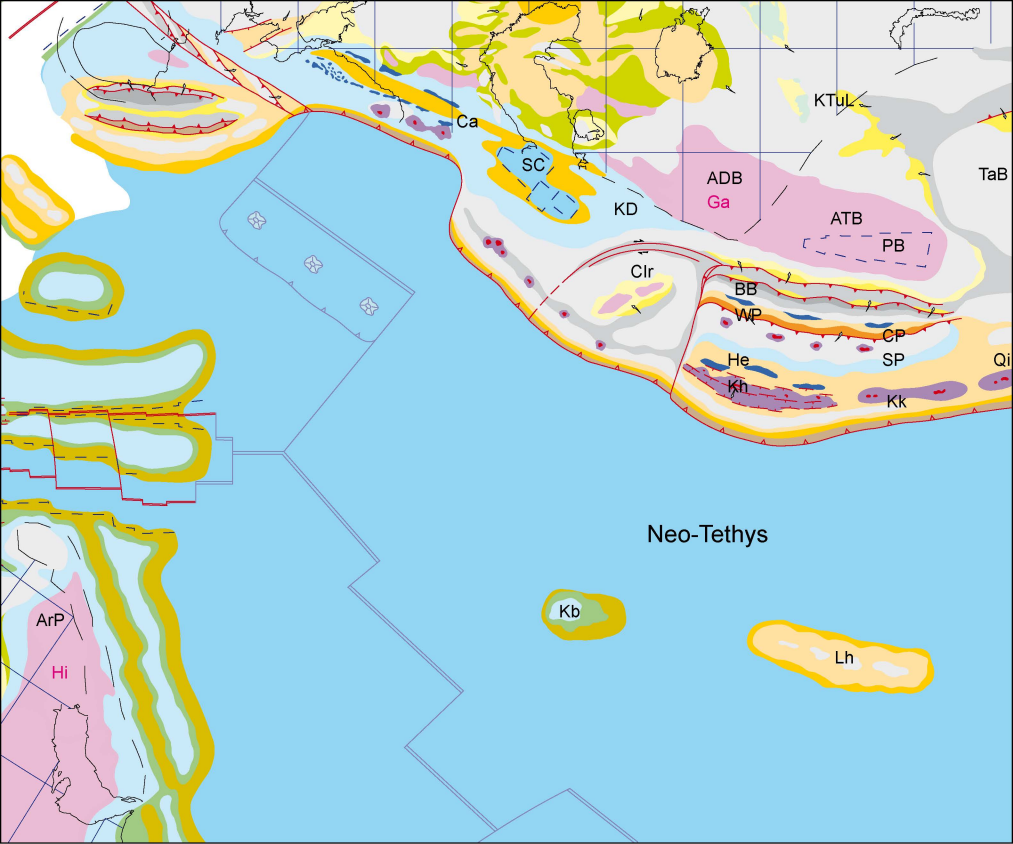
Ca
SC
KD
ADB
Ga
KTuL
TaB
ATB
PB
Clr
BB
WP
CP
SP
Qi
He
Kh
Kk
Neo-Tethys
Kb
Lh
ArP
Hi